EXPLORING SPATIAL REUSE EFFECTS ON PERFORMANCE ENHANCEMENTS IN WIRELESS MULTIHOP NETWORKS

Basel Alawieh

A thesis

in

The Department

of

Electrical and Computer Engineering

Presented in Partial Fulfillment of the Requirements

For the Degree of Doctor of Philosophy

Concordia University

Montréal, Québec, Canada

September 2008

Your file Votre référence
ISBN: 978-0-494-45647-7
Our file Notre référence
ISBN: 978-0-494-45647-7

Abstract

Exploring Spatial Reuse effects on performance enhancements in Wireless Multihop Networks

Basel Alawieh, Ph.D.

Concordia University, 2008

Recent years have witnessed a remarkable interest in wireless multihop ad hoc networks that need little or no infrastructure support. Such networks have enabled the existence of various applications ranging from the monitoring of herds of animals to supporting communication in military battle-fields and civilian disaster recovery scenarios as well as providing an emergency warning system for vehicles on the road. Currently, the distributed coordination function (DCF) of the IEEE is the industry dominant MAC protocol for wireless multihop ad hoc environment due to its simple implementation and distributed nature. Nevertheless, the DCF access method does not make efficient use of the shared channel due to its inherent conservative approach in assessing the level of interference. Moreover, the implementation of DCF in multihop ad hoc networks suffers from the exposed and hidden terminal problems; both of these problems highly affect the spectrum spatial reuse and accordingly causes serious throughput deterioration. To date, various methods have been proposed to enhance the throughput of the DCF; namely, tuning the carrier sensing threshold, the transmission attempt probability through changing the binary exponential backoff, controlling the frame transmit power, adapting the physical transmission rate of data frame, and the use of directional antennas. In this thesis, we develop mathematical tools to study the effectiveness of the interplay among the various tunable parameters and propose suitable protocols for achieving better utilization of the wireless spectrum.

Acknowledgments

I am indebted to my professors Dr. C. Assi and Dr. H.T. Mouftah, who supervised my thesis and introduced me to the world of wireless communications, for their tremendous help throughout my PhD work. I would like to express my appreciations to the doctoral thesis committee members for their insightful remarks during this work. I would like to extend my thanks to my friends Ibrahim Salloum, Ali Kanso and Archer for their tremendous support. Finally, I am especially grateful to my parents for their continuing support and encouragement.

Contents

List of Figures

List of Tables

List of Publications

Conference papers (Accepted):

- Basel Alawieh, Yongyang guo, Chadi Assi, and Hussein Mouftah. An efficient Rate Adaptation Scheme for MANET using Kalman Filter. *Proceedings of IEEE ISCC 2008.*

- Yongning Zhang, Basel Alawieh and Chadi Assi. A Novel Physical Carrier Sensing Scheme for Enhancing Spatial Reuse in Multihop Wireless Networks. *Proceedings of IEEE WoWMoM 2008.*

- Bassel Alawieh, Yongning Zhang and Chadi Assi. A Distributed Power and Rate Control Scheme for MANET. *Proceedings of IEEE Wiopt 2008.*

- Basel Alawieh, Chadi Assi and Hussein Mouftah. Investigation of Power-Aware IEEE 802.11 in multihop networks. *Proceedings of LNCS - MSN 2007.*

- Basel Alawieh, Chadi Assi. Power Control using directional antenna in ad hoc networks: Models and Analysis. *Proceedings of IEEE ISCC 2007.*

- Basel Alawieh, Chadi Assi,Wessam Ajib. Distributed Power Control Scheme for MANET using Prediction Filters. *Proceedings of IEEE AINA 2007.*

- Basel Alawieh, Chadi Assi, Wessam Ajib. A Power Control Scheme for Directional MAC Protocols in MANET. *Proceedings of IEEE WCNC 2007.*

Journal papers (Accepted):

- Basel Alawieh, Chadi Assi and Wessam Ajib. Distributed Power Control using Directional Antenna. *IEEE Transaction of Vehicular Technology*, May 2008. 2008.

- Basel Alawieh, Chadi Assi and Hussein Mouftah. Investigating the Performance of Power-Aware IEEE 802.11 in Multi-hop Wireless Networks to appear in *IEEE Transactions on Vehicular Technology.*

- Basel Alawieh, Chadi Assi , Hussein Mouftah. Power-Aware Ad Hoc Networks with Directional Antennas: Models and Analysis. To Appear in *Journal of Ad hoc Networks.*

- Basel Alawieh, Yongning Zhang and Chadi Assi. Improving Spatial Reuse in Multihop Wireless Networks: A Survey. To Appear in *IEEE Communications Surveys and Tutorials.*

Journal papers (Under Review):

- Yongning Zhang, Bassel Alawieh and Chadi Assi. A Spatiotemporal Contention Resolution for Enhancing Spatial Reuse in Multihop Wireless Networks. Submitted to *IEEE Transactions on Mobile Computing.*

- Basel Alawieh, Yongning Zhang and Chadi Assi. Improving the Performance of MultihopWireless Networks Through Power and Rate Control. Submitted to *IEEE Trans- actions on Vehicular Technology.*

Book Chapters (Accepted):

- Basel Alawieh, Chadi Assi and Hussein Mouftah. Mobile Ad hoc Networks with directional Antennas. To appear as a Book Chapter in Encyclopedia on Ad Hoc and Ubiquitous Computing. World Scientific Book company 2008.

- Basel Alawieh, Chadi Assi and Hussein Mouftah. Transmission Power Control for Mobile Ad hoc Networks. To appear in the Handbook of Communication Networks and Distributed Systems. World Scientific Book company 2008

- Basel Alawieh, Chadi Assi and Hussein Mouftah. Collision Avoidance Aware MAC protocols for Multihop Ad hoc Networks: Challenges and Open issues. To appear in the Handbook of Communication Networks and Distributed Systems. World Scientific Book company 2008

List of Acronyms

ACK – Acknowledgement

AIFS – Arbitration Interframe Space

AIMD – Additive Increase Multiplicative Decrease

AODV – Ad Hoc On Demand Distance Vector

AoA – Angle of Arrival

AP – Access Point

CBR – Constant Bit Rate

CSMA/CA – Carrier Sense Multiple Access with Collision Avoidance

CTS – Clear To Send

CW – Contention Window

DCF – Distributed Coordination Function

DIFS – Distributed Inter Frame Space

DNAV – Directional Network Allocation Vector

DVCS – Directional virtual carrier sensing

EIFS – Extended Inter Frame Space

FIFO – First in First out

HOL – Head of line Blocking

IEEE – Institution of Electrical and Electronics Engineers

MAC – Media Access Control

MANET – Mobile Ad Hoc Network

NAV – Network Allocation Vector

PCS – Physical Carrier Sensing

PRAS-CP – Power and Rate Adaptive Scheme with Collision Prevention

RTS – Request To Send

SIFS – Short Inter Frame Space

SINR – Signal to Interference plus Noise Ratio

VCS – Virtual Carrier Sensing

WLAN – Wireless Local Area Network

Chapter 1

Introduction

1.1 Overview

Wireless communications have become an essential part of modern life, allowing users to maintain network and Internet access without being tied to a particular location by a wire. As the bandwidth and throughput of wireless technologies have increased, it has become possible to support true multimedia applications, including, voice, and video traffic.

In wireless networking, there are two main classes of communication paradigms, infrastructure-based networks and ad hoc networks. Infrastructure-based networks include cellular networks and wireless LANs. The network operator deploys a network infrastructure within the coverage area to provide wireless connectivity to the vicinity. The infrastructure is known as base stations in cellular networks, access points in wireless LANs, and are connected together to a backbone network by wires. All communications on the wireless medium occurs in one hop between the mobile nodes to the local base station/access point. A mobile node acts as the source or the sink of a communication circuit.

Mobile Ad hoc Networks [1] (MANET), on the other hand, preclude the use of any wired infrastructure and enable communications only over wireless channels. These

networks are applicable to environments in which a prior deployment of network infrastructure is impossible. Current applications are mostly confined to military and rescue operations for long range outdoor networks, or to indoor network settings such as a conference room with a collection of laptop computers. The emergency wireless personal area networks (WPAN) is an example of an indoor MANET that will be used to connect home appliances. Multi-hop wireless networks, known as last-mile solution, are another example of MANET that will likely increase in popularity, and may become the dominant solution for the wireless networks community. In multihop ad hoc networks, mobile nodes are connected together to form a network on the fly. Nodes also have routing capabilities and each node may act as the source, sink or a forwarding node to relay packets for other nodes.

Today, we have around three billion wireless users worldwide [2], each may require a mixture of real-time traffic (e.g., voice, video, etc.) and data traffic (e.g., email, messaging, web browsing, file transfer, etc.); hence, efficient utilization of the limited shared wireless spectrum has become an essential design goal for researchers [1], [3], [4]. Indeed, since the wireless channel is a shared channel, an efficient medium access control (MAC) protocol is needed to regulate the channel access among multiple contending nodes.

MAC protocols can be classified into reservation-based protocols or contention-based protocols. Reservation-based protocols apply to static networks or networks in which a central access point has control over when and which station can access the channel. In contention-based MAC protocols [1], the nodes contend for the channel when they have a packet to send (i.e, individual decision). This type of MAC is attractive due to its simplicity, robustness and suitability for bursty traffic. Moreover, due to the lack of centralized control points, contention-based MAC protocols are often more useful in wireless multihop networks.

Currently, the distributed coordination function (DCF) of the IEEE 802.11 [5] is

the dominant MAC protocol for both wireless LANs and wireless multihop ad hoc environment due to its simple implementation and distributed nature. A station running the DCF protocol uses carrier sensing to determine the status of the medium (e.g., assess its current interference level) before initiating any transmission to avoid collisions. Two types of carrier sensing are used, a mandatory physical carrier sensing (PCS) and an optional virtual carrier sensing (VCS). In the former, a node monitors the radio frequency (RF) energy level on the channel and initiates channel access for transmission only if the power of the detected signal is below a certain carrier sense threshold (CS_{th}) [5]. In the latter, each node regards the channel busy for a period indicated in the MAC frames defined in the protocol. Namely, nodes hearing the RTS/CTS (request-to-send and clear-to-send) exchange (typically nodes in the transmission range of these frames) will adjust their network allocation vector (NAV) to the duration of the complete four-way handshake. Hence, a node contends for a channel only if the conditions for both carrier sense mechanisms are satisfied. Thus, DCF using the former is called basic two-way handshake (i.e, DATA and ACK) and when using RTS/CTS is called the four-way handshake (RTS, CTS,DATA and ACK).

1.2 Problem Formulation and Motivation

It has been shown that the DCF access method does not make efficient use of the shared channel due to its inherent conservative approach in assessing the level of interference. For example, when a station senses a busy medium (either through the PCS or VCS functions of the IEEE 802.11), it simply blocks its own transmission [5] to yield for other ongoing communication. However, if the transmission of this station does not cause enough interference to corrupt the frame reception of the ongoing transmission, then blocking that transmission would be unnecessary. This problem has been referred to in the literature as the *exposed terminal problem* as

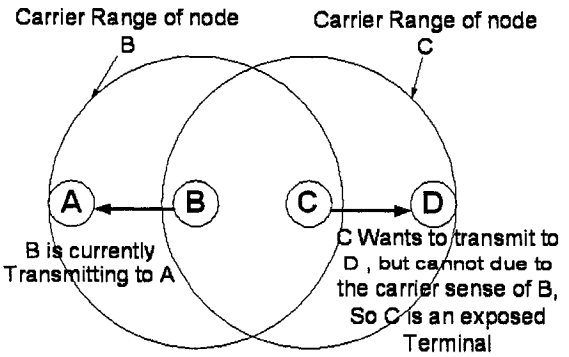

Figure 1.1: Exposed Terminal Problem

shown in Figure 1.1 and has been shown to severely affect the ***spatial reuse*** of the spectral resource and thus limit the network capacity. Here, spatial reuse is considered one of the most dominant performance issue related to wireless ad hoc networks. Being an important metric which value the performance of MAC protocol under investigation, spatial reuse determines the number of simultaneous communications allowed in a given region. Now, after a node senses an idle medium, a node can initiate a transmission; the signal to interference plus noise ratio (SINR) perceived at the receiver determines whether this transmission is successful or not. Namely, if the SINR is smaller than a minimum threshold (ζ), the transmission cannot be correctly decoded. However, the interference contributed by concurrent transmissions outside the carrier sense range of the sender may corrupt the ongoing communication. Those potential interfering nodes that are outside the carrier sense range of the sender are commonly known as the *hidden terminals*, as shown in Figure 1.2. Thus, the optimal spatial reuse and hence optimal performance can be achieved through a balance between the exposed and hidden terminals.

Although the IEEE 802.11 DCF has many drawbacks, nevertheless the request for a standard change faces both technical difficulties and market resistance (millions of commercial products in the market are deploying the DCF at this time). To date, various mechanisms have been proposed to improve the capacity of IEEE 802.11-based multi-hop wireless networks. These mechanisms (as shown in Figure 1.3) can

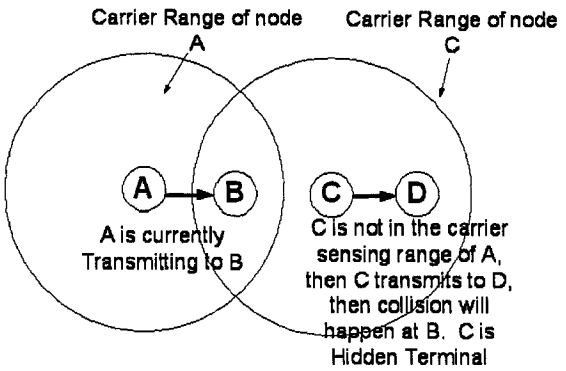

Figure 1.2: Hidden Terminal Problem

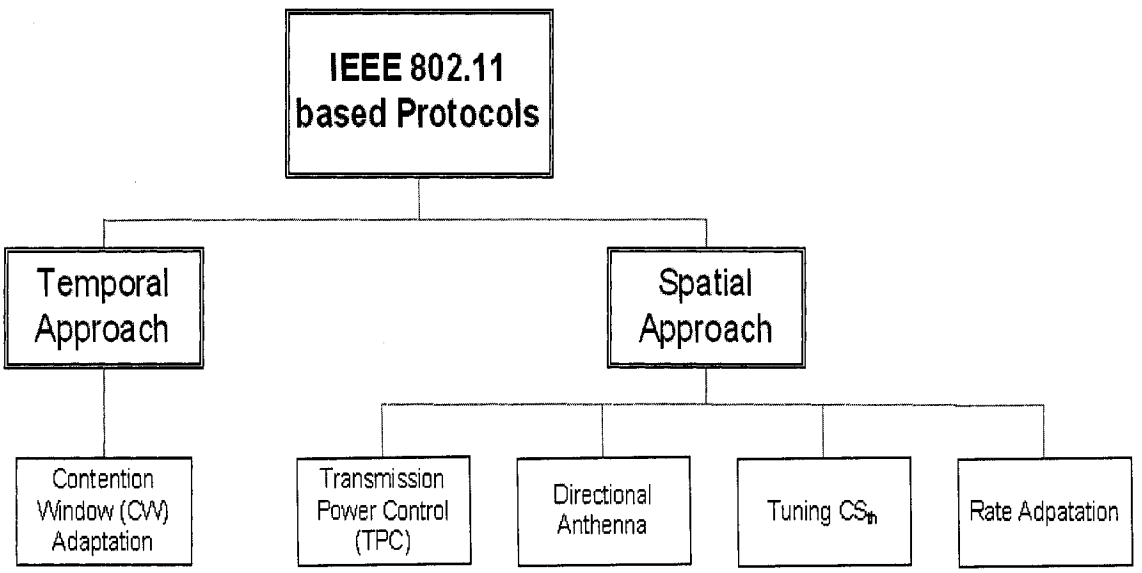

Figure 1.3: Techniques to enhance the performance of IEEE 802.11 based multihop networks

be broadly classified as temporal and spatial approaches depending on their focus of optimization on the channel bandwidth. The temporal approaches [6], [7] attempt to better utilize the channel along the time dimension by optimization or improving the binary exponential backoff algorithm (BEB) of the DCF protocol. Alternatively, the spatial approaches try to find more chances of spatial reuse without significantly increasing the chance of collisions. These mechanisms include the tuning of the carrier sensing threshold, the data rate adaptation, the transmission power control, and the use of directional antennas.

1.3 Thesis Objective

In this thesis, protocols and mathematical tools that target the efficient utilization of the wireless spectrum in IEEE 802.11 multihop-based Ad hoc networks are developed. Specifically, analytical models to study the effect of the interplay between transmit power control, data rate adaptation, tuning the CS_{th}, tuning the CW and the use of directional antennas. Based on the insights from these models, efficient protocols are designed.

1.4 Thesis Contributions

- The effects that transmission power control, data rate adaptation and tuning carrier sensing threshold have on network throughput are investigated and the interplay between them is studied. To accomplish this, a realistic analytical model is developed that characterizes the transmission activities governed by the IEEE 802.11 DCF in a single channel, power-aware, multihop wireless network. Conclusions drawn from the model states that selecting a smaller carrier sensing (CS) threshold (i.e, larger carrier sensing range) will severely impact the spatial reuse while a larger CS threshold will yield excessive interference among

concurrent transmissions. Accordingly, performing power control has either minor or negligible effect in both situations respectively. Furthermore, when the CS threshold is selected appropriately, power control shows its effectiveness in reducing collisions and hence improving system performance. Finally, using the model, the potential adverse impacts of RTS/CTS control packets on the network capacity is demonstrated and its performance is compared with the two-way basic access method.

- A decentralized, localized, heuristic to adjust the transmit power and rate according to the level of interference in the network is proposed. The Heuristic outlines the rules for performing power and rate assignment so that higher performance is obtained. A realistic analytical model to study the performance of the proposed heuristics is presented; analytical results show that the proposed algorithm, indeed, finds the balance between spatial reuse and transmission quality through its appropriate search for the suitable transmission parameters. Simulation experiments are conducted and performance of the proposed algorithm to other heuristics is compared; the results indicate a remarkable performance both in terms of achieved throughput and energy consumption.

- A dynamic spatiotemporal algorithm using the joint control of carrier sense threshold and contention window is presented with the objective of controlling the access to the channel in order to enhance the spatial reuse and optimize the overall network throughput. Furthermore, a policy to distinguish the causes of transmission failures is proposed. Then, based on this, the CS_{th} and CW are selectively adjusted in order to eliminate the likelihood of collisions both from hidden terminals and contending hosts while also enhancing the spatial reuse by reducing the number of exposed terminals. Specifically, a node adjusts its CS_{th} based on both its success/failure history and the information it receives from neighboring nodes through clear-to-send packets. Moreover, to reduce

the effect of exposed terminals, the RTS/CTS exchange is only employed for the purpose of informing neighboring nodes of their CS_{th} but not to silence them. Then, the scheme will adaptively performs a dynamic switch between the (request-to-send) RTS/CTS access scheme and the basic scheme based on a predefined policy in order to reduce the additional overhead caused by the RTS/CTS exchange.

- A model to calculate future interference in networks with directional antennas is presented, and based on this model, the relations that should exist between the required transmission power of RTS, CTS, DATA, ACK frames for successful data packet delivery are derived for MANETs based on directional version of IEEE 802.11 DCF. From these relations, a distributed power control scheme is proposed. Furthermore, the simulations show that the true potentials from the proposed control scheme cannot be shown due to the imperfection of the model derived. Based on these observations, another class of power control algorithm is proposed that deploys prediction filters (Kalman or extended Kalman) to estimate the interference in future. Simulation experiments for different topologies are used to verify the significant throughput and energy gains that can be obtained by the proposed power control schemes.

- The benefits of transmission power control on throughput and energy consumption in a uniformly distributed power aware ad hoc network where nodes are equipped with directional antennas is investigated. An interference model for directional antenna based on a honey grid model is constructed to calculate the maximum interference. Further, a directional collision avoidance model is derived and based on the integrated interference/collision model and Signal to Interference Requirements (SIR), the maximum end-to-end throughput under the maximum interference is calculated. Furthermore, the effect of collisions on

the energy consumption is investigated through proposing an energy consumption model that utilizes all aspects of energy wastage.

1.5 Thesis Outline

The rest of the thesis is organized as follows. Chapter 2 introduces the background and reviews the related work in this area. In Chapter 3, an accurate analytical model for wireless multihop networks is presented to study the effects of power control, tuning the carrier sensing threshold, impacts of packet size and transmission rates. The distributed localized power and transmission rate heuristics are presented in Chapter 4, whose performance improvements are verified by both analytical and simulation results. In Chapter 5, the dynamic spatiotemporal algorithm using the joint control of carrier sense threshold and contention window is presented. Chapter 6 introduces an alternative technique to enhance spatial reuse by coupling power control scheme with directional antenna. The spatial reuse study using directional antenna is further extended in Chapter 7 to investigate analytically the merits of coupling directional antenna with power control. Chapter 8 summarizes our conclusions and presents some future directions.

Chapter 2

Background and Related Work

In this chapter, the background and the literature survey for topics investigated in this thesis are presented. The rest of this chapter is as follows. Sections 2.1 and 2.2 present the IEEE 802.11 DCF and the communication model adopted in this thesis. Section 2.3 discusses existing analytical models for IEEE 802.11. Sections 2.4, 2.5, 2.6, 2.7, 2.8 survey the related literature that considers the use of spatial reuse techniques. Finally, alternative solutions that do not make use of these techniques are presented in section 2.9.

We begin our discussion with the introduction of IEEE 802.11 DCF and the model background that will adopted in the thesis. Then, the techniques (shown in Figure 1.3) used to enhance spatial reuse are discussed and categorized.

2.1 IEEE 802. 11 DCF

The IEEE 802.11 DCF relies on carrier sensing multiple access with collision avoidance (CSMA/CA). DCF employs two different channel access modes for data packet transmission; the default 2-way (basic access) and the optional four-way handshaking (RTS/CTS) access scheme [5]. Here, the optional (RTS/CTS) scheme assumes the transmission of short request-to- send (RTS) and clear-to-send (CTS) control packets

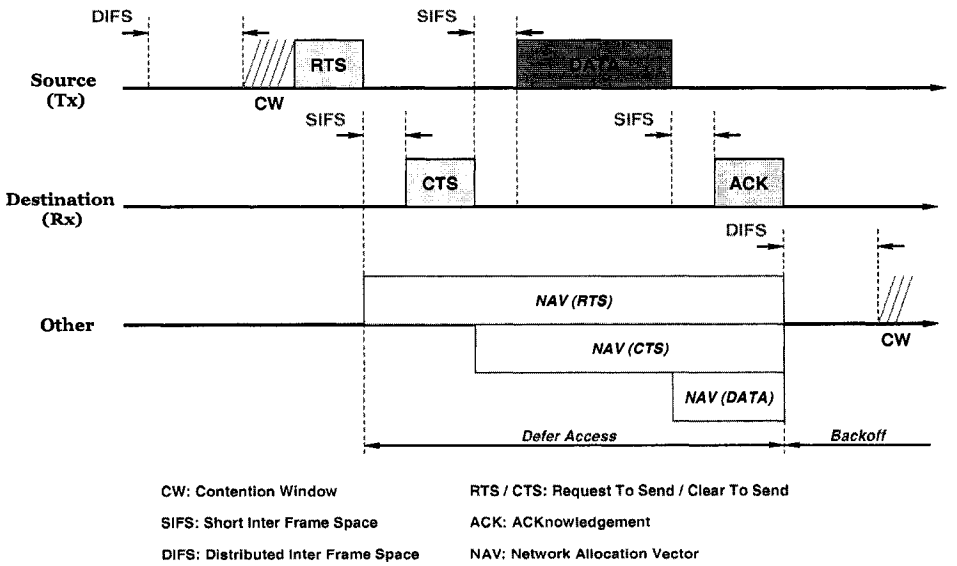

Figure 2.1: IEEE 802.11 DCF

prior to the data packet transmission. In the (RTS/CTS) access scheme, a node with packets to transmit first senses the medium through physical carrier sensing (PCS). If the medium is idle for at least a certain period DIFS (Distributed Interframe Space), it will immediately request the channel by sending a short control frame request to send (RTS) to the receiver node. If the receiver correctly receives the RTS, it will reply with a short control frame clear to send (CTS) after waiting a SIFS (Short Interframe Space) period. Once the sender receives the CTS, it will start to transfer DATA. After the successful reception of DATA, the receiver sends an ACK to the sender. SIFS duration is the shortest of the interframe spaces and is used after the RTS, CTS, and DATA frames to give the highest priority to CTS, DATA and ACK, respectively. Nodes implementing IEEE 802. 11 maintains a NAV (Network Allocation Vector) which shows the remaining time of the on-going transmission sessions. Using the duration information in the RTS, CTS, and DATA packets, nodes adjust their NAVs whenever they receive a packet. This is shown in Figure 2.1. For the basic scheme, nodes upon sensing the DATA or ACK packet will refrain from transmitting any packet for EIFS.

Moreover, if the channel is sensed busy, the station has to wait until the channel is sensed idle for a DIFS time. At this point, the station generates a random backoff time interval before transmission, in order to minimize the probability of collisions with packets being transmitted by other stations. DCF adopts an exponential back off scheme. At each packet transmission, the back off time is uniformly chosen in the range $[0, CW]$. The value CW is called contention window, and depends on the number of failed transmissions for the packet. At the first transmission attempt, CW is set to CW_{min}. After each retransmission, CW will be exponentially increased until the maximum value CW_{max}. Upon successful transmission, CW will be reset to CW_{min}.

2.2 IEEE 802.11 Ranges

Assume a sender A transmits to its receiver B and another node F (hidden node) unaware of the transmission of A, may start to transmit to its intended receiver as shown in Figure 2.2. Here, the two signals from A and F may overlap in time at the receiver B. Whether the signal from sender A can be correctly decoded depends on the so-called capture effect, i.e., the stronger signal will capture the receiver modem, while the weaker signal will be rejected as noise.

While in the literature there exist various models that characterize the capture effect [8], [9], in this chapter, the most widely adopted model is used. The receiver B can correctly decode the signal if the signal to interference plus noise ratio (SINR) exceeds a certain predetermined threshold denoted by ζ. This results in the following constraint:

$$P_r \geq \zeta \times (P_n) \tag{2.1}$$

where P_n is the total allowed interference power which consists of interference power

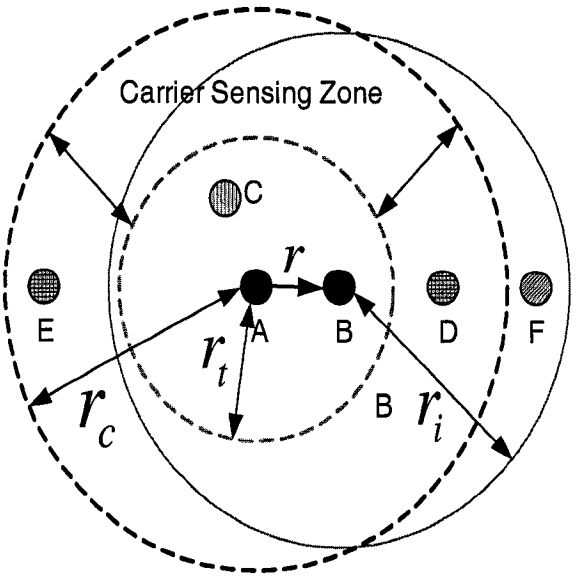

Figure 2.2: Different Ranges according to IEEE 802.11

from interfering nodes and background thermal noise. Here, the value of ζ is determined according to the rate at which a packet is received at the receiver.

Moreover, due to the pathloss constraints, the receiver B is able to receive and correctly decode a packet when the received power (P_r) of a frame from a transmitter (with a transmission power P_t) is higher than or equal κ (the receiver sensitivity). Accordingly, and adopting the two-ray model with antenna heights and gains equal to one, the transmission range (r_t) is:

$$r_t = (\frac{P_t}{\kappa})^{\frac{1}{4}} \tag{2.2}$$

where κ is dependent on the rate the packet is received at the receiver; note that the higher the rate, the smaller κ is [5].

Furthermore, a transmitter cannot initiate any communication if it senses a signal with a power level larger than a predefined CS_{th}. Hence, the CS_{th} specifies the signal strength above which a node determines that the medium is busy and will not attempt for transmission. Let the Carrier Sense set of a transmitter A (denoted as CS_A) be defined as the set of nodes, if any of them transmits, node A will sense the medium

busy [10]. Formally,

$$CS_A = \{A' \mid \frac{P_{A'}}{d^4} \geq CS_{th}\}$$

where d is the distance between the sender A and node A'(in the carrier sense set) and $P_{A'}$ is the transmission power of A'. If all nodes use the same transmission power, P_t, then the carrier sense range r_c, defined as the maximum value of d such that the above constraints hold, can be expressed as:

$$r_c = (\frac{P_t}{CS_{th}})^{\frac{1}{4}} \tag{2.3}$$

Note that, however, if nodes use different power, the carrier sense region (CS_A) will have an arbitrary shape (not circular). Another acronym of interest is the silence area that results from the transmission of node A. The silence set of a transmitter A (denoted as SL_A), assuming fixed CS_{th} for all nodes, is the set of nodes that will detect the channel to be busy if A transmits [10]. Formally:

$$SL_A = \{A' \mid \frac{P_A}{d^4} \geq CS_{th}\}$$

Clearly, $SL_A \equiv CS_A$ if all nodes use the same transmission power.

Next, the interference range [11] is explained. Consider an ongoing communication between nodes A and B that are r distant apart. If node A transmits with power P_t, node B receives this signal with a power $P_r = \frac{P_t}{r^4}$. Moreover, if the thermal noise is neglected, P_n in equation 2.1 can be expressed as $P_n = P_{cn} + P_{tn}$. Here, P_{cn} is the current measured interference at node B and P_{tn} is the maximum remaining interference that node B can tolerate while it is still able to decode correctly the packet that it receives from node A. Accordingly, and making use of equation 2.1,

P_{tn} can be expressed as follows:

$$P_{tn} \leq \frac{P_t}{r^4 \cdot \zeta} - P_{cn} \tag{2.4}$$

Now assume that an interfering node F which is d meters away from node B initiates a communication with a power P_i while node B is receiving a packet from node A. The received power $P_{ri} = \frac{P_i}{d^4}$ at node B from node F should satisfy the condition that $P_{ri} \leq P_{tn}$ such that node B is still able to receive and correctly decode the packet from node A. Accordingly, the interference set of a receiver B (denoted as IN_B) is defined as the set of nodes whose transmission, if overlapping with the transmission of a sender, will cause collision at the receiver. Specifically, if node F transmits,

$$IN_B = \{F \mid \frac{P_i}{d^4} \geq \frac{P_t}{r^4 \cdot \zeta} - P_{cn}\} \tag{2.5}$$

With the condition of the interference set from equation 2.5, the interference range r_i is defined as the maximum value of d such that the inequality in equation 2.5 holds:

$$r_i = \left(\frac{P_i}{\frac{P_t}{r^4 \cdot \zeta} - P_{cn}} \right)^{\frac{1}{4}} \tag{2.6}$$

Based on the above equation, both ζ (whose value depends on physical transmission rate) and the power value (P_t) of an ensued packet can be seen to determine the interference range at the receiver.

2.3 IEEE 802.11 Models

Many of the analytical performance modeling of wireless MAC protocols that focused on the single hop wireless networks have originated from the analytical principles proposed for the analysis of ALOHA protocol [12] and carrier sense multiple access

(CSMA) protocol [13]. One of the approaches to model the IEEE 802.11 was presented in [14]. Their model does not capture accurately the true number of hidden nodes, moreover the exponential backoff principle is not modeled.

Bianchi [15] was among the first who modeled the IEEE 802.11 DCF in WLAN environment. He studied the behavior of a single station with a Markov model, and accordingly obtained the stationary probability that the station transmits a packet in a generic (i.e., randomly chosen) slot time. He later proved that the operation of the RTS/CTS scheme can lead to a significant performance enhancement, in comparison with the basic scheme, for the case of saturated network or very long data frame. Cali et al. [16] derived analytic models that characterize the system capacity under the p-persistent version of IEEE 802.11. Here, the capacity is defined as the maximum fraction of channel bandwidth used for successful packet transmission.

The authors in [11] show that the RTS/CTS handshake for data rate of 2Mbps is not effective when the transmitter-receiver distance is larger than 0.56 times the transmission range.

The authors in [17] analyzed saturation throughput of collision avoidance protocols in multihop ad hoc networks. The impact of the hidden terminals were analyzed only when transmitting an RTS or CTS packets, whereas the hidden terminals that may interrupt the receiving of the DATA/ACK packets were not included. Moreover, the physical carrier sensing aspect together with the exponential backoff scheme were also not captured. In [18], the authors calculated the throughput by including all hidden terminals that may impact the reception of all the control and data packets by considering the physical carrier sensing attribute, moreover, their model captures the exponential backoff.

2.4 Transmit Power Control

Transmit power control (TPC) is extremely important in wireless networks due to three major reasons:

- the transmission power determines the transmission range according to Equation 2.2, which in turn can affect the connectivity and network topology. The network topology, in turn, has considerable impact on the throughput performance of the network.

- mobile nodes in ad hoc networks are usually energy constrained, hence they have to be as energy efficient as possible. Power control is essential in reducing the energy consumption while meeting the required SINR value at the receiver.

- transmitting at high power can degrade other ongoing transmissions and can unnecessarily silence future transmissions. Reducing the transmission power can reduce the interference on neighboring on-going transmissions and may enhance the overall network throughput, thereby allowing more concurrent transmissions.

Although the idea of power control is simple, achieving this in an IEE802.11-based multihop network is challenging. When reducing the transmission power, the number of nodes included within the transmission range of the sender competing for wireless channel access is reduced and hence the number of collisions from contending nodes is reduced. Moreover, it is intuitive that using reduced power may minimize the interference level among neighboring nodes. However, since there is an increase in the number of concurrent transmissions due to the fact that less nodes are silenced, the aggregate interference level in the network may increase. Consequently, the overall SINR might degrade and this may lead to an increase in frame loss rate. Further, lower SINR forces the sender to transmit at lower PHY rates (more robust modulation) to overcome the higher level of interference at the receiver. On the other hand,

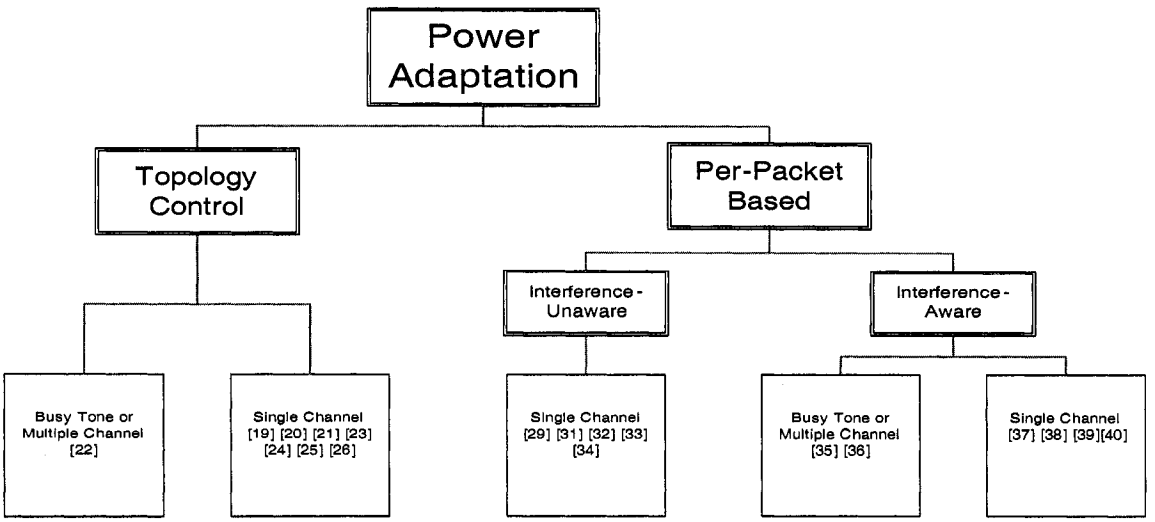

Figure 2.3: Categorization of power control schemes

reducing the transmit power may indeed decrease the energy consumption for one transmission attempt; however, the likelihood of packet corruptions (error or collisions) during packet reception becomes high, and hence retransmissions of the same packet could yield to higher power consumption.

We classify power control schemes into two classes; namely topology-based and per-packet based as shown in Figure 2.3 and they are surveyed in the following subsections.

2.4.1 Topology Control

A topology control protocol *COMPOW*, that requires that all the nodes use a common minimum transmission power, was developed in [19]. The authors showed that spatial reuse can be enhanced and energy is conserved if nodes agree on the minimum common power that maintains the network connectivity. In *COMPOW*, each node tries to find the best minimum power by locating the route entry that maximizes the throughput among other entries. This is accomplished by running several routing daemons in parallel, one for each power level. However, COMPOW suffers from

overhead problems due to link-state messages exchanged by nodes. Moreover, COMPOW is inefficient in cluster topologies since it tends to use higher power. Finally, COMPOW is highly affected by mobility; if a node moves away, redetermination of the common power is triggered, and thus global reconfiguration is required.

A cone-based topology control scheme was proposed in [20]. Here, each node determines the minimum power that preserves its connectivity with at least one neighbor existing in every cone of degree ϕ. In order to find its neighbors, a node broadcasts a Hello message at the lowest power and gradually increases its power. Thereafter, a node stores the direction in which replies are received for every Hello packet transmitted at a certain power level. Based on the saved directions, a node is able to determine whether its neighbor lies in a cone of degree ϕ. The algorithm has been analytically proven to maintain network connectivity for $\phi = \frac{5 \cdot \pi}{3}$.

A distributed position-based topology control algorithm is proposed in [21]. Through this algorithm, each node (e.g., node i) periodically broadcasts its position information and builds a sparse graph named enclosure graph with the position information contained in the broadcasting packets from its neighbors. Then node i assigns a cost metric respectively for each neighbor node j included in the enclosure graph. Here, the cost metric is defined as the minimum required power to establish a link between node i and j, and this is also broadcasted by node i. Afterwards, all nodes are able to select an optimal link on the enclosure graph using the distributed Bell Ford shortest path algorithm.

A power controlled dual channel ($PCDC$) MAC that constructs the network topology by considering the interplay between the MAC and network layers was proposed in [22]. $PCDC$ employs two separate channels one for control packets (RTS/CTS/ACK) and the other for data packets. In order to allow for future concurrent transmissions without corrupting the ongoing transmission, a receiver-dependent interference margin is defined and accordingly the data packet is transmitted at a

power level that accounts for this interference margin. This margin is broadcasted through the CTS packet. With this information, each node calculates the optimal required power to each of its directed neighbors and accordingly construct the network topology (i.e., select the optimal next hop destination).

The authors of [23], [24], [25] and [26] also studied the problem of topology maintenance, where the objective is to preserve network connectivity, reduce power consumption, and mitigate MAC-level interference and thus increase the spatial reuse. Comprehensive surveys for topology control schemes are presented in [27], [28].

2.4.2 Per-Packet based

Interference-Unaware

A simple power control MAC protocol that allows nodes to vary transmission power on a per packet basis is presented in [29]; the main idea is to allow nodes to use different power levels for RTS/CTS and DATA/ACK frames. More specifically, a maximum transmission power is used for sending the RTS/CTS frames and a lower power level, necessary to communicate, is used for DATA/ACK packets. This protocol is referred to as the *BASIC* protocol and the authors of [29] have pointed out its deficiencies. *BASIC* was proposed to enhance the energy efficiency; it however suffers severely from high collision rate from hidden terminals due to asymmetrical link problems. This, in turn, increases the energy consumption and deteriorates the throughput.

To elaborate more on the asymmetrical link problem, consider two nodes A and B, which are a distance r away from each other, exchanging their RTS and CTS frames at the maximum power (Figure 2.4); nodes E and F back off for EIFS since they lie in the silence range of RTS and CTS frames. Now, nodes A and B exchange their DATA and ACK packets at the minimum transmission power. Hence, nodes E and F are no longer inside the silence zone of both nodes. After an EIFS duration,

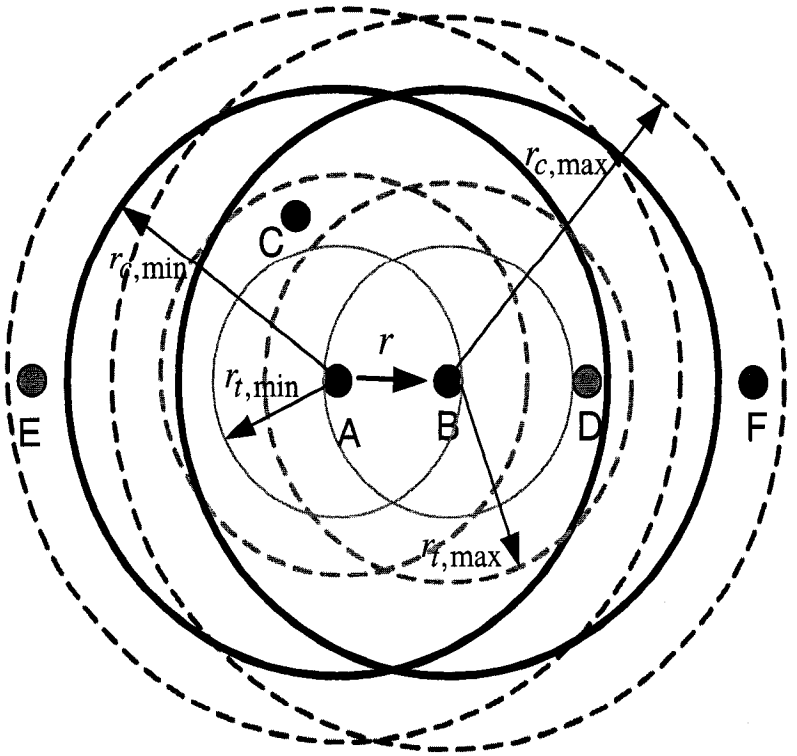

$r_{t,max}$ The Transmission range resulting from maximum powe
$r_{t,min}$ The Transmission range resulting from minimum power
$r_{c,max}$ The silence range resulting from maximum power
$r_{c,min}$ The silence range resulting from minimum power

Figure 2.4: Asymmetrical link Problem

they will contend for the channel if they have a packet to transmit. If the duration of the DATA packet (from A to B) is long, node F may corrupt the frame reception at the receiver, B. Similarly, node E may also corrupt the ACK packet reception. The authors in [30] further studied analytically the performance of *BASIC* scheme by proposing a model to analyze the maximum throughput and the consumed energy under maximum interference achieved by the BASIC scheme. They adopted the honey grid model for accumulative interference measurement. The proposed model showed the deficiencies of *BASIC*.

In order to address this problem, the authors in [29] proposed to transmit the DATA packet periodically at maximum power. Here, the transmitter every 190 μs

raises the DATA power level to its maximum for a period of 15 μs so that potential interfering nodes will now be able to detect the transmission and accordingly defer their future transmissions and prevent collisions with the current transmission. The receiver, then, transmits an ACK frame using the minimum required power to reach the source node, similar to the BASIC scheme. The calculation of the periodic time for increasing the power is dependent on the duration of $EIFS$. Here, $EIFS = SIFS + DIFS + [(8 * ACKsize) + PreambleLength + PLCPHeader - Length]/BitRate$, where $ACKsize$ is the length (in bytes) of an ACK frame, and $BitRate$ is the physical layer's lowest mandatory rate. The $PreambleLength$ is 144 bits and $PLCPHeaderLength$ is 48 bits. Using a 2 Mbps channel bit rate, EIFS is equal to 212 μs. Here, the 15 μs should be adequate for carrier sensing, 5 μs to up and down the power level. So the time will be 210 μs which is less than the 212 μs. In this way, the ACK packet is well protected and the energy is assumed to be conserved. However, the spatial reuse is not improved since the RTS and CTS packets, which are sent at maximum power, may still unnecessarily silence future concurrent transmissions. A similar approach to that of [29] which relies on periodical increase of transmission power to silence hidden nodes was also proposed in [31].

It was suggested in [32], as another enhancement to the BASIC scheme, that a node should be aware of the success and failure of its own transmissions. To achieve this, a node maintains a table that keeps a record of all the previous RTS-CTS-DATA-ACK transmission power levels used to communicate with each of its neighbors. Given this information, a transmitter would be able to adjust adaptively the transmission power of its future communication according to a predefined policy. Here, the policy dictates that each transmitter increases/decreases its transmission power to its receiver if the last transmission to the same receiver fails/succeeds. As opposed to the BASIC scheme, a node uses the reduced power level for all its transmissions (i.e., RTS-CTS-DATA-ACK). This algorithm yields higher throughput because

of the enhanced spatial reuse and lower energy consumption compared with the IEEE 802.11 MAC protocol. Here, the channel reuse is enhanced since the RTS/CTS packets are exchanged at a reduced power level, allowing for simultaneous transmissions to exist. Nevertheless, this mechanism still suffers from hidden terminals since it does not provide an efficient protection for DATA packet. Moreover, asymmetric link problem is not completely addressed here.

Another enhancement for BASIC was proposed in [33]. The authors argued that through knowing the received signal pattern, a node can foretell if the signal belongs to a transmitted CTS packet. Upon recognizing the CTS packet, the node accordingly sets its NAV so as not to interfere with the upcoming DATA packet reception. A solution has been proposed in [34] to overcome the asymmetric link problem of the BASIC scheme by allowing nodes in the carrier sensing zone of an RTS/CTS transmission to acknowledge the transmission duration information of the up-coming DATA packet. Although these nodes are not able to correctly decode the RTS/CTS packet, they can still detect, the time duration when the physical carrier is sensed or not. The physical duration of the RTS/CTS frames is increased by simply adding a few bits to them. Thus, the ALCA protocol provides a discrete set of N different Carrier Durations (CD) for RTS/CTS frames, and each CD is mapped to different durations for the DATA packet transmission duration. A node in the carrier sensing zone of RTS/CTS transmission senses the physical carrier of RTS/CTS duration and can extract the CD for the RTS/CTS frame. Correspondingly, it can acknowledge the transmission duration for the DATA packet, and set its NAV to this value, instead of setting the NAV to the standard EIFS value.

Interference-Aware

A power controlled multiple access protocol (*PCMA*) has been proposed in [35]; in *PCMA*, the receiver advertises its tolerable interference margin on an out-of-band

channel and the transmitter selects the transmission power that does not disrupt any ongoing transmissions. To elaborate more, each receiver transmits busy-tone pulses over separate channel to inform its interference margin to its neighbors (potential interferers). A potential interfering node, upon receiving the pulse, determines its signal strength and accordingly takes a decision to bound its future transmission or not. Specifically, a potential interfering node first senses the busy-tone channel to calculate an upper bound on its transmission power on all of its control and data packets complying to the most sensitive receiver in its transmission zone. This potential interfering node, upon determining this upper bound value, will transmit an RTS packet and waits for the CTS from the receiver. If the receiver is able to correctly decode the RTS packet (i.e., it lies within the RTS range of the transmitter node) and the power needed to send back the CTS packet is below the power bound at the receiver, the receiver then transmits back a CTS allowing the DATA packet transmission to begin. Implementation of PCMA shows significant throughput gain (more than twice) over the IEEEE 802.11. Nevertheless, the collision resulting from contention among busy-tones is not addressed.

Performing TPC with the use of a separate control channel for (RTS, CTS, ACK) in conjunction with a busy-tone scheme was proposed in [36]. A transmitter sends the DATA packets and busy-tones at reduced power, while the receiver transmits its busy-tones at the maximum power. Upon receiving the busy-tone, a potential interfering node estimates the channel gain and decides to transmit if the interference value from its future transmission does not add more than a fixed interference on the ongoing reception. The protocol is shown to achieve considerable throughput enhancements. Nevertheless, the assumptions made in the design of the protocol are not realistic. Specifically, that the antenna system neglects the interfering power of a signal that is less than the power of the "desired" signal (i.e., they assume perfect capture) and that there is no requirement for any interference margin. Moreover,

when addressing the energy consumption, the power utilized in transmitting busy tones is not considered. The collision from contention among busy-tones is also not addressed as well. Although these algorithms claim to achieve good throughput and less energy consumption, the implementation of dual or multi-channels in the framework of IEEE802.11 faces both technical difficulties and market resistance as such algorithms would require a complete change of the standards.

The authors in [37] extended the work of in *PCMA* [35] to a single channel power controlled MAC protocol named *POWMAC*. Instead of delivering the interference margin information on a second channel, *POWMAC* exchanges the interference information and DATA packet using only one channel. To achieve this, POWMAC employs an access window (AW) to allow for a series of RTS/CTS exchanges to take place before several concurrent DATA packet transmissions can commence. Thus, during the AW, each node is aware of the interference margin of its neighboring nodes and accordingly bounds its transmission power as in *PCMA* such that DATA transmissions can proceed simultaneously as long as collisions are prevented.

In [38], the authors investigated the correlations that exist between the required transmission power of RTS, CTS, DATA and ACK frames to guarantee a successful 4-way handshake. Based on these correlations, they proposed *Core-PC*(a class of correlative power control schemes). The scheme argues that all the packets should be transmitted at the same power value to achieve the best throughput performance. In their scheme, they considered the accumulated interference from all interfering nodes. Moreover, they protected the CTS or the ACK packet from collisions by forcing the transmission range of the RTS or DATA packet to be equal to the interference range of the CTS or ACK packet. Moreover, they proposed localized heuristics to determine the average power of the accumulative interference.

The authors of [39] introduced the a collision avoidance power control (*CAPC*)

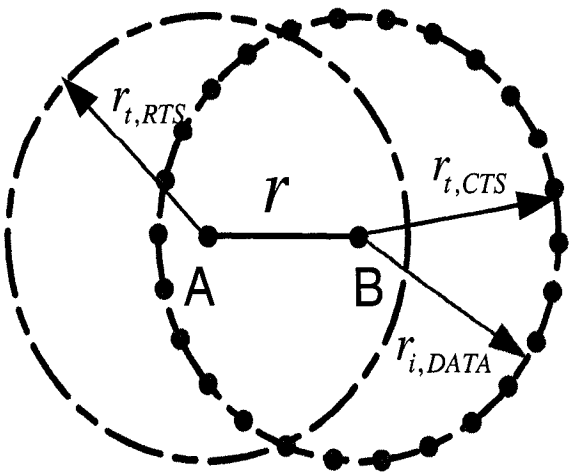

Figure 2.5: transmission range of CTS protect DATA

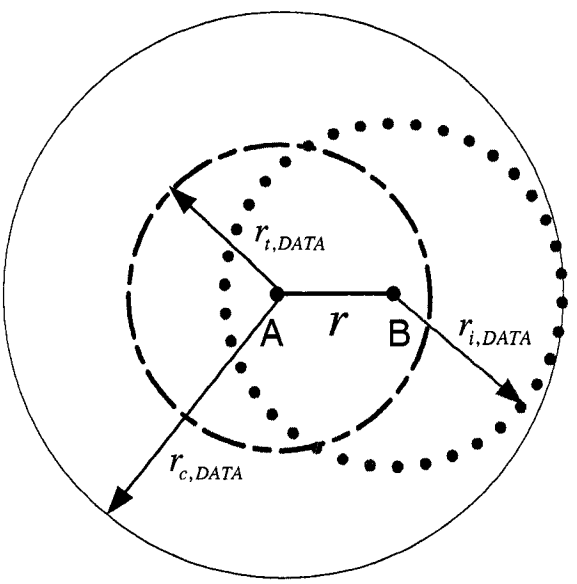

Figure 2.6: Carrier sensing range of DATA protect DATA

MAC protocol to protect the transmission of DATA and ACK packets by appropriately selecting their power values; for example, a DATA packet may be protected if the interference range at its receiver (equation 2.6) is set equal to transmission range (equation 2.2) of the ensued CTS packet, as shown in Figure 2.5. Here, the authors assumed that an interfering node always sends at maximum power to derive the interference range. Similar to *BASIC*, RTS and CTS frames are sent at maximum power and that may impact the spatial reuse in the network.

More recently, the authors of [40] extended the work in [39] and proposed an adaptive range-based power control (*ARPC*) MAC protocol for avoiding collisions and conserving energy consumption. They derived four mechanisms and studied their performances. Carrier-sensing Range Cover Mechanism (SCRC), Receivers Carrier-sensing Range Cover Mechanism (RCRC), Senders Transmission Range Cover Mechanism (STRC) and Receivers Transmission Range Cover Mechanism (RTRC)) to adapt the transmission power for a node. In SCRC, the RTS and CTS packets are transmitted at maximum power and the transmission power of DATA and ACK packets are calculated such that the carrier sensing range of DATA packet covers the entire interference range of DATA packet,as shown in Figure 2.6. In RCRC, the RTS packet is also transmitted at maximum power and the DATA packet is transmitted at minimum power while the transmission power of the CTS frame is determined such that the carrier sensing range of the CTS equals the interference range of the DATA packet given that the size of DATA packet is small. Moreover, in RCRC, the ACK packet is transmitted at a maximum power. In the other two mechanisms, STRC and RTRC, RTS and CTS packets are transmitted at maximum power while DATA or ACK packet is transmitted at adapted power such that the interference range of DATA packet is protected by the transmission range of RTS or CTS packets (as shown in Figure 2.5) respectively. The authors further derived an adaptive algorithm that selects between the proposed mechanisms based on the distance between

the sender and the receiver. The performance evaluation has shown that the proposed scheme has completely eliminated the hidden terminal problem and thus the DATA collision rate becomes negligible. Additionally, in the proposed mechanisms, the interference range is always calculated under the worst case scenario, in which the potential interfering node is considered to transmit at maximum power which does not reflect the real channel condition. However in their methods, the RTS (and most of the time CTS) frame is always transmitted at maximum power, which, as mentioned earlier, affects the channel spatial reuse.

2.5 Tuning Carrier Sensing threshold

Recently, tuning the physical carrier sensing threshold (CS_{th}) has been proposed as an efficient mechanism to enhance the network throughput in an IEEE 802.11-based multihop ad hoc networks. The physical carrier sensing method reduces the likelihood of collision by preventing nodes in the vicinity of each other from transmitting simultaneously, while allowing nodes that are separated by a safe margin (carrier sensing range) to engage in concurrent transmission.

The authors of [41] were the first to introduce the concept of tuning the CS_{th} for throughput enhancement. By setting the physical silence range, r_c, such that it covers the interference range (i.e., $r_c = r_i + d$), the interference impact from hidden terminals is eliminated. Accordingly, they derived the optimal CS_{th} for several grid topologies to achieve maximum network throughput (via enhancing the spatial reuse) given a predetermined transmission rate and Signal to Interference plus Noise Ratio (SINR); the authors in their work did not however consider the MAC overhead.

The *ECHOS* architecture [42] improved the network capacity in hotspot wireless networks through dynamically tuning the CS_{th} to allow more flows to co-exist. Here, hot spot deployment operate in infrastructure where an Access Point (AP) services connectivity to multiple clients. *ECHOS* adjusts CS_{th} based on interference measured

at both AP and client side. The clients report the measured interference to their APs. Then each AP estimates the maximum tolerable future interference for the clients and set its CS_{th} to avoid hidden terminals.

On the contrary, the authors of [43], [44], [45] studied analytically the effect of CS_{th} on the performance of ad hoc networks and showed through theoretical analysis, and verified later via simulations, that the optimum CS_{th} that maximizes the throughput allows hidden terminals to exist.

The authors of [46] further explored the interactions between MAC and PHY layers and studied the impact of MAC overhead on the choice of optimal carrier sense range and the aggregate throughput. They concluded that the optimal CS_{th} depends on the degree of channel contention, packet size and MAC-overhead.

Besides numerical analysis, an experimental testbed in [47] has been developed to investigate the effectiveness of carrier sensing in a practical system for improving network throughput. The authors argued that in order to get the true potentials from tuning the carrier sense threshold, the carrier sense algorithm in design should employ the capture effect, i.e., it should make transmission deferral decisions based on the bit rates being used and the received signal strength ratios observed at all of the nearby receivers. To elaborate more on this, consider two senders, A and B, both are within transmission range of each other. The intended recipients of their transmissions, nodes A' and B' respectively, are each within range of only one transmitter. If A' can capture the transmission of B, carrier sense should be used to defer node B to prevent it from interfering with A's transmission. On the other hand, if A' can sustain a parallel transmission from B without significantly affecting A delivery rate, carrier sense should be suppressed to make efficient use of the available transmission opportunities (spatial reuse).

Based on the insights from the analytical model and testbed experiment, the authors of [48], [49] and [50] proposed heuristic algorithms for tuning the CS_{th} based

on the network performance. Here, a transmitter periodically measures the SINR as in [49] or FER (frame error rate) as in [48] and [50]. Then, the node compares the measured value with pre-defined thresholds (simulation parameters) and accordingly decides whether it should increase or decrease its CS_{th}. These proposed schemes do not completely avoid collisions from hidden terminals. This is due to the fact that a node adjusts its CS_{th} only in order to improve its own performance, without considering whether such an adjustment may adversely impact the transmission of neighboring nodes.

The authors of [51] found that carrier sense can unnecessarily suppress an 802.11 receiver from responding to RTS messages. They observed that a successful reception of a RTS message is a good indication that subsequent transmissions from the RTS sender can overcome the current noise levels observed at the receiver, even when the noise level is within carrier sensing range. To increase efficiency, they propose 802.11 receivers use a different threshold for carrier sense prior to transmitting a CTS message.

In [52], the transmitter collects the RTS/CTS success ratio and the signal strength, and builds a mapping table between the two. This mapping table is updated after every access request. Before each transmit attempt, the sender looks up the mapping table with the current sensed signal strength to obtain the estimated success ratio. If the obtained success ratio is higher than certain threshold, the transmitter starts transmission. Otherwise, it blocks itself until it decides the channel is clear.

In [53], the authors first through an analytical study claimed that the CS_{th} which allows certain number of hidden terminals to exist can enhance the network capacity. Moreover, they proposed that the number of contending nodes (n_c) is determined by CS_{th} and they derived an optimal value of n_c that can maximize the throughput. They also presented an algorithm that adjusts n_c through tuning CS_{th}. In this algorithm, a node first estimates n_c from the measured information, such as the time

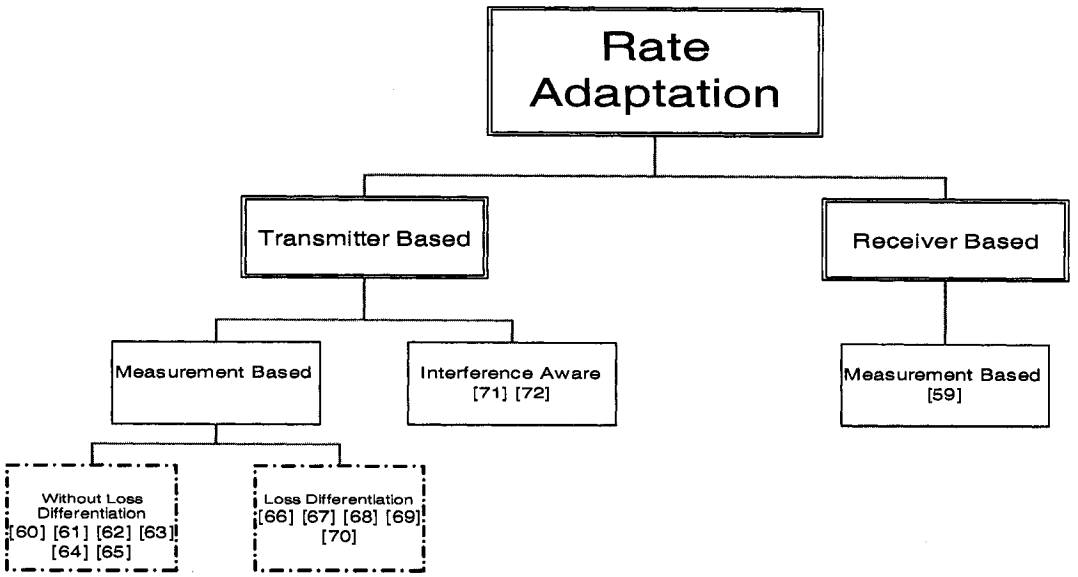

Figure 2.7: Categorization of rate adaptation schemes

that the node senses the channel as idle, busy and captured for receiving, then the node adjusts its CS_{th} in order to achieve an optimal n_c.

2.6 Rate Adaptation

The IEEE 802.11 wireless networks support a wide range of transmission rates between 1 and 54Mbps by employing different sets of modulation and channel coding schemes. For example, the IEEE 802.11a supports 8 PHY channel rates ranging from 6 Mb/s to 54 Mb/s based on different modulation schemes and coding rates and the IEEE 802.11b supports 4 PHY channel rates ranging from 1 Mb/s to 11 Mb/s.

To utilize the multiple rate capacity of IEEE 802.11, various DATA rate adaptation schemes have been proposed for throughput enhancement. The basic idea for rate adaptation is to select appropriate transmission rates according to the channel condition. More specifically, one should exploit good channel conditions by using higher rates for improved efficiency (i.e, throughput), and improve the transmission reliability by lowering the rate in the presence of channel impairments.

In [54], [55], [56], [57], [58] analytical models were presented to investigate the goodput under the rate adaptation for 802.11a-based WLANs. The authors in [58] further investigated the RTS/CTS mechanism in the absence of hidden terminals and showed that the collision time reduction is practically vanished whenever the control rate is lower than that of the data rate and concluded that the concept of deploying RTS/CTS for network improvement is questionable. Furthermore, the authors in [56] showed that RTS/CTS mechanism is effective against hidden node interference only for low transmission rates. When high rates are used, both schemes achieve similar performance. Nevertheless, they have assumed collision-free transmissions and only considered interference from nodes placed just outside the maximum CTS coverage range of the receiver. Moreover, the authors of [57] showed for multi-rate environment that as the data transmission time increases the RTS/CTS handshake becomes less and less beneficial due to the added overhead.

Rate adaptation schemes usually consist of two phases: 1) estimating or probing the channel condition and 2) rate selection based on the estimated channel condition. Moreover, DATA rate adaptation schemes fall into two categories: transmitter-based and receiver-based as shown in Figure 2.7. For the first category, the channel condition estimation and rate selection is at the sender side and vice versa. In [59], an RBAR (Receiver-Based Auto-Rate) protocol was proposed. In RBAR, the SINR measured at the receiver is used to estimate the channel conditions, and accordingly, the receiver selects the DATA rate based on this information. The selected rate is sent back to the sender through the CTS packet.

Various sender-based rate adaptation schemes that estimate the channel condition with the information measured at sender (such as transmission success/failure, or SINR) were proposed. We refer these schemes as "measurement based" schemes. An ARF (Automatic Rate Fallback) algorithm was proposed in [60]. In ARF, a node determines the status of the channel condition as good after a certain number of

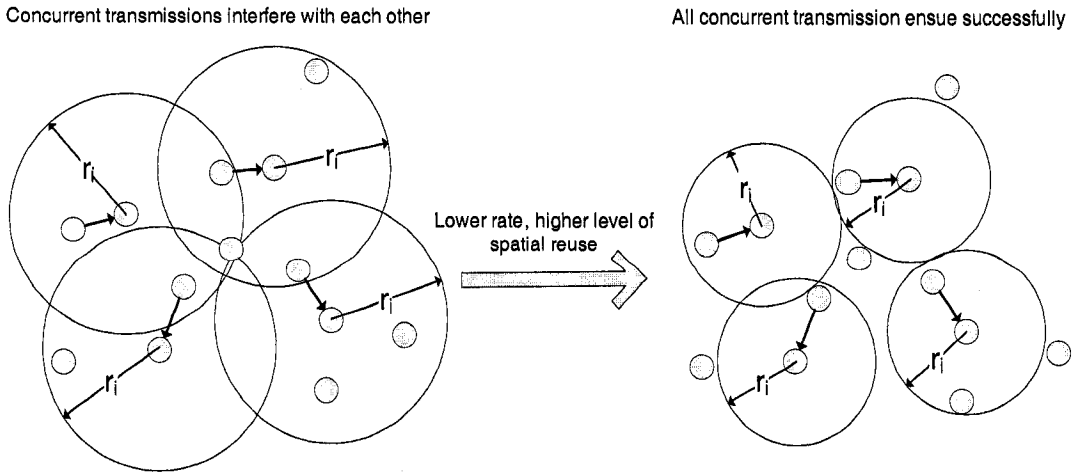

Figure 2.8: Rate adaptation enhances spatial reuse

consecutive transmission successes and accordingly increase the rate, and it decreases the rate after a frame loss. ARF is now the common standard for IEEE 802.11 rate adaptation, thanks to its simple implementation. In [61], a *SampleRate* rate selection algorithm was proposed. Here, in order to estimate the channel condition, *SampleRate* periodically transmits a DATA packet at some other rates in order to update a record of that rate's loss ratio. *SampleRate* then switches to a different rate if the throughput estimate based on the other rate's recorded loss ratio is higher than the current throughput. The MADWIFI driver in [62] provides ONOE, a rate adaptive scheme that estimates channel condition and selects transmission rate based on the frame error rate (FER) measured during certain time period.

The authors in [63] proposed a Hybrid Rate Control algorithm which adjusts transmission rate based on the combination of physical layer information (e.g. SINR) and MAC layer information (e.g. FER). Moreover, the authors in [64] proposed two algorithms for high and low latency system: Adaptive Auto Rate Fallback (AARF) and Adaptive Multi-Rate Retry (AMRR). AARF is based on ARF while AMRR is based on ONOE. Both algorithms dynamically adapt the success threshold (number of packets successfully received) for increasing the rate.

In [65], an OAR (Opportunistic Auto Rate) is proposed and works by opportunistically transmitting multiple back-to-back packets whenever the channel quality is good.

The above measurement based rate adaptive schemes treat transmission failure as an indicator of bad channel conditions. However, as pointed out in [66], transmission failures can be caused either by collisions or channel errors. Here, channel error can be due to fading, shadowing ,etc. Thus, in order to accurately estimate channel condition, those transmission failures caused by collisions should be excluded. Various rate adaptation schemes have been proposed in order to differentiate collisions with channel errors. Here, these schemes are referred to as "loss differentiation" schemes, which form a sub-category of measurement-based schemes, as shown in Figure 2.7. The basic idea of loss differentiation schemes is to avoid unnecessary rate decreasing when encountering collisions. More specifically, when facing a transmission failure, a node first identifies the causes of this transmission failure, then it only decreases the transmission rate if this transmission failure is caused by channel error. On the other hand, it fixes the transmission rate when encountering collisions.

The authors of [67] introduced a new NAK packet to differentiate packet collision and channel error. A receiver node transmits an NAK to the sender if it successfully receives the MAC header but fails in receiving the packet payload. Upon receiving the NAK, the sender acknowledges that this transmission failure is due to channel errors but not collisions and accordingly adapts the rate. Another scheme is proposed in [68], which differentiates collisions and errors based on the transmission time information for lost packets. Moreover, the authors of [66] proposed a Collision-Aware Rate Adaptation (CARA). CARA employs RTS probing to differentiate between packet collision or packet error. And to reduce RTS/CTS overhead, in CARA, the RTS/CTS exchange is switched off after certain number of consecutive packets success and switched back on after certain packets failure. A Robust Rate Adaptation Algorithm

(RRAA) is proposed in [69] which combines the selective RTS/CTS scheme from CARA with FER threshold-based scheme from ONOE.

In [70], the authors proposed a model to investigate analytically the impact of rate switching thresholds (i.e, when to switch from higher rate to lower rate and vice-versa) on the performance. Accordingly they showed that dynamic adjustment of thresholds is an effective way to enhance the throughput. Based on these observations, they proposed a rate adaptation scheme that adjusts the rate-increasing and decreasing parameters based on link-layer measurement.

The measurement based rate adaptation scheme, listed above are aimed at selecting the optimal transmission rate corresponding to varying channel conditions. Moreover, according to Equation (2.6), lowering transmission rate can reduce the size of interference range, allowing more concurrent transmissions to coexist without corrupting each other, as shown in Figure 2.8. Consequently, sender-based rate adaptation schemes that take into account either the interference range or accumulative interference has been proposed.

In [71], the authors proposed to enhance energy efficiency through rate adaptation techniques in an IEEE 802.11-based multi-hop network. Specifically, they formulated the average power consumption on a link as an optimizing problem subject to some specific traffic requirements. Further they showed that this problem tend to be NP-hard in nature, and accordingly they proposed a distributed cooperative rate adaptation (CRA) heuristic as a suboptimal solution. The authors proved that CRA converges and verified later by simulation results that implementing CRA scheme can enhance the network lifetime.

A link adaptation scheme called ILARI (Integrated link Adaptation with Rate selection and interference avoidance) was presented in [72]. Here, ILARI adopts the RTS/CTS access mechanism for the purposes of both probing the channel quality and preventing interference from the hidden terminals. Moreover, ILARI adaptively

performs a dynamic switch between the RTS/CTS access scheme and the basic scheme based on a predefined policy in order to avoid the additional overhead caused by the RTS/CTS exchange. When operating using the basic access scheme, ILARI utilizes the physical carrier sensing (PCS) to protect DATA packet reception from the interferences from hidden terminals. Based on the fact that when a hidden node lies inside the physical sensing zone of the transmitter, the reception of the DATA packet transmission is guaranteed even without the RTS/CTS access mechanism. Furthermore, given a fixed power, transmitting at a lower data rate decreases the interference range of the receiver since the required SINR for successful transmissions decreases. Accordingly, and based on the receiver's channel quality and the size of data frame, ILARI chooses lower data rates such that the physical carrier sensing range covers the interference range of the receiver so that the RTS/CTS handshake is not required.

Other rate adaptation schemes for enhancing spatial reuse were proposed in [73], [74] , and [75]. However in those schemes, besides DATA rate adaptation, other parameters such as transmission power, CS_{th} and DATA packet length are also jointly considered. We will elaborate the details in later section.

2.7 Interplay among the Tunable Parameters

Different variants of access methods have been proposed to optimize the operation of DCF by helping nodes to either select optimal contention window size or optimal transmission probabilities which may yield to a decrease in collision among contending hosts and ultimately minimizing both the collision and idle periods. The authors of [76] suggested to turn off BEB and proposed a new method to dynamically tune the contention window size . In their new access method, termed as *Idle Sense*, each host measures the average number of consecutive idle slots between transmission attempts and make sure that this number is close to an optimal number (the optimal

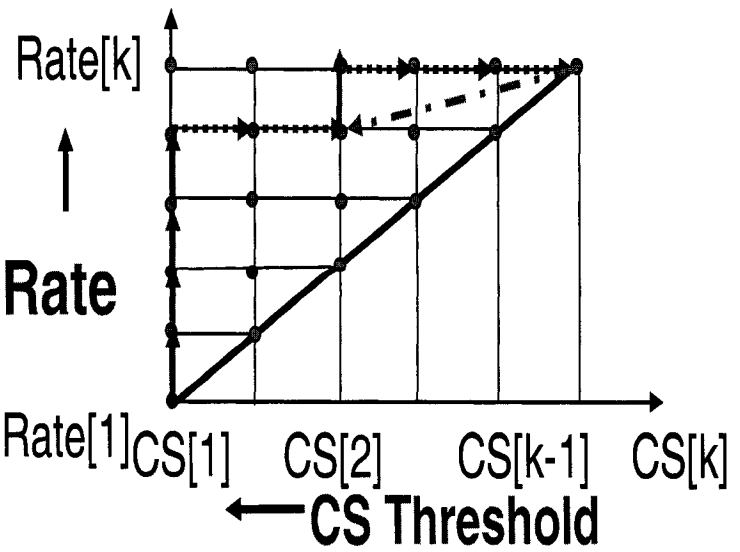

Figure 2.9: Spatial Backoff

number that maximizes the throughput is derived from analytical study) by either increasing or reducing the contention window size in an additive increase, multiplicative decrease (AIMD) manner. Furthermore, they also studied the impact of rate adaptation and noted that a node should switch to a lower transmission rate only if the throughput obtained at the lower rate is at least equal to that obtained at higher rate. Accordingly, a frame error rate threshold exists, above which it is beneficial to switch the transmission rate. For example, for IEEE 802.11b, one needs to switch from 11Mbps to 5.5Mbps when the frame error rate exceeds 50 %.

An RAF (Rate Adaptive Framing) scheme was proposed in [75]. In RAF a receiver node predicts the channel condition and accordingly jointly calculates the optimal DATA transmission rate and frame size in order to fully utilize the channel bandwidth while avoiding interference from neighboring nodes. Here, the channel condition prediction is based on the number of idle (busy) time slots during which the channel is sensed as idle (busy).

In [77], the authors proposed an energy efficient scheme (MiSer) by jointly controlling both transmit power and PHY transmission rate. They compute offline an

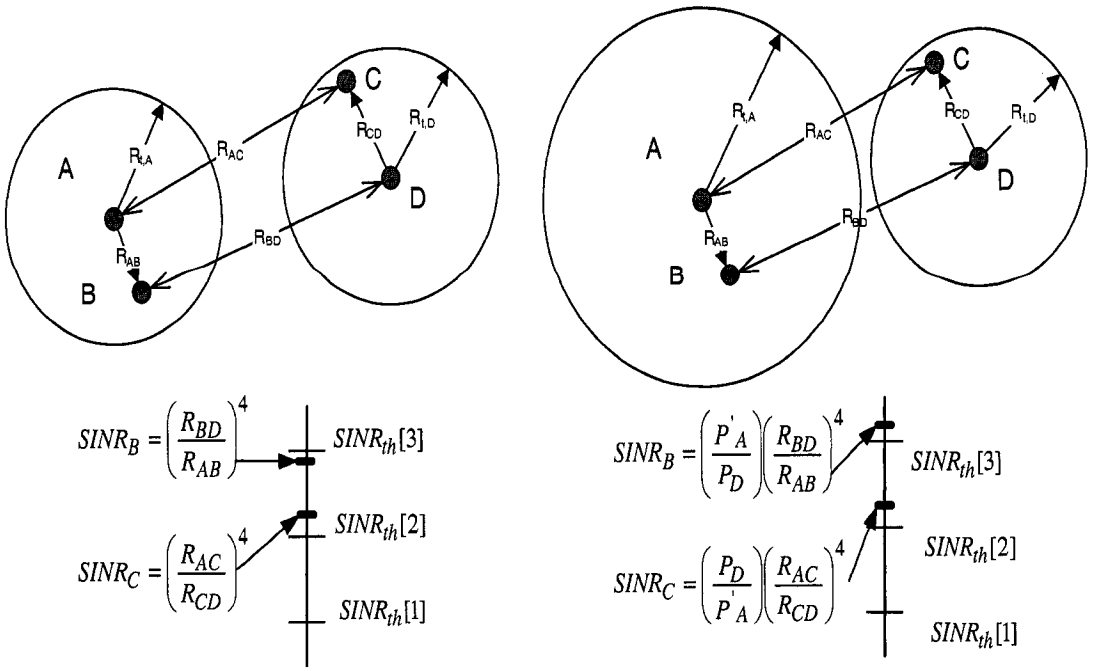

Figure 2.10: Illustrative example to show when power control is more beneficial than tuning CS_{th}

optimal rate-power combination table, and then at runtime, a wireless station determines the most energy efficient transmission strategy for each data frame.

The authors observed in [74] that the space occupied by each transmission can be adjusted by tuning some protocol parameters (e.g., CS_{th} and transmission rate) and accordingly they proposed the concept of spatial backoff. More specifically, in order to allow more concurrent transmission to be initialized, CS_{th} should be increased. On the other hand, in order to make sure that these transmissions can take place simultaneously without corrupting each other, one should reduce the size of the interference range through lowering the transmission rate. To conclude, a lower rate and higher CS_{th} result in smaller occupied space. Accordingly, they proposed an algorithm for improving the spatial reuse by dynamically adjusting the CS_{th} and transmission rate as shown in Figure 2.9. The Y axis represents the different transmitting rate levels, which are in an increasing order, while the X axis represents the different CS_{th} levels in a decreasing order. A node at point (CS[i], Rate[j]) means the

node is using carrier sensing threshold CS[i], and transmitting rate Rate[j]. Assuming that the interference at the transmitter equals the interference at the receiver, the authors derived a minimum CS_{th} associated with each transmission rate, represented by the diagonal in the figure. A node adjusts its transmitting rates and CS_{th} based on the network performance. More specifically, when a node faces certain number of consecutive transmission successes, it increases its transmitting rate by 1 level and CS_{th} remains the same. This action is presented by the solid arrow in Figure 2.9. When the node faces certain number of consecutive transmission failures and the CS_{th} threshold does not reach the minimum value for the current transmission rate, the node decrease the CS_{th} by 1 level, and the transmitting rate remains the same as represented by the dotted arrows in the figure. When the transmission fails and the CS_{th} has already reached the minimum value for the current rate, the node decreases the transmission rate by one level, and increases the CS_{th} to the one it used with the lower rate before, represented by the dashed arrows in the figure.

Another algorithm that jointly tunes the CS_{th} and the transmission rate was proposed in [78]. Here, all source nodes assume a fixed predefined interference range and accordingly adapt their transmission rate based on the distances from their receivers. The CS_{th} is tuned in a similar way to [48].

Moreover, the authors in [79] argued that for the CSMA protocols, the product of the transmit power and the carrier sensing threshold should be kept constant. That is, the lower the transmit power, the higher the carrier sensing threshold and hence the smaller the carrier sensing range and vice versa. Further, the authors proposed a heuristic algorithm to improve spatial reuse by incorporating this proposition.

Similarly, the authors of [73] studied the impact of spatial reuse on network capacity and derived the network capacity as a function of both transmission power and CS_{th}. They showed that in the case where discrete data rates are available, tuning the transmission power offers several advantages that tuning CS_{th} cannot, provided

there is a sufficient number of power levels available. The merits from power control is elaborated in the following example shown in Figure 2.10. Here, both nodes A and D are transmitting concurrently to their intended receiver B and C. Let $r[1]$, $r[2]$ and $r[3]$ denote the available transmission rates with SINR thresholds $SINR_{th}[1]$, $SINR_{th}[2]$ and $SINR_{th}[3]$ respectively. Moreover, let P_A and P_D denote the initial transmission power for node A and D and we assume that $P_A = P_D$ and the same transmission rate $r[2]$ is adopted for both senders. With transmission power control, node A can increase its transmission power P_A up to an appropriate value, P'_A, where it sustains a higher data rate $r[3]$ with SINR threshold $SINR_{th}[3]$, while not disturbing the other concurrent transmission from D to C with data rate $r[2]$. Here, the increase in interference at node C from the increase in transmission power of node A, does not make the SINR value at node C fall below $SINR_{th}[2]$. In contrast, when tuning the carrier sensing threshold of node A to achieve the rate $r[3]$, then node A should decrease its CS_{th} such that node D is included within its carrier sense range. As a result, the two transmissions can not take place at the same time. Further more, the authors also pointed out that in the case the achievable channel rate follows the Shannon capacity, spatial reuse depends only on the ratio of transmission power and CS_{th}. This is contrary to the work of [79] where they showed that transmitters should keep the product of transmission power and CS_{th} fixed at a constant. Accordingly, they proposed a localized heuristic algorithm that adjusts the space occupied by a node through joint dynamic tuning of transmission power and rate.

Yong [10] et al. proposed an analytical model to investigate the impact of transmit power and carrier sense threshold on network throughput in the basic access mechanism; they extended both Bianchi's [15] and Kumar's [80] models to derive the single node's throughput. Through their model, the authors argued that an optimum throughput can be achieved for a specific carrier sensing threshold. Moreover, they concluded that a higher system throughput can be achieved with the use of smaller

transmit power (subject to network connectivity) and carrier sense threshold.

Yu [81] et al. investigated the interaction between the carrier sensing threshold, contention window size CW, and discrete data rates for IEEE 802. 11 DCF. To accomplish this, they adopted and extended Cali's [16] model to derive the capacity of the network as a function of the carrier sensing threshold and SINR. The theoretical analysis results verified that the throughput can be maximized at various transition points of the carrier sensing threshold. Thus, the capacity is strictly not a monotonically increasing/decreasing function of the carrier sensing threshold. Moreover, the throughput can be further enhanced by tuning the contention window size. A spatial reuse optimization mechanism is considered in [82] for multihop wireless networks where the authors considered variable transmission power and different receiver sensitivities.

More recently, the authors in [83] proposed a model to study analytically the impact of CS_{th} on the network capacity in wireless multihop networks. In their model, the effect of collisions caused by accumulative interference is considered. Additionally, they claimed that the transmission attempt probability is a function of both contention window size and CS_{th} and accordingly, they showed that in order to enhance throughput, the attempt probability should remain large, allowing some collisions to exist. To achieve high attempt probability, the size of the contention window should be fixed to smaller values while higher CS_{th} should be used.

2.8 Directional Antennas

Directional antennas offer clear advantages for improving the network capacity by increasing the potential for spatial reuse [84]. Allowing a sender to direct his transmissions in the direction of the intended receiver clearly reduces the level of contention with other nodes, thereby allowing for more simultaneous transmissions. Moreover, directional antennas can increase the signaling range without spending extra power

(as opposed to omni-directional) and accordingly, some receivers outside the omni-directional range may be reached in one hop transmission. This longer range results in a smaller number of hops on end-to-end paths, yielding an increase in connection throughput. The integration of directional antennas with transmission power control scheme can further give more benefits than anticipated [84] in terms of enhancing the spatial reuse as elaborated in Figure 2.11. Here, Figure 2.11 illustrates this very easily by comparing the four combinations assuming an angle of 10 degrees and applying the pathloss law a) no power or directional b) power control without using directional antenna c) directional antenna d) power control with directional antenna. Neglecting the side lobes of directional antenna and taking into account the ratio of the areas resulting from applying the four combinations, the merits achieved in terms of spatial reuse from integrating power control with directional antenna are shown. With power control and without the use of directional antenna, the area is reduced by a factor of 4 if the distance between the sender and the receiver is half the distance of the maximum range. With directional antenna and without power control, the same area is reduced by a factor of 6 if the beamwidth is $\frac{\pi}{18}$. Finally using directional antenna with power control, the area is reduced by a factor of 144% with the same distance and beamwidth. It can be seen that coupling directional antenna is far better than using each technique separately.

According to the path-loss, energy is directly proportional to the distance between the sender and receiver raised to power of path-loss factor. The path loss factor can take values between 2 and 6 depending on the wireless medium. With the use of directional antenna, energy is directly proportional to the beam width angle and the distance between the sender and the receiver. Applying power control with directional antenna can enhance the energy savings by 144% [84] if using path-loss free space model.

The authors of [85], [17], [86], [87], [88] have studied analytically the capacity of

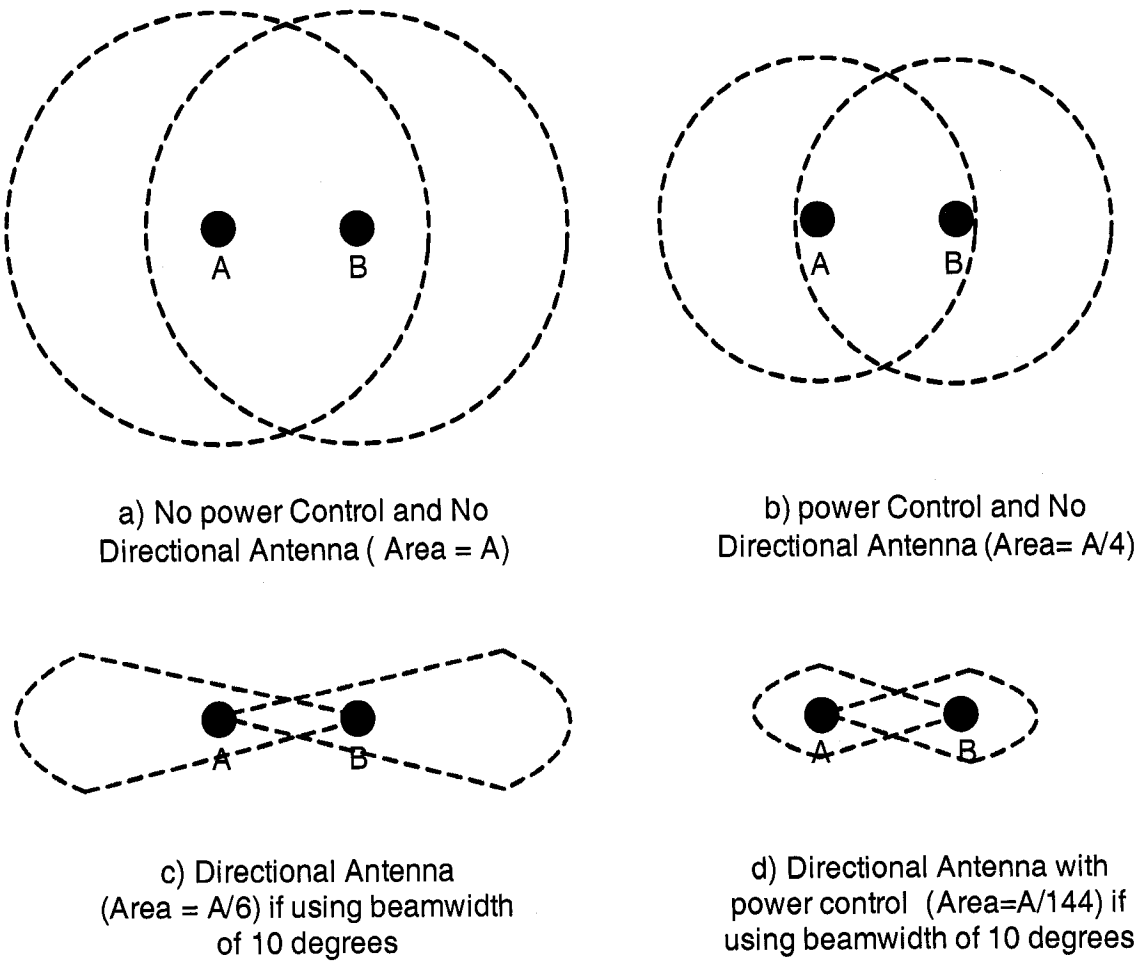

a) No power Control and No Directional Antenna (Area = A)

b) power Control and No Directional Antenna (Area= A/4)

c) Directional Antenna (Area = A/6) if using beamwidth of 10 degrees

d) Directional Antenna with power control (Area=A/144) if using beamwidth of 10 degrees

Figure 2.11: Theoretical study of coupling directional antenna with power control

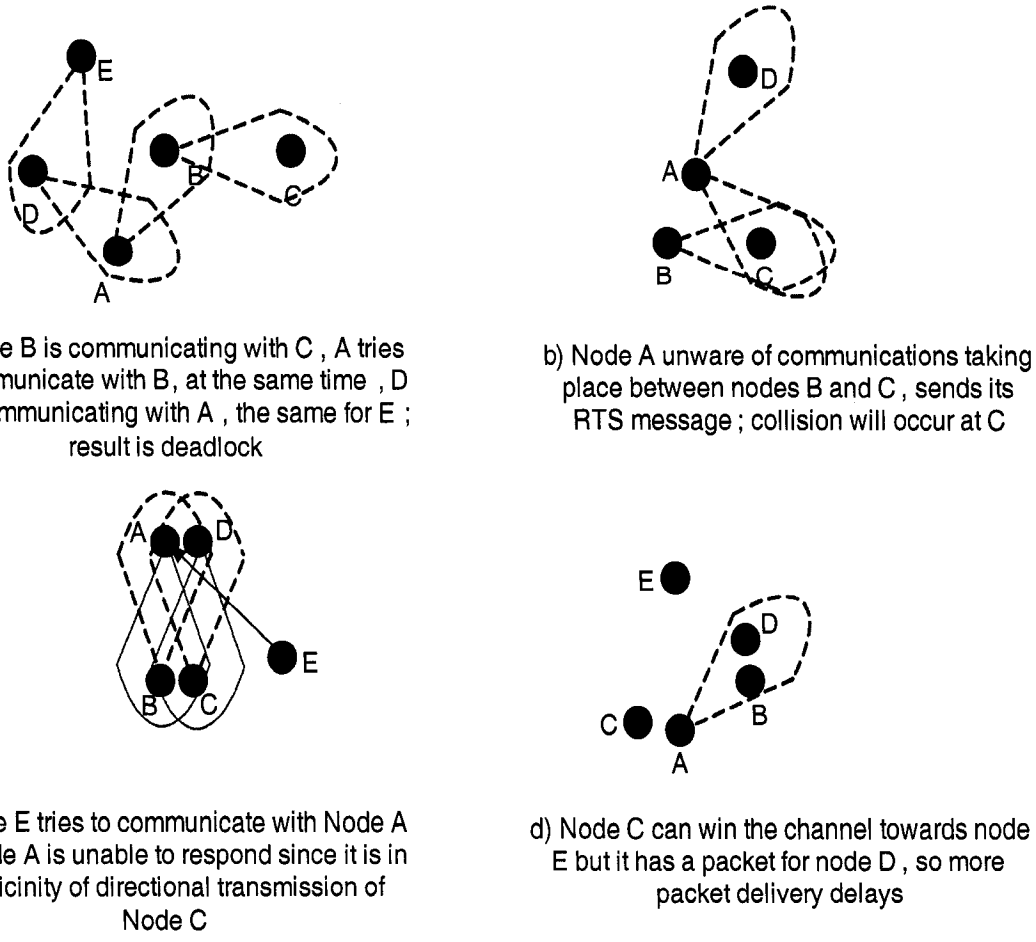

Figure 2.12: Directional Antenna Operational Burdens

multihop ad hoc networks with nodes equipped with directional antennas and showed that directional antennas offer great throughput gains. Directional MAC [3] was the first MAC to include the directional version of IEEE 802.11 DCF. Here, RTS, CTS, DATA and ACK are transmitted all directionally. However, D-MAC faced operational obstacles such as deafness, hidden terminals, head of line blocking. We identify the origin of each problem and evaluate its impacts on the network performance.

Deafness

The deafness problem [89] results when an intended receiver fails to reply to an RTS message initiated by an intended sender since the intended receiver beam is set in

a direction away from the intended sender. Figure 2.12 (a) illustrates this problem; an ongoing directional communication is occurring between nodes B and C. Node A attempts to initiate a communication with node B by sending Directional RTS towards node B after sensing the channel in that direction to B idle. As a result, node B will be unable to respond to node A's RTS message, since its beam is directed towards node C. This is termed as deafness. Moreover, node A is ignorant about the cause node B is not replying for. Node A assumes packet collision and exhaust its RTS retry limit and in the case where the communication between nodes B and C takes longer times than the time needed for RTS retry limit, node A will drop the packet. Now suppose there are more than such scenario in the network, the network will be jammed and the overall performance interms of energy savings and throughput will definitely decrease. Now, consider the same scenario as before where node D is trying to communicate with node A while node A is attempting to communicate with node B. Another node, say E, initiates a communication towards node D while node D is trying to communicate with node A. Deadlock is reached and severe consequences may result. To conclude, deafness is a severe phenomena which may hinder to a great extent the merits of using directional antennas if left unsolved.

Hidden Terminal

The hidden terminal problem [90] is due to the combination of inefficient timing criteria of the IEEE 802.11 and the directional transmission of RTS/CTS/DATA/ACK messages. To elaborate more on this, let us consider the simple scenario depicted in Figure 2.12 (b). While node A was communicating with node D , it was not able to hear the RTS/CTS messages between node B and C. If node A has a packet to send to node C, node A sends an RTS message towards node C at the same time node B starts sending DATA message towards node C; consequently collision will occur at node C. Collision has high effect on increasing energy consumption and declining

capacity throughput.

Exposed Terminal

Exposed Terminal problem [91] reduces spatial reuse and thus the throughput performance decreases. Figure 2.12(c) illustrates this problem; node A cannot initiate any transmission to node B while node C is communicating with node D and vice versa since all nodes lies in the directional vicinity of each other. Another problem that is built on the exposed terminal problem is the jointly exposed terminal problem and the receiver blocking problem [90]. We illustrate this further in Figure 2.12 (c); node A cannot reply with a CTS message to an initiated RTS message from node B, since node A lies in the vicinity of the ongoing directional communication of node C. Node B will keep sending an RTS message according to the number of retries allowed and configured in RTS retry limit , thinking that the previous messages collided. This term of problem has the same effect on the network as deafness.

Head of Line Blocking

Networks implementing First-In-First-Out (FIFO) queuing service rule suffers from Head-of-Line blocking Problem [91]. Networks with such queuing schemes suffers to a great extent when using directional antenna. Nodes contend to win a channel before transmitting their packets. Suppose nodes A in Figure 2.12(d) has a packet to transmit to node B, node C has a packet to transmit to node D. Node A wins the channel and transmits the data message to node B. On the other hand, node C can win the channel in the direction of node E and transmit any intended packet to node E, but it is unable to do so since it has a packet for node D. This is termed as HOL blocking problem. This problems adds more delay for packet delivery and thus affect the overall network throughput.

Solutions to these problems can be found in [92], [3], [93], [94]. In what follows,

the new accomplishment on the use of directional antennas and the integration of directional antenna with power control are listed.

2.8.1 Directional MAC

The Tone-based directional MAC (ToneDMAC) protocol [95] has been proposed to alleviate Deafness; in other words to get nodes to understand that other nodes are deaf. Two channels are adopted a data channel and a narrow control channel. RTS/CTS, Data and ACK packets are transmitted on the data channel and tones are transmitted on the control channel. Tones are sent omnidirectional after the directional Data/ACK exchange has been completed. By this, a neighboring node can conclude deafness if it overhears a tone from its targeted destination. Every node is assigned a unique identifier by which its neighbor can recognize it through and this identifier is transmitted in the busy tone. Identifying a node is performed via a hash function that contains both the tone frequency and duration. Multiple Tones usage in the network was an obstacle and was rectified via frequency tone reuse through the hash function implementations. Furthermore, the location information regarding the neighboring nodes was used to reduce the probability of tone mismatching.

Directional Antenna Medium Access protocol (DAMA) [96] designed to effectively pass the limitations incurred by DMAC. Directional four-way handshake is considered to take the benefit of increased gain obtained by directional antennas. DAMA employs a sweeping circular transmission of RTS and CTS to prevent the problems if deafness and hidden terminal problems. In order not to overwhelm the network with these control packets, DAMA performs an optimized transmission of RTS/CTS. A Node discovers all its neighbors and consequently sent its RTS through the antenna beams associated with these neighbors. Worst case scenario is the dense network topology where the node has to use all of its antennas beams to reach all its neighbors, thus performance issue regarding overhead pops out. The mentioned technique

showed a performance gain in case of sparse network. DAMA employs a three way handshake in a way Directional RTS is sent then followed by directional CTS then at the same DRTS/DCTS are sent directly via sweeping through all the selected beams. Finally ACK is sent. DAMA implements an adaptive mechanism where it learns and caches information about those sectors with neighbors. Various topologies have been considered for performance evaluation. Simulation showed that DAMA performs better than IEEE 802.11 DMAC and CRM in all scenarios except in the linear topology. The linear topology case is particularly degrading to all directional MAC protocols, but DAMA is still observed to perform best in terms of all directional MAC protocols considered, while IEEE 802.11 performs best overall. MAC for directional Antenna (MDA) [97] another fruitful work by the same authors consider enhancing DAMA by employing an efficient sweeping procedure for sending circular RTS and CTS called the Diametrically Opposite Directional (DOD). An enhancement to the MDA protocol has been recently proposed in [98] by a incorporating Wait To Send Control (WTS) packet. Here, WTS packets are simultaneously transmitted by the transmitter and the receiver after the successful exchange of directional RTS and CTS to notify the on-going communication to potential nodes that are unaware of this ongoing communication.

SYN-DMAC a directional MAC protocol for Adhoc Networks with Synchronization is investigated in [91]. Nodes are assumed to be equipped with GPS receivers for synchronization purposes. A switched-beam antenna is adopted for this protocol. SYN-DMAC proposes a timing-structure different than that of the IEEE 802.11 to alleviate the hidden and deafness problems. The timing structure in each cycle is made up of three phases. The first phase is the Random channel access multiple nodes contend to win out a channel. Neighbor discovery is carried along with channel contention in the same phase. One or more node-pair may win out a channel on a condition these node-pairs should not collide with each other. Simultaneous

Data transmissions occur in second phase. Based on the variation of the channel, each node-pair modify its power or rate accordingly. Finally parallel contention-free ACKs are transmitted in phase three. The protocol also addresses the HOL problem. Simulations showed significantly improvement gain over the IEEE 802.11 MAC protocol.

To fully exploit the benefits of directional antennas, DBSMA [99], a MAC protocol for Multi-hop Ad-hoc Networks with Directional Antennas, considers all transmissions, receptions, and idle listening to be directional. The authors describe a set of requirements that should be met by directional MAC protocol and then proposed DBSMA as a voted MAC. DBSMA uses novel concepts of idle directional listening, beam sweeping, Invitation Signal and directional back-off windows. Listening is performed via sweeping to cover the whole space. Every beam sector for each direction in a switch beam antenna implements its own back off window. Implementing the same back off window would result in unfairness to channel contention. Increasing a backoff window of a node due to collision in one direction affects the node's ability to content for a channel in the remaining directions due to the fact the node implements the same backoff window for all directions. If such a collision occurs in an un-congested area, this will deteriorate the node's capability to send in congested -area. Thus, the network condition becomes more un-stable. Independent backoff window for every direction rectifies this problem. An Invitation signal is introduced before an RTS control packet. This signal is sufficiently long to make all neighbors hear it. Upon hearing it, all nodes stop listening in all directions and lock their antenna beam in the direction of IS signal and waits for RTS message. After receiving an RTS, a destination node starts transmitting a busy tone till the end of the DATA and ACK transmissions. The busy signal is a narrow bandwidth, out of band signal. Simulations showed that implementing independent backoff window for every direction has enhanced the throughput by factor greater than 20%. The author observed

the that the minimum back-off window using directional antennas should be smaller compared to the single back-off window due to the reality that the number of nodes existing in within the directional transmission range is smaller than the number of all possible neighbors. It is also shown that IS duration highly affects the throughput. Finally, DBSMA achieved higher performance gain over the popular DMAC in the case the control packet is much smaller than the data packets.

2.8.2 Directional MAC with power Control

The use of directional antennas for single- hop packet radio network was first proposed in [100] where a slotted ALOHA packet radio network was considered. Authors derived an equation model to calculate the performance improvement that can be obtained in a slotted ALOHA channel by the use of directional antennas and multiple receivers. The idea was then reformulated to multi-hop networks but using directional antenna with power control. The throughput performance was investigated through a derived equation model. The derived model showed that the throughput increases dramatically if power controlled directional antennas are used for transmission. Moreover, the authors argue that using narrow beams antenna, the risk of destructive packet collision is reduced and nodes will be able to communicate with higher transmission probability. Thereafter, several studies have been carried in to benefit from the controlled transmission power gains of directional antennas.

Performance evaluation of directional antenna with power control was studied in [101]. The RTS message is sent at a predetermined power - the maximum power. The receiver will find the difference between the received power of the RTS message and its threshold power. The threshold power is the minimum power needed to decode the packet correctly. The value of the difference is sent within the CTS message. The source node will use power value that is equal to maximum power minus the difference value. A simulation experiment consisted of 40 static nodes equipped with directional

antenna were randomly distributed in an specific area. Since the packets considered in simulation are large packets, the delay metric is a better indicator of performance. Adding power control with directional antenna dramatically reduced the delay by up to 28% where as with only directional antenna the factor of delay is around 2% to 3%. Throughput enhancement of 118% was recorded.

The authors in [102] proposed the use of adaptive antenna arrays. RTS/CTS messages are sent omnidirectional with maximum power P_{max} whereas DATA/ACK are sent directionally with controlled power. A $SHORT_{NAV}$ term is used to alleviate the exposed terminal problem. Two power control schemes were introduced 1) global power control (GPC) 2) local power control (LPC). DATA/ACK power values in GPC are determined based on a factor α such that $P_{data/ACK} = \alpha \times P_{max}$; whereas the power of DATA/ACK packets is set for each transmission so the Signal to Noise ratio (SNR) is a pre-determined value. This can be done by using the values of the received RTS/CTS power levels to compute how much power reduction is required. Performance evaluation of GPC and LPC showed the following; normalized system capacity for GPC was 475% over IEEE 802.11, LPC was 525% over IEEE 802.11, where as with only the use of directional antenna it is 260% over IEEE 802.11.

Based on the omni-directional BASIC power control protocol , a similar scheme but with the use of directional antenna was investigated in [103]. They name it directional antenna based MAC protocol with power control (DMACP). Here, all the control and data packets are sent directionally; the RTS and CTS messages are sent with maximum power but the data packets are transmitted with power control. Through the RTS-CTS handshake, the power value for transmitting the data packet is assigned. Moreover, a destination node upon receiving an RTS packet, it calculates the difference between the values of signal to interference plus noise ratio (SINR) of the RTS packet and the SIR_{min} threshold. This difference value is encapsulated in the CTS message sent to the source. Based on this value, the source reduces the power

value needed for ensuing the data packet by an amount that is equal to this difference minus a margin 6 dB, not exceeding the maximum power level of the transmitter. The performance evaluation of DMACP showed that integrating power control with use of directional antenna does not have a significant impact on the throughput but on energy consumption.

A distributed power control (DPC) protocol has been introduced for ad hoc nodes with smart antennas in [104]. In this protocol, the receivers measures the local interference information and send it to the transmitters; upon receiving this information, the transmitter use it together with corresponding minimum SINR (signal to interference plus noise) to estimate the power reduction factors for each activated link. DATA and ACK transmissions are in (beamformed) array-mode since smart antennas are used at both ends of the link. In DPC protocol, the interference information is collected during both omni-directional RTS/CTS transmission and the beamformed DATA/ACK transmission. RTS /CTS packets are always transmitted with full power in omni-directional mode, and the power level of DATA/ACK transmission is determined by a power reduction factor which is determined by the maximum interference. Protocol performance evaluation showed significant performance improvement has been achieved when compared the conventional IEEE 802.11 protocol.

A directional medium access protocol with power control (DMAP) was presented in [90]. RTS message sent omnidirectionally while CTS/DATA/ACK messages are sent directionally. The main target of DMAP was to alleviate some of the problems associated with directional antenna use. Moreover, DMAP minimizes the energy consumption by integrating transmission power control with the use of directional antennas. Separate data and control (RTS/CTS/ACK) channels were used to rectify the hidden terminal problem due to unheard RTS/CTS messages. In DMAP, a transmitter sends an omnidirectional RTS . The receiver, before replying with directional CTS (D-CTS), will sense the data channel towards the transmitter and measures the

interference. A power control factor is encapsulated within the D-CTS packet for the transmitter to read so as to assign a power value for data packets. The CTS message is sent with a power that is multiplied by directional gain factor as if the RTS message is sent directionally. The author argues that deafness would be eliminated due to the power scaling of D-CTS. Performance evaluation of DMAP when compared with IEEE 802.11b showed throughput enhancement by a factor of 200% and energy consumption reduction by a factor of 82%.

A load-based concurrent access protocol (LCAP) was proposed in [105]. LCAP aims at increasing spatial reuse by allowing interference-limited, simultaneous transmissions to take place within the same vicinity by using transmission power control. RTS messages are sent omnidirectionally with maximum power , CTS/DATA/ACK messages are sent directionally. Similar to its predecessor (DMAP), LCAP uses separate data and control channel to alleviate the hidden terminal problem due to unheard RTS/CTS messages. LCAP uses the same procedure in DMAP for scaling and finding the power of CTS to solve deafness. Moreover, the receiver uses a *load control* technique to determine the power value of the data packets and encapsulate it within the CTS message. This data power value is determined so as to ensure a balance between energy consumption and spatial reuse. Furthermore, upon finding the data power value, the receiver calculates the difference between this value and the minimum power value needed to decode the packet correctly. The difference is also encapsulated in the CTS packet and is used by the nodes hearing the CTS messages to find in case they have to initiate any communication, the amount of interference they can put on the receiver. Thus the difference value is interference margin that nodes decide on the maximum value of their future interfering transmissions . LCAP showed interesting performance metrics when compared with IEEE 802.11b for different network topologies.

Three channels power control scheme with the use of directional antennas is presented in [106]. The protocol proposed uses one channel for data packets, a second channel for control packets and a third channel for busy tone. Busy tones are sent directionally, RTS message is sent omnidirectionally with maximum power, CTS/DATA/ACK sent directionally with CTS/ACK messages with maximum power. The busy tone is used to solve the deafness problem. An Interference model is calculated to estimate the interference around the receiver. Based on this interference calculated, a proposed power control scheme is designed. A node receiving an omnidirectional RTS will calculate the maximum interference using the mention model then decide on the power value the source node should send its DATA message by. Data power value is advised as follows. The receiver computes the difference between the maximum interference calculated by the model and subtracts from it the total measured noise power; then adds to this difference the minimum power needed to transmit the packet. The minimum power to transmit the packet is simply the minimum power needed to decode the packet correctly upon reception times the channel loss gain. Two busy tones are defined: transmit busy tone and receive busy tones. Both of these busy tones are sent at maximum power and with the RTS/CTS messages respectively. The protocol showed enhancement in the channel utilization and energy consumption when compared with IEEE 802.11 performances.

2.9 Other Schemes

Another category of alternative collision avoidance schemes that do not consider all the above proposed techniques have been proposed in [107] and [108]. Both schemes embed extra information regarding the upcoming transmission in the PLCP (physical layer convergence procedure) header so that a larger group of potential interferers become aware of the transmission. The information can be the locations of the transmitter and receiver as in [108] or the interference range as in [107]. Upon

receiving the PLCP header, a neighboring node is able to determine whether it lies inside the interference range of the receiver and accordingly, decide whether to block its own transmission or not. However, mandating extra information in the PLCP header of every control or data packet adds extra overhead.

Another enhanced carrier sensing (ECS) scheme was proposed in [109]. Here, the MAC frame type is encapsulated into the PLCP header. Upon receiving the PLCP header, neighboring nodes can distinguish the type of transmitted frame and accordingly back off for a specific duration that is assigned based on the MAC frame type information.

An aggressive virtual carrier sense mechanism is presented in [110]. The basic idea is that a node which overhears either an RTS packet or a CTS packet, but not both, would not consider the media as busy and accordingly may attempt for transmission.

Chapter 3

Investigating the Performance of Power-Aware *IEEE 802.11* in Multi-hop Wireless Networks

In this chapter, both access mechanisms of the IEEE 802.11 (the two-way handshake (basic) and four-way handshake) are considered and the impact of the interplay between power control, tuning carrier sensing threshold on the throughput performance of multihop networks is studied. It is shown that through controlling the transmit power or tuning the carrier sensing threshold, there exists a tradeoff between the amount of spatial reuse and the probability of collisions due to both the hidden and exposed terminal problems. For instance, in the RTS/CTS access method, increasing the transmission power of RTS/CTS control packets will severely affect the spatial reuse and add interference to other nearby communicating nodes regardless of the power at which DATA packets are transmitted. Similarly, in the basic handshake, increasing the DATA transmission power will result in increasing the data collision rates, reducing the spatial reuse, and adding interference to nearby communicating nodes.

To achieve this objective, an accurate analytical model is presented that characterizes the transmission activities as governed by the IEEE 802.11 DCF . Through this model, the effects of power control, tuning the carrier sensing threshold, impacts of packet size and transmission rates are studied. Moreover, the potential adverse impacts of RTS/CTS control packets on the network capacity are demonstrated and then compared with the two-way basic access method.

The rest of this chapter is as follows. Section 3.1 proposes the analytical model. In Section 3.2, comprehensive study of IEEE 802.11 DCF mentioned attributes is presented using the derived model after which the reliability of the model is verified using discrete event simulations in Section 3.3. Finally, the conclusion is presented in Section 3.4.

3.1 Analytical Model

3.1.1 Model Background

We assume that RTS/CTS messages are sent with equal fixed power. Accordingly, the transmission ranges of RTS a_{RTS} and CTS packets are a_{CTS} are equal. The DATA/ACK messages are sent with power value that is less than the fixed power to cover the distance between the transmitter and the receiver as has been shown in Figure 2.2, thus, the transmission ranges of DATA/ACK messages are denoted as a_{data} and a_{ack} respectively and accordingly are equal. Moreover, all nodes have identical CS_{th}, and accordingly the silence range (r_c) and transmission range (r_t) are related according to the carrier sense threshold (CS_{th}) and the reception power threshold (κ)assuming two-ray channel model:

$$r_c = r_t \cdot C \tag{3.1}$$

where $C = (\frac{\kappa}{CS_{th}})^{\frac{1}{4}}$. Here, C varies when tuning CS_{th} (the carrier sensing threshold) since $\kappa = 3.652e^{-10}$ W (the reception sensitivity) is fixed.

Hence, we have two silence sensing ranges according to equation 3.1. These are ($r_c = r_{c,RTS} = r_{c,CTS}$) for RTS/CTS packets and ($r_c = r_{c,DATA} = r_{c,ACK}$) for DATA/ACK packets.

Further, the power relation between the control messages (RTS/CTS) and the DATA/ACK packets values using the path loss law [30] are expressed as:

$$P_{data|ack} = P_{RTS|CTS} \cdot (\frac{a_{data}}{a_{RTS}})^4 \tag{3.2}$$

With the definition of the interference set from equation (2.6) and assuming $P_{cn} = 0$, the interference ranges of node B when receiving either an RTS packet or a DATA packet is determined as follows. First, the case when the transmitter A is sending its RTS packet is considered. In this case, $P_{tA} = P_{RTS}$. We assume the worst case interference scenario; that is the interfering node F is sending an RTS packet $P_{tF} = P_{RTS}$. Accordingly the interference range of node B (when receiving an RTS packet) $r_{i,RTS}$ is defined as the maximum value of d such that the inequality in equation (2.6) holds:

$$r_{i,RTS} = \zeta^{\frac{1}{4}} \cdot a_{data} \tag{3.3}$$

For example, if an RTS/CTS channel rate of 2 Mbps with ζ equals to 10 dB is adopted, $r_{i,RTS} = 1.78 \cdot a_{data}$. Similarly, the interference range of the transmitter A when receiving the CTS packet can be derived and is given as $r_{i,CTS} = \zeta^{\frac{1}{4}} \cdot a_{data}$.

Assuming a successful RTS/CTS handshake, node A sends DATA packet at different power $P_{tA} = P_{data} < P_{RTS}$. Assume the worst case interference scenario; that is the interfering node F is sending an RTS packet $P_{tF} = P_{RTS}$, and by substituting equation (3.2) into equation (2.6), the interference range of the receiver B when

receiving the DATA packet can be re-derived as:

$$r_{i,DATA} = \zeta^{\frac{1}{4}} \cdot a_{RTS} \tag{3.4}$$

Note that, $r_{i,DATA} = 1.78 \cdot a_{RTS}$ for data channel rate of 2 Mbps, $\zeta = 10dB$. As can be seen from equation (3.4) under worst case assumption, the lower the power value of the DATA packet a transmitter uses, the larger the interference range of the receiver is when receiving the DATA packet. Similarly, the interference range of the transmitter A when receiving the ACK packet can be derived and is given as $r_{i,ACK} = \zeta^{\frac{1}{\alpha}} \cdot a_{RTS}$.

Finally, the value of ζ is based on the rate a packet is received with. The higher the rate is the higher ζ is [5]. For instance, for a receiver to correctly receive a DATA packet transmitted at 11 Mbps, ζ is set to 15 dB [5]. Now, consider the RTS, CTS, ACK packets are transmitted at 2Mbps while DATA packet is transmitted at 11 Mbps. The interference ranges are calculated as follows: $r_{i,RTS} = r_{i,CTS} = 1.78 \cdot a_{data}$, $r_{i,DATA} = 2.37 \cdot a_{RTS}$, and $r_{i,ACK} = 1.78 \cdot a_{RTS}$.

3.1.2 Model Preliminaries

We assume that the system time is slotted with σ seconds. RTS, CTS, DATA and ACK packets are assumed to be with fixed length of L_{RTS}, L_{CTS}, L_{DATA} , L_{ACK} bits. The channel DATA bit rate is assumed to be R (Mbps) and that of the control channel is R_c (Mbps). Thus the transmission of an RTS/CTS/DATA/ACK packets will last for $T_r = \frac{L_{RTS}}{R_c \cdot \sigma}$, $T_c = \frac{L_{CTS}}{R_c \cdot \sigma}$, $T_d = \frac{L_{DATA}}{R \cdot \sigma}$, $T_a = \frac{L_{ACK}}{R_c \cdot \sigma}$ respectively.

Each node in the network initiates a transmission to one of its neighbors in a randomly chosen virtual time slot for a duration of T_{avg}. Here, T_{avg} denotes the expected time interval between the beginning instants of two consecutive virtual slots. T_{avg} may be much longer than the physical slot size σ [15].

We also assume that the network operates under the saturation condition, i.e., the transmission queue of a sender is always nonempty. Now, the channel activities are modeled from the perspective of an individual sender in order to be able to derive the single node throughput S. However, a first parameter of interest is the attempt probability τ that a node transmits in a randomly chosen virtual slot. This attempt probability is given by [18]:

$$\tau = \frac{2 \cdot (1 - 2 \cdot P_c) \cdot (1 - p)}{(1 - 2 \cdot P_c) \cdot (W_0 + 1) + P_c \cdot W_0 \cdot (1 - (2 \cdot P_c)^m)} \tag{3.5}$$

where $m = log_2(W_m/W_0)$, W_0 and W_m are the minimum contention window and maximum contention window respectively. P_c is the conditional collision probability (to be derived next) and is calculated for the RTS/CTS access method as follows:

$$P_c = 1 - (1 - p_{rts}) \cdot (1 - p_{cts}) \cdot (1 - p_{data}) \cdot (1 - p_{ack}) \tag{3.6}$$

p_{rts}, p_{cts}, p_{data}, p_{ack} are the probabilities of RTS, CTS, DATA, and ACK collision respectively. Moreover, p is the probability that a node senses the channel busy and is given by $p = 1 - (1 - \tau)^{N_c}$, where $N_c = \rho \cdot \pi r_c^2$ is the number of nodes in the carrier sensing range of the transmitter and ρ is the active density.

3.1.3 Collision probability

In this section, the RTS/CTS/DATA/ACK collision events that may occur within a considered virtual time slot are analyzed in order to calculate P_c as a function of τ. The analysis is based on the probability that the packet will be received correctly at the receiver.

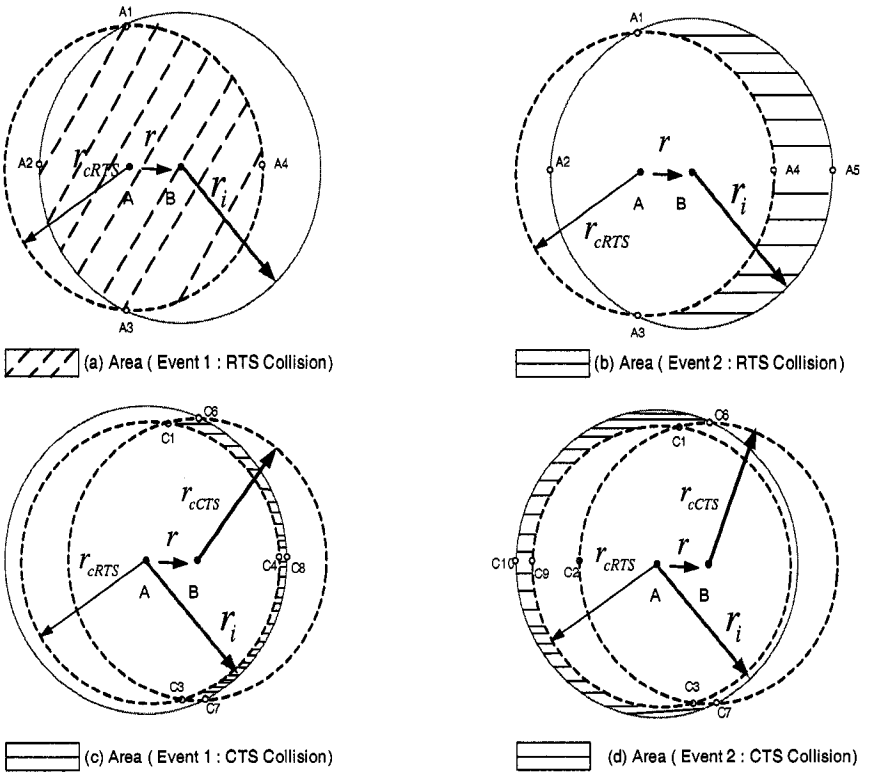

Figure 3.1: RTS Collision Event 1

RTS/CTS Handshake Collision Events

We now consider the RTS/CTS handshake is taking place between nodes A and B separated from each other by a distance r as shown in Fig. 3.1. Four cases need to be investigated and these are $r_c \geq r_i + r$, $r_i \geq r_c + r$, $r_c \geq r_i$, $r_c < r_i$; here, $r_c = r_{c,RTS} = r_{c,CTS}$ and $r_i = r_{i,RTS} = r_{i,CTS}$ (equation 3.3). We will only analyze the case $r_c < r_i$ since in this case, the reasons behind the RTS/CTS collisions (as will be shown shortly) can be illustrated more delicately. Other cases, $r_c > r_i + r$, and $r_i > r_c + r$, $r_c > r_i$ will follow the same line of analysis.

- *RTS Collision Events* are the various events behind the failure of an RTS packet transmission that yield to an unsuccessful transmission. Node A is initiating an RTS transmission towards node B (Figure 3.1): In order to determine the probability of RTS packet collision, the following two events are to be considered:

1. Event 1-RTS: There are one or more transmissions initiated from nodes N_{ci} located in the intersection of the interference range area of the receiver (node B) and the carrier sensing range of the transmitter (node A), the area (A1A2A3A4) as shown in Figure 3.1(a) at time t_r, the time an RTS packet initiated and it is the first time slot in T_r. These nodes will sense the channel busy if they do not transmit at the first time slot. Assuming that the nodes in the carrier sensing area will sense the same channel status as that sensed by the transmitter (node A), then the probability P_{rts1} of this event can be approximated by:

$$p_{rts1}(r) = 1 - (1 - \tau)^{N_{ci}(r)} \tag{3.7}$$

   if $A(r)$ is the area where $N_{ci}(r)$ nodes are located, then $N_{ci}(r) = \rho \cdot A(r)$.

2. Event 2-RTS: A collision occurs if there are one or more transmissions initiated during the vulnerable interval $[t_r - T_r + 1, t_r + T_r - 1]$ from nodes N_h located in the hidden area as shown in Figure 3.1(b) (A1A4A3A5A1). Those nodes if they transmit during the vulnerable period (period during which data packet is transmitted), a collision will occur. The probability of this event p_{rts2} is

$$p_{rts2}(r) = 1 - (1 - \tau)^{N_h(r) \cdot \frac{T_r}{T_{avg}}} \tag{3.8}$$

   where $\frac{T_r}{T_{avg}}$ is the number of virtual slots in the vulnerable period. Since at the beginning of each of these virtual slots a node may attempt for transmission, the term $(1 - \tau)^{N_h(r)}$ has to be raised to a power of $\frac{T_r}{T_{avg}}$.

Therefore, the probability of RTS collision (p_{rts}) is simply:

$$p_{rts}(r) = 1 - (1 - p_{rts1}(r)) \cdot (1 - p_{rts2}(r)) \tag{3.9}$$

- *CTS Collision Events* are the events that a collision occurs during a CTS packet transmission. Assuming RTS packet has succeeded, node B will reply with a CTS. Nodes within the carrier sensing zone of node A and outside the transmission zone will defer their transmission to EIFS duration. Thus, these nodes will not interfere with the CTS reception at node A since EIFS is a sufficient period for CTS to be transmitted and received at the sender. Two reasons exist for a CTS packet to collide.

  1. Event 1-CTS: There are one or more transmissions initiated from nodes N_{cci} as shown in Figure 3.1(c) located in the area (C1C6C8C7C3C4C1))at t_c (the time a CTS packet initiated and it is the first time slot in T_c). Following the same assumption as event 2 for RTS packet collision, p_{cts1} is derived as:

$$p_{cts1}(r) = 1 - (1 - \tau)^{N_{cci}(r)} \tag{3.10}$$

  2. Event 2-CTS: A collision occurs if there are one or more transmissions initiated during the interval T_c (vulnerable period) from nodes N_{hct} (as shown in Figure 3.1(d)) located in the hidden area (C1C6C10C7C3C9C1) any time slot within $[t_c - T_c + 1, t_c + T_c - 1]$. The probability $P_{cts2}(r)$ of this event is:

$$p_{cts2}(r) = 1 - (1 - \tau)^{N_{hct}(r) \cdot \frac{T_c}{T_{avg}}} \tag{3.11}$$

  Therefore, $p_{cts}(r)$ is simply:

$$p_{cts}(r) = 1 - (1 - p_{cts1}(r)) \cdot (1 - p_{cts2}(r)) \tag{3.12}$$

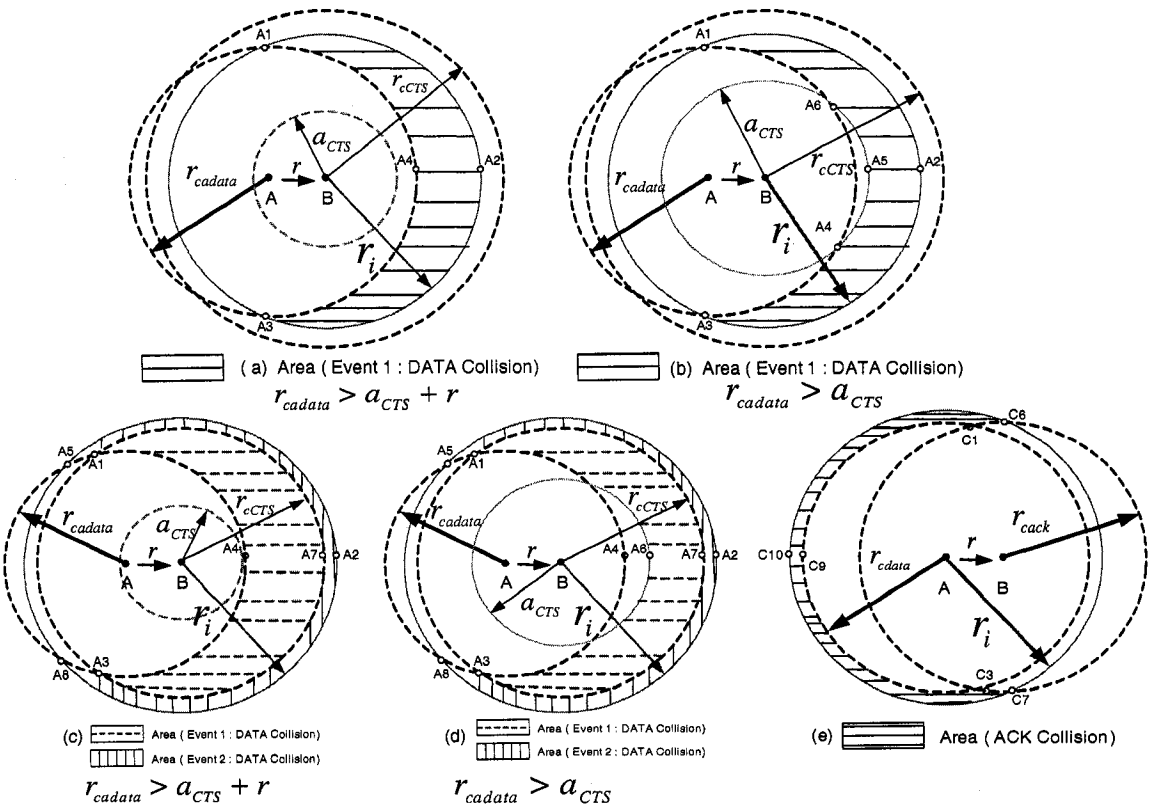

Figure 3.2: DATA/ACK Events

DATA/ACK Handshake Collision Events

Now node A and node B decided to reduce the transmit power for DATA-ACK so as only to cover the distance between them as discussed earlier. Hence, the transmission range ($a_{data} = a_{ack}$) for DATA-ACK becomes smaller than that of RTS-CTS ($a_{RTS} = a_{CTS}$). Similarly, the new carrier sensing range $r_{c,DATA}$ for DATA-ACK also becomes smaller (since it will be a function of a_{data} according to equation (3.1)) than that of RTS-CTS. Now, depending on the distance between nodes A and B ($r = a_{data}$), and assuming a successful RTS/CTS handshaking has taken place, four scenarios should be distinguished in order to determine the collision probabilities of DATA/ACK: $r_c > r_i$, $r_c \geq r_i + r$, $r_c < r_i$, $r_i \geq r_c + r$. Here, $r_c = r_{c,DATA} = r_{c,ACK}$ and $r_i = r_{i,DATA} = r_{i,ACK}$. Similarly, the case $r_c < r_i$ i analyzed.

Now, two types of DATA collision events are distinguished.

- Event1-DATA: Nodes N_{hd} that mainly lie in the carrier sensing zone of node B when transmitting the CTS message may become active after EIFS and can start transmission during any time slot within $[t_d - T_d + 1 - EIFS, t_d + T_d - 1 - EIFS]$, t_d (the time node A starts transmitting its data packet) and thus may corrupt the packet reception at node B. So, the probability p_{data1} of this event is

$$p_{data1}(r) = 1 - (1 - \tau)^{N_{hd}(r) \cdot \frac{T_d - \frac{EIFS}{\sigma}}{T_{avg}}} \tag{3.13}$$

- Event2-DATA: Hidden nodes N_{hd1} that are mainly located outside the carrier sensing zone of node B when transmitting the CTS message and within the interference range can start transmission any time slot within $[t_d - T_d + 1, t_d + T_d - 1]$. The probability p_{data2} of this event

$$p_{data2} = 1 - (1 - \tau)^{N_{hd1}(r) \cdot \frac{T_d}{T_{avg}}} \tag{3.14}$$

$p_{data}(r)$ can be calculated as follows:

$$p_{data}(r) = 1 - (1 - p_{data1}(r)) \cdot (1 - p_{data2}(r)) \tag{3.15}$$

The calculation of the number of hidden nodes N_{hd} and N_{hd1} are dependent on the transmission power of the data packet. This is what is going to elaborated shortly. If the DATA packet is transmitted at a power such that $r_{i,DATA} > r_{c,DATA}$, two different scenarios are to be considered within this case: $r_{c,CTS} \geq r_i$, ($r_{c,CTS}$ is the carrier sensing range of the transmitted CTS packet and depends on the power at which the CTS is transmitted) and $r_{c,CTS} < r_{i,DATA}$.

- $r_{c,CTS} \geq r_i$: In this case, the probability of data packet collision will result from Event1-DATA. Within this scenario, the following cases are distinguished: $r_{c,DATA} \geq a_{CTS} + r$ or $r_{c,DATA} > a_{CTS}$;

  1. $r_{c,DATA} \geq a_{CTS} + r$ (Figure 3.2(a)): In this case,the collision probability for data packet, p_{data1}, will be the result of nodes N_{hd} existing in the shaded area (A1A2A3A4A1).

  2. $r_{c,DATA} > a_{CTS}$ (Figure 3.2(b)): p_{data1} for this case will be the result of nodes N_{hd} existing in shaded area (A1A2A3A4A5A6A1).

- $r_{c,CTS} < r_i$: Both p_{data1} and p_{data2} exist for this scenario and we distinguish between the following: $r_{c,DATA} \geq a_{CTS} + r$ or $r_{c,DATA} > a_{CTS}$ to determine p_{data1} ;

  1. $r_{c,DATA} \geq a_{CTS} + r$:(Figure 3.2(c)) The collision probability for data packet, p_{data1}, will be the result of nodes N_{hd} existing in shaded area (A1A4A3A7A1) .

  2. $r_{c,DATA} > a_{CTS}$:(Figure 3.2(d)) will be the result of nodes N_{hd} existing in shaded area (A1A7A3A6A1).

p_{data2}, on the other hand, will be the result of nodes N_{hd1} existing in shaded area (A1A5A2A4A3A7A1) Figures Figure 3.2(c)-(d).

We proceed now to define the ACK collision event and determine the probability of ACK collision accordingly. Since nodes in the carrier sensing zone of node A defers for EIFS, the ACK packet can be correctly received by node A without any interference from these nodes (in the carrier sensing zone of node A). This due to the fact that EIFS duration is sufficient time for an ACK packet to be transmitted and received correctly at the DATA packet sender. Hidden nodes,N_{hack}, that may interrupt the ACK reception exist only in the case when $r_{i,ACK}$ is larger than $r_{c,ACK}$. Since $r_{i,ACK} > r_{c,ACK}$ scenario is considered, the nodes N_{hack} that might interfere while the ACK packet is received at the sender will be those located in area (C1C6C10C7C3C9C1C6) as shown in Figure 3.2(e). The probability for ACK packet collision , p_{ack}, is:

$$p_{ack}(r) = 1 - (1 - \tau)^{N_{hack}(r) \cdot \frac{T_a}{T_{avg}}} \tag{3.16}$$

The average CTS, DATA and ACK collision probabilities are determined in a similar way to that of RTS.

3.1.4 Throughput

We analyze four possible channel activities from the perspective of a node attempting to send a packet in a virtual slot in order to determine T_{avg}.

- idle: This indicates that there is no transmission on the channel (i. e. , the received power level is below the carrier sense threshold η). The probability of the virtual slot to be an idle slot is simply $P_i = (1 - \tau)^{N_c+1}$. That is none of the nodes in the carrier sensing range of the transmitter transmits at this time slot. The duration of this slot is $T_i = \sigma$.

- collision: If the transmitter does not receive a CTS (ACK) within an interval of SIFS after the RTS (DATA) frame is transmitted, it determines that a collision has occurred. The probability that a virtual slot is a collision slot is τp_{col} with a duration T_{col}.

- success: This activity shows that node A has received an ACK frame within an interval of SIFS after the DATA frame is transmitted, for which it determines that the transmission is successful. The duration of this activity is $T_{transmit}$; the probability of the virtual slot to be a success slot is $P_t = \tau(1 - P_c)$. That is given a node transmits at this slot and the transmission was successful.

- busy: A node will sense the channel busy when the received signal is above the carrier sensing threshold. This results from transmission of other nodes. The probability of the virtual slot to be a busy slot with duration T_{busy} is simply $(1-\tau)p$. Here, $T_{busy} = (1-P_c)\cdot T_{transmit}$ is the average busy period approximated on the assumption that a node will be silenced for the whole communication duration on a condition the transmitting node does not incur any transmission failure.

Based on the above analysis , T_{avg} can be calculated as follows:

$$T_{avg} = P_i T_i + P_t T_{transmit} + \tau p_{col} T_{col} + (1 - \tau) p T_{busy} \tag{3.17}$$

where $p_{col}T_{col} = (1-(1-p_{rts})(1-p_{cts}))T_{rr}+(1-(1-p_{data})(1-p_{ack}))T_{dd}$. Here, $T_{transmit}$, T_{rr}, T_{dd} are respectively the successful time needed for successful data packet delivery,

Table 3.1: Model and Simulation Parameter

Parameter	Value	Parameter	Value
SIFS	10 μs	DIFS	50 μs
EIFS (1Mbps)	364 μs	σ	20 μs
PCLP Length	192 bits @ 1 Mbps	ζ	10dB
Packet size	1000 bytes	$[W_0, W_m]$	$[31, 1023]$
RTS packet	20 bytes	CTS/ACK packets	14 bytes
MAC_{hdr}	34 bytes	α	4
R_c	2 Mbps	R	2 Mbps

RTS timeout duration, and DATA timeout duration. These can be calculated as:

$$\begin{cases} T_{transmit} = \dfrac{4 \cdot PHY_{hdr}}{r_h} + \dfrac{MAC_{hdr}}{R} + DIFS \\ \qquad + 4 \cdot \omega + 3 \cdot SIFS + (T_r + T_c + T_a + T_d) \cdot \sigma \\ T_{rr} = \dfrac{PHY_{hdr}}{r_h} + T_r \cdot \sigma + DIFS + \omega \\ T_{dd} = \dfrac{3 \cdot PHY_{hdr}}{r_h} + \dfrac{MAC_{hdr}}{R} + DIFS \\ \qquad + 3 \cdot \omega + 2 \cdot SIFS + (T_r + T_c + T_d) \cdot \sigma \end{cases} \tag{3.18}$$

where ω is is propagation delay, PHY_{hdr} is the header of physical layer and MAC_{hdr} is the header of MAC layer. $\frac{PHY_{hdr}}{r_h}$ is the transmission time of PLCP preamble and PLCP header.

Finally the throughput, (S), for each transmitter is calculated as follows:

$$S = \frac{P_t \cdot L_{DATA}}{T_{avg}} \tag{3.19}$$

3.2 Model Analysis

The common parameters at the MAC and physical layers used in our model (equations (3.5)-(3.19)) are presented in Table 3.1. The two-ray model is adopted. In our model verification, a_{data} is initialized to $d = \frac{1}{\sqrt{\rho\pi}} = 56m$ for $(\rho = 100 nodes/km^2)$, which

is the average distance for a receiver to exist within the transmission range of the sender. a_{RTS}, the transmission range of RTS/CTS control packets is also a function of d and $a_{data} \leq a_{RTS}$. Please note that a_{DATA} and r_{DATA} a_{RTS} and r_{RTS} are used interchangeably throughout the simulation analysis part.

3.2.1 Analysis of the Four-way handshake

Varying Transmission Range of a_{RTS}/a_{CTS}

We start by first analyzing the throughput performance as the transmission power for DATA packets (i.e., a_{data}) is varied and for different transmission ranges for RTS/CTS packets (i.e, a_{RTS}). Figure 3.3 shows the performance result of the RTS/CTS handshake when C = 2.78. Figure 3.3(a) shows that the highest throughput is obtained for shorter ranges of RTS (i.e., lower power for RTS packets), while the throughput decreases for longer ranges for RTS packets. This is due to the fact that by increasing the RTS transmission range (a_{RTS}), the control messages will silence larger number of nodes (that fall in the carrier sensing range of the transmitter and may not be in the interference range of the receiver) which has the effect of reducing the spatial reuse as verified by the decrease in the transmission probability as shown in Figure 3.3(b), and ultimately leading to a lower throughput. Moreover, at a larger a_{RTS}, the interference range for DATA and ACK (equation 3.4) increases as well, leading to more DATA/ACK collisions and hence reduced throughput. This is shown in Figure 3.3(c). On the other hand, when a_{RTS} is smaller, the interference range for DATA and ACK packets (equation 3.4) (interference area around the receiver when the transmitter is sending its DATA packet or receiving its ACK packet) decreases, thereby reducing the impact of hidden terminals on the reception of DATA/ACK packets.

Next, the effect of varying the transmission power of DATA packet on the system performance is analyzed. When a_{data} is small (e.g., $a_{data} << a_{RTS}$), the carrier

sensing range of DATA is also small while the interference range of the receiver (of DATA packet) is very large ($r_{i,DATA}$ is a function of a_{RTS} (equation 3.4)); hence, the interference area of DATA packets that is not covered by the carrier sensing range of the transmitter becomes large (i.e, more hidden nodes) and therefore there is a higher likelihood for DATA packet collision (as shown in Figure 3.3(c)).

Note that a small a_{data} has a negligible effect on either RTS or CTS packet collision; that is, when both the transmitter and the receiver are close to each other, while a_{RTS} is large, the interference range of RTS/CTS becomes completely covered by the carrier sensing range of the RTS/CTS which yields a very small RTS/CTS collision probability (as shown in Figure 3.3(c)). Figure 3.3(a) shows the poor performance obtained at very small a_{data} ($a_{data} << a_{RTS}$) and this is due to the higher DATA packet collision rate.

On the other hand, as a_{data} increases, the interference area of RTS/CTS increases too and the hidden terminal problem is amplified and hence the RTS/CTS collision probabilities increase (as shown in Figure 3.3(c)). In addition, increasing a_{data} will increase the carrier sensing range of DATA packet ($r_{c,DATA}$) which will start to cover more nodes in the interference zone of the DATA packet (i.e, reduces the effect of hidden nodes in the reception of DATA packet); this will result in lower DATA packet collision rate (the same analysis applies to ACK packet). Note that at very large a_{data} (e.g., a_{data} approaching a_{RTS}), the carrier sensing range of DATA packet becomes unnecessarily very large and the transmitter may suppress nodes outside the interference area of DATA packet from transmitting, limiting the spatial reuse. This is shown in the slight decrease of the transmission probability and throughput at larger a_{data} as shown in Figures 3.3(a),(b). Similar analysis applies to ACK transmission.

Tuning carrier sensing threshold

Next the impact that the carrier sensing (CS) threshold may have on the network performance is investigated as the data packet transmission power is varied and the interplay between them is studied. Here, $a_{RTS} = 2d$, where d is the minimal separation distance between source and destination, $d = 56m$; we observe from Figure 3.4(a) that there exists an optimal carrier sensing threshold that achieves best system performance. In addition, the larger the CS threshold (smaller C), the more effective power control schemes are and the smaller the CS threshold (larger C), the less effective power control becomes. Consider the case where $a_{data} = d$; a larger C will yield a larger carrier sensing range for RTS (e.g., $C = 4$ implies $r_{c,RTS} = 8d$), much larger than the interference range of the control packet ($r_{i,RTS} = 1.78 \times a_{data} = 1.78d$) which will unnecessarily silence more nodes and thereby affect excessively the spatial reuse. Now, when transmitting the DATA packet, the nodes that may affect the reception of the frame are those in the interference range of the receiver ($r_{i,DATA} = 1.78 \times a_{RTS} = 3.56d$) and outside the transmission range of the CTS packet ($r_{t,CTS} = a_{RTS} = 2d$) and the carrier sensing range of the DATA packet ($r_{c,data} = C \times a_{data} = 4d$), which already covers the transmission range of the CTS packet. Those nodes may affect the reception of the DATA packet if they transmit during the *vulnerable period.* Clearly, the larger value of C results in a large carrier sensing range for data packet and hence smaller data frame collision probability (as shown in Figure 3.4(c)). Accordingly, the effect of spatial reuse outweighs the benefits obtained from reduced data collision and hence lower throughput is obtained. As we slowly start reducing C, we observe the improvement in the system performance, since the spatial reuse is having lesser effect, until we reach a maximum throughput that corresponds to a $C \simeq 2$, beyond which further reducing C will start to affect the network performance. This is due to the fact that at a very small C, the data frame collision becomes higher (now due to the larger effect of hidden nodes) and its

impact outweighs the benefits we obtain from spatial reuse.

It is interesting to notice that when C is large, varying the transmission power of data packet does not add any benefits. This is clearly due to the major impact of spatial reuse. Conversely, when selecting a smaller C, it is more advantageous to perform power control and our results showed that it is always good to transmit data packet at larger power (i.e., larger a_{data}) in order to obtain better performance. This is mainly attributed to the fact that a larger a_{data} will yield a smaller data frame collision, although the collision rate of RTS packets increases (which is due to the larger interference range, $r_{i,RTS} = 1.78 \times a_{data}$, and hence larger number of nodes that may affect the reception of the RTS), with an overall packet collision that is lower. Figures 3.4(b) (c) and (d) show the packet collision probabilities for different values of C and a_{data}.

Impact of Packet size on the network performance

The network performance by varying the packet size is investigated and the impact of tuning carrier sensing threshold and controlling the transmission power is studied. Here, $a_{RTS} = 2d$. Similar to the earlier observation, larger C impacts the spatial reuse and smaller C yields larger data frame collision, hence there is an optimal carrier sensing threshold that yields best system performance. Unlike our earlier observation, however, the smaller the size of the data frame as shown in Figure 3.5(a), the lesser the impact of small C on DATA frame collision probability. This is due to the fact that those nodes in the interference area of the receiver of the DATA frame (and outside the carrier sensing of both DATA and CTS packets) may only interfere during a *vulnerable period* which corresponds to the transmission duration of the DATA packet. Given that the packet size is very small, this vulnerable period becomes small and hence the DATA collision rate as well becomes small. In addition, changing the transmission power of the DATA packet has also minor effect, even at

smaller C, for the same reason mentioned above.

When the packet size becomes larger (512 bytes in Figure 3.5(b), 1000 bytes in Figure 3.4(a)), the DATA packet will become more vulnerable to collisions (due to the increase in the duration of the vulnerable period, the hidden nodes will have stronger effect) especially at smaller C. It is clear, however, that in this case, controlling the DATA transmission power plays an important role in improving the system throughput when the carrier sensing (CS) threshold is large.

3.2.2 Evaluation of the basic access scheme

Here, the performance of the basic access mechanism is studied. the node throughput is measured as we vary (1) the carrier sensing threshold (2) the DATA packet transmission power. Here, the DATA/ACK collision events for the basic scheme are identical to that of the RTS/CTS collision events. Figure 3.6 (a) shows the throughput vs. the DATA carrier sensing range ($r_{c,DATA} = C.a_{data}$) for different network densities and for fixed distance d ($d = \frac{1}{\sqrt{\rho\pi}}$ is the distance between the transmitter and receiver). Here, as the carrier sensing threshold decreases (i.e, C increases), the carrier sensing range may completely cover the interference range of the receiver and hence the transmitter may be suppressing other transmissions which may yield a severe impact on the spatial reuse and accordingly results in lower throughput. As $r_{c,DATA}$ decreases, the spatial reuse starts to improve and the node's throughput starts to increase. Further, decreasing $r_{c,DATA}$ (e.g., $r_{c,DATA} << r_i + d$) will yield a carrier sensing range that is not sufficient to eliminate or reduce the effect of hidden terminals (that is data frame collision rate gets larger). Here, $r_i = 1.78 \cdot a_{data}$. This results in a decrease in the node's throughput. Similar results are obtained for different node densities. Note that the maximum throughput corresponds to $r_{c,DATA} < r_i + d$ (a point that is computationally expensive to find [10]). The authors of [10] have highlighted this issue and noted that the condition at which the carrier sensing range

just entirely covers the interference range ($r_{c,DATA} = r_i + d$ which corresponds to C = 2.78) is well suited to be used in the design of of distributed and localized algorithm as pointed in Figure 3.6(a). Hence, this condition is used to study the system throughput as the transmission power is varied. Figure 3.6(b) shows that as a_{data} increases, the throughput decreases. At larger a_{data}, the interference area at the receiver increases and accordingly the number of nodes in that area increases. Therefore, the likelihood for DATA collision from these nodes, transmitting simultaneously with the transmitter, increases. Additionally, as a_{data} increases (while maintaining $r_{c,DATA} = r_i + d$), the area covered by the carrier sensing range and outside the interference range increases (the exposed terminal area), therefore impacting the spatial reuse and ultimately the throughput. Moreover, as can be seen from Figure 3.6(b), an optimum carrier sensing threshold exists for a particular a_{data} (for instance, the throughput at a_{data} = 150 m for C = 2.78 is higher than that at C = 1.5 , whereas it is vice versa at a_{data} = 100 m). Note that the ACK message does not experience any collision under this condition ($r_{c,DATA} = r_i + d$, however all nodes falling in its carrier sensing range will be silenced for EIFS period. Accordingly, a large a_{data} further impacts the spatial reuse.

3.2.3 Basic access vs RTS/CTS access scheme

The basic and RTS/CTS handshake schemes (Figures 3.7(a),(b)) are compared in this subsection. In the RTS/CTS access method, we set $a_{RTS} = a_{data}$ (recall that a larger a_{RTS} showed earlier worse performance). We set $C = 2.78$ (i.e., the case when the probability of RTS collision resulting from hidden nodes is zero for RTS/CTS access scheme and the DATA collision probability of the basic access scheme is zero) and the throughput is measured as a_{data} is varied.

We observe in Figure 3.7(a) that the basic scheme slightly outperforms the RTS/CTS

scheme for larger packet size (i.e, 1000 bytes) and the throughput becomes more identical for higher a_{data} (the same analysis as before explains the reason the throughput decreases as we increase a_{data} in both cases). Note that in both schemes, we observed a similar data collision probability. However, it is intuitive to understand why the basic access scheme has shown a slight improvement, since an (inefficient) RTS/CTS exchange is introduced per each transmission (i.e., more control overhead). Notice that for smaller packet sizes (e.g., 64 bytes), the overhead introduced by the RTS/CTS exchange becomes more pronounced and thus the basic access scheme shows better performance than the RTS/CTS access scheme; for example, a difference of 20Kbps is observed when a_{data} is small. As a_{data} increases, we observe a decrease in the transmission probability, impacting equally the spatial reuse for both access methods. As before, the throughput in both methods decreases and the difference between them becomes less noticeable.

Figure 3.7(b) shows the same comparison, but using higher transmission rates (11Mbps). The results show that the two way handshake always outperforms the four way handshake, with the two way performing much better at lower a_{data} for both smaller and larger payloads. At larger a_{data} the spatial reuse limits the performance of the network and hence we focus our discussions on smaller a_{data}. First we note that control messages are always transmitted at 2Mbps [5]. As the data rate (transmission rate for DATA packets) increases, the SIR threshold ζ increases; for example, for a data rate of 11 Mbps , ζ becomes 15dB [5] which yield a new interference range for the receiver of a DATA packet of $2.37 \times a_{data}$. Since control packets are always transmitted at the lowest rate, the interference range remains $1.78 \cdot a_{RTS}$.

We observe higher collision rates in the basic access method than in the four-way. This is due to the fact that (1) RTS in the RTS/CTS mechanism experiences less collision than DATA in the basic ($r_{i,RTS} < r_{i,DATA}$) and (2) DATA collision in the RTS/CTS mechanism is either small (for larger data payloads) or negligible (for

smaller payloads). Notice that the interference range of the DATA packet falls inside the carrier sensing range for CTS packet. Nodes in the interference range for DATA packet receiver, and outside the carrier sensing range for DATA, will be silenced for EIFS period, upon the transmission of a CTS. Given the high data rate, the transmission duration of DATA packet becomes very small, and even smaller when the payload is small. Hence, the vulnerable period becomes either small or negligible. Alternatively, in the basic access method, DATA packet collision is larger because of the larger interference range ($r_{i,DATA} = 2.37 \times a_{data}$) and hence more hidden nodes.

On the other hand, as the transmission rate increases, the transmission duration for DATA packet becomes small and hence the overhead from control packets becomes excessive. This explains the better performance obtained in the basic access method (it has been also verified that the busy time in the RTS/CTS handshake is much larger than that in the basic access). One additional observation at smaller payloads is that RTS/CTS will affect the spatial reuse; that is, nodes in the carrier sensing range of both RTS and CTS will defer for EIFS period, while it will take much smaller time for the transmission of DATA packet at larger data rates. Accordingly, RTS/CTS will unnecessarily force nodes to defer their transmission for longer times.

3.3 Simulation Results

Here, we validate our analysis of the proposed model and compare the analytical results obtained for the throughput with simulation results obtained using Qualnet [111]. In the network, 100 nodes are regularly placed in a $10x10$ grid topology within an area of $1000 \times 1000m^2$.The distance between a node and its closest neighbor is 100 m. We consider CBR (constant bit rate) traffic of packet size 1000 bytes, unless otherwise specified. Each source node transmits packets to its receiver at a distance $a_{data} = r$ and r is varied for different experiment runs. For example when $r = 100m$, there exists 50 CBR flows (5 in each row of the grid) and when $r = 200m$, there

exists 30 flows (3 in each row) in the network. The packet generation rate is high enough to saturate the network; that is a node always has packets to send out. The carrier sensing threshold is set to - 87 dbm and the received threshold to -78 dbm. The throughput is calculated by taking the average of the received bytes of these flows divided by the simulation time (300 seconds). We use 5 simulation seeds to calculate the average single node throughput. 95% confidence levels are also plotted for each simulation run. The corresponding transmit power values used to reach 100 , 200, 300 and 400 meters are respectively 0.5 dBm, 12.5 dBm, 20 dBm and 24.5 dBm. We compare first the RTS/CTS access mechanism with basic scheme for different $a_{data} = r$. Figures 3.8 (a) and (b),(c), (d) compare the analytical and simulation results for single node throughput for the basic and RTS/CTS schemes respectively for different r. Now we consider the scenario when the RTS packet is transmitted to cover range $a_{RTS} = 200m$ and $a_{RTS} = 300m$ and we study accordingly the effect of changing the data power value to cover range a_{data}. The results are shown in Figures 3.8 (e), (f). The average relative error in prediction of the individual throughput recorded is 8.9 % for two-way handshaking and 10.02 % with four-way handshake.

3.4 Conclusions

In this chapter, a realistic analytical model for power-aware multi-hop wireless networks is presented to study the interplay between tuning carrier sensing threshold and transmission power control. The model has been validated through simulations using Qualnet simulator. Our results showed that both carrier sensing threshold and transmit power have major impact on network performance. While decreasing the CS threshold impacts the spatial reuse, a larger CS threshold will yield severe interference among concurrent transmissions rendering power control ineffective. We observed that there exists an optimal CS threshold that strikes a balance between

spatial reuse and collisions resulting from interfering nodes. Controlling transmission power while selecting an appropriate CS threshold showed to be quite effective. Moreover, the smaller the size of the data frame is, the more advantageous to tune the CS rather than perform power control. The model has also been used to expose the performance of the RTS/CTS access scheme; although these control messages may slightly reduce the collision among contending hosts, their impact on spatial reuse and the added overhead outweighs their benefits and specifically when using higher rates. The comparative study showed that the basic access always outperforms the RTS/CTS access method.

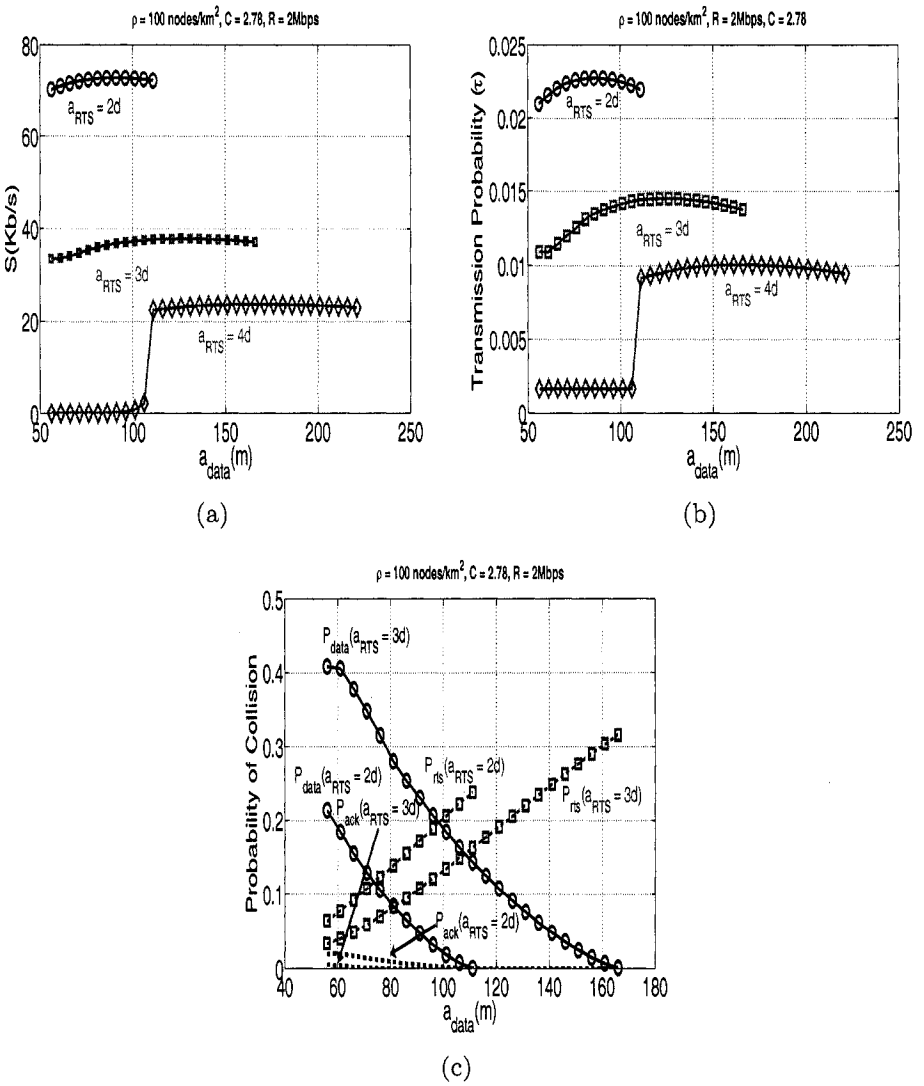

Figure 3.3: Throughput 4-way handshake for different a_{RTS}

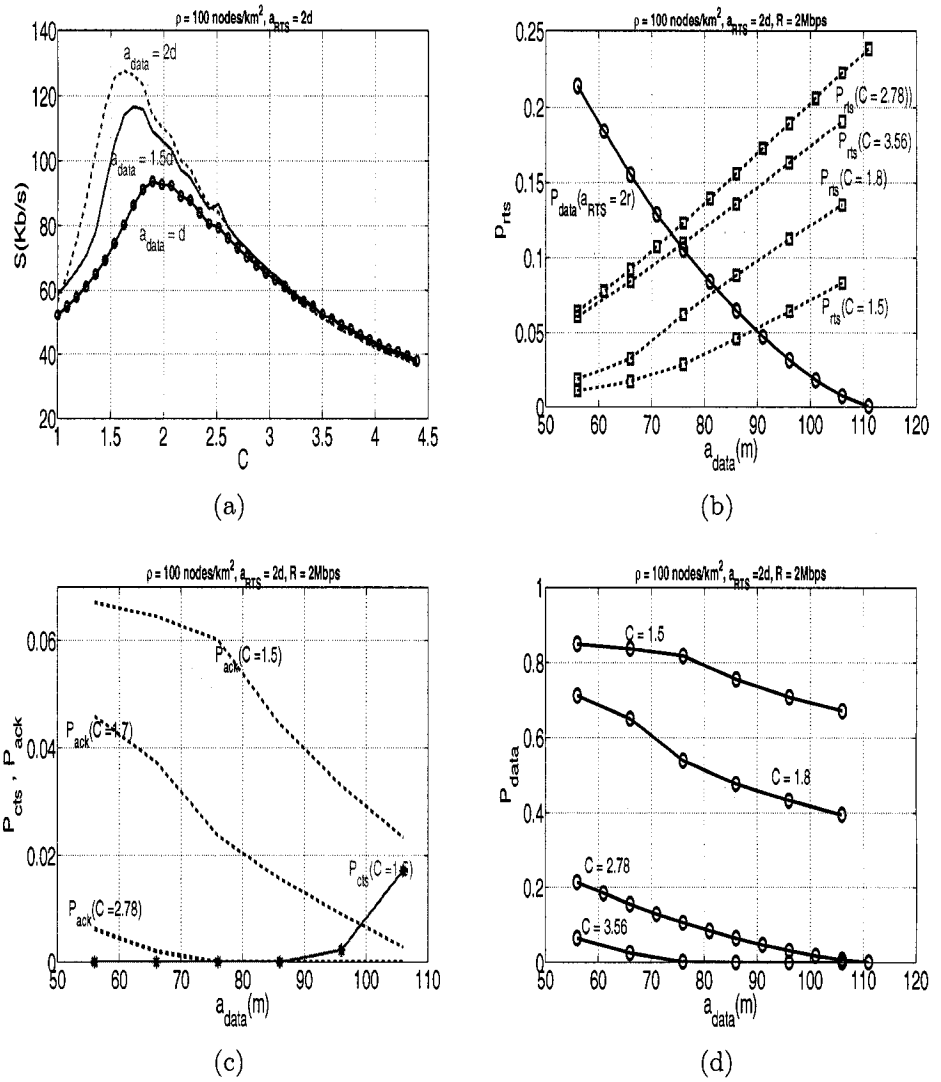

Figure 3.4: Throughput 4-way handshake R = 2 Mbps for different carrier sensing thresholds

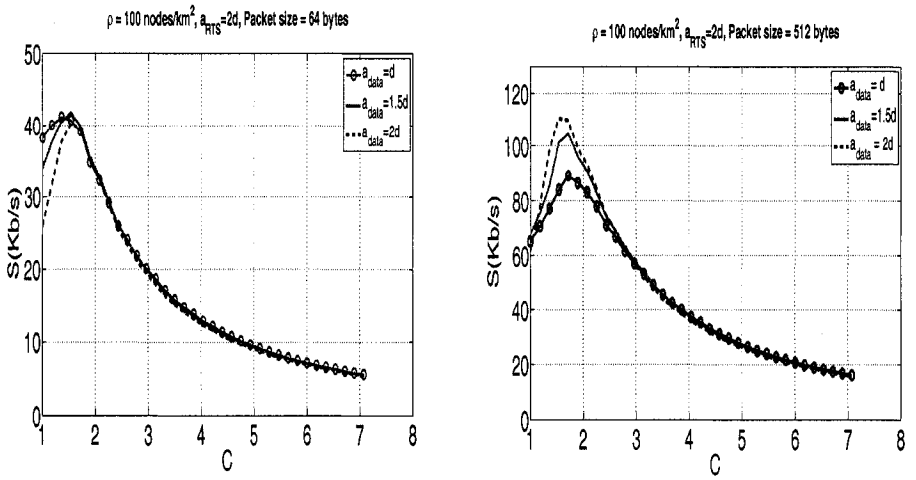

Figure 3.5: Throughput 4-way handshake R = 2 Mbps for different packet sizes

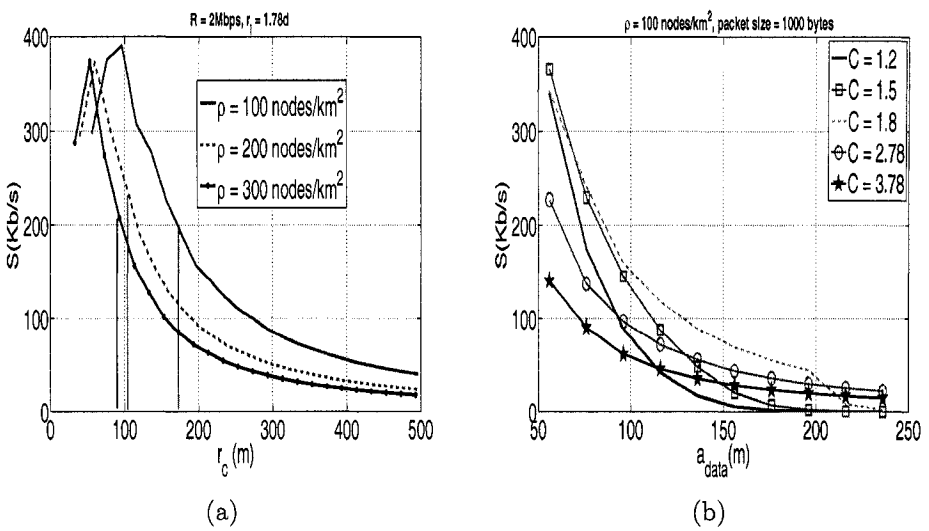

Figure 3.6: Evaluation of basic access method

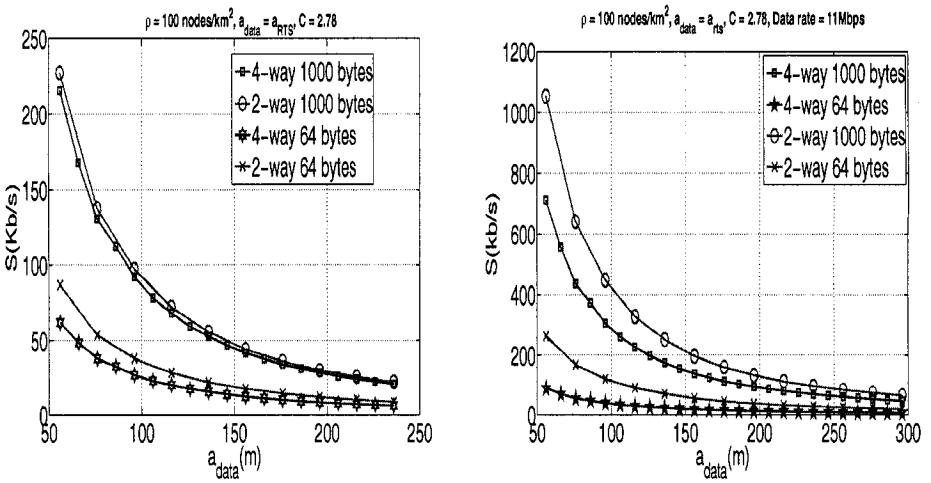

Figure 3.7: four-way vs 2 way handshake for different packet sizes

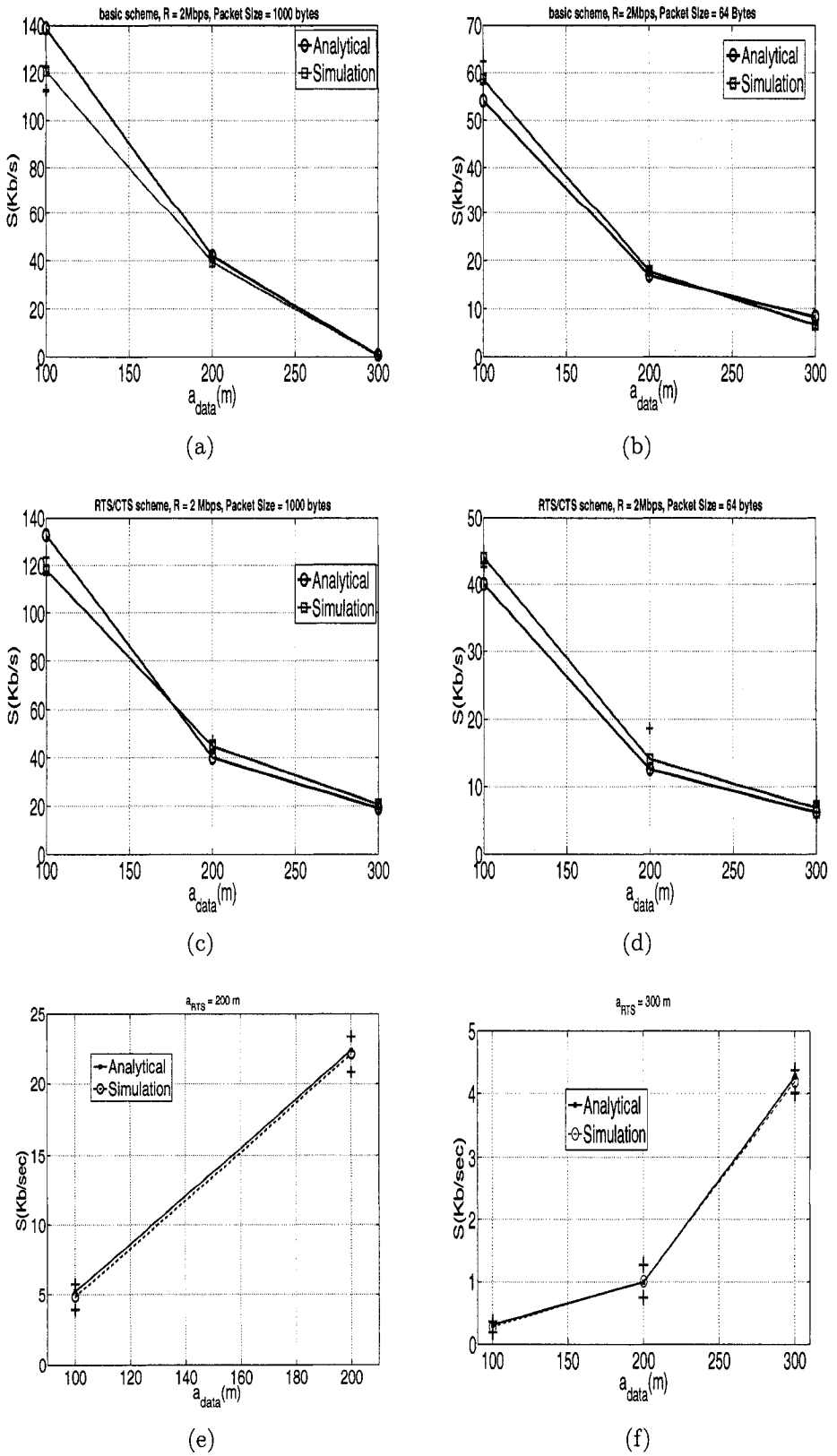

Figure 3.8: Simulations vs Analytical

Chapter 4

Improving the Performance of Multihop Wireless Networks Through Power and Rate Control

In multihop, multi-rate wireless networks, simultaneous transmissions can interfere with one another and prevent correct frame reception. Hence, achieving high network capacity in these networks requires a balance between the spatial reuse and the transmission quality. Spatial reuse can be increased by tuning the carrier sense threshold to reduce the carrier sense range or by controlling the transmission power. However, high spatial reuse results in more concurrent transmissions and accordingly the transmission quality is affected either because of the increased interference level or due to a weak received signal (resulting in both cases in a lower signal to interference plus noise ratio, SINR). As a result, the sustained transmission rate may decrease. To achieve a tradeoff between spatial reuse and transmission quality, a decentralized power and rate control algorithm (PRAS) is proposed in this chapter that allows a sender and receiver pair, using the four way access method, to adjust the transmit power and rate for their frames according to the level of interference

in the network. The algorithm outlines the rules for performing power and rate assignment so that higher performance is obtained. A realistic analytical model to study the performance of the proposed heuristic is then presented; analytical results show that the proposed algorithm, indeed, finds the balance between spatial reuse and transmission quality through its appropriate search for the suitable transmission parameters. Simulation experiments are carried to compare the performance of the proposed algorithm to other heuristics; our results indicate a remarkable performance both in terms of achieved throughput and energy consumption.

The rest of the chapter is as follows. Section 4.1 presents the concepts for the proposed power and rate control scheme and proposes different heuristics supported by sound analysis. Section 4.2 presents the performance evaluation and comparisons of the methods and finally, the conclusion of the work is presented in section 4.3.

4.1 Distributed Power and Rate Adaptive Scheme (PRAS)

4.1.1 Preliminaries

Clearly, the level of spatial reuse plays a key role in determining the capacity of a multihop wireless network [46]. As mentioned earlier, one can increase the level of spatial reuse either through reducing the transmission power or increasing the CS_{th}. We focus in this work on the former approach and assume a fixed CS_{th}. While decreasing the transmission power allows multiple concurrent transmissions to co-exist, a reduced transmission power, however, yields a lower SINR which results from either a weaker received signal or increased interference level [73]. This consequently yields to a lower data rate that is sustained by each transmission, ultimately affecting the system performance. Additionally, a lower transmission power would result in a higher interference range (Eq. 2.6) and hence more hidden nodes that may corrupt

the transmission between a sender and a receiver. Alternatively, increasing the transmission power enhances the capture effect (SINR) and thus decrease the possibility of collision from hidden terminals. With enhanced SINR, a node can use higher rates for sending its packets and this would yield to a better throughput. However, larger sender transmission power adversely impacts the spatial reuse by unnecessarily suppressing concurrent communications. Hence, in order to achieve higher level of spatial reuse and thus network throughput, one needs to find a balance between the transmission power and the transmission rate. To achieve this, one can derive analytically the network capacity as a function of both the transmission power and the SINR threshold (hence the transmission rate) [10] and study the interplay among these parameters so that a maximum capacity can be achieved. In this work, a localized heuristic method for power and rate control is presented.

It is to be noted first that in [10] the authors observed that a high system throughput can be achieved when the area silenced by a sender is reduced as much as possible under the premise that the interference area of its intended receiver is covered by the silence area. An alternative method for protecting the sender transmissions by appropriately selecting the transmission power and rate while minimizing the exposed terminals is derived. The four-way handshake mode of operation of the DCF is assumed. Furthermore, a realistic analytical model is presented that characterizes the transmission activities governed by the proposed heuristic in a single channel, power-aware, multihop wireless network.

4.1.2 Methodologies

Consider a data frame transmission between two nodes A and B (Figure 4.1). We assume an RTS frame, whose silence range is $r_{c,RTS}$, has been successfully transmitted and we consider first the protection of the CTS packet reception. Here, if the receiver (B) selects a transmission power for its CTS frame such that the interference range

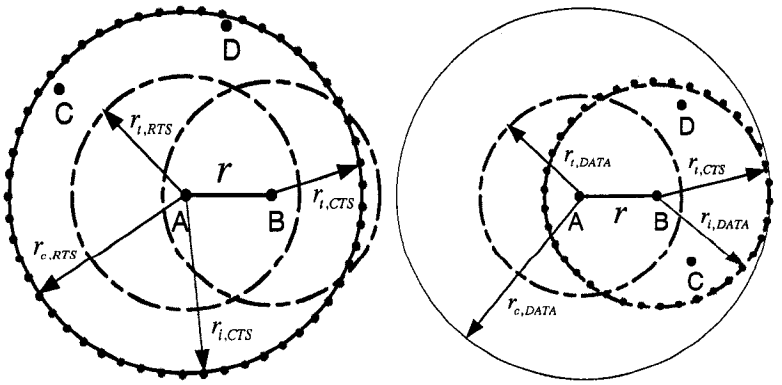

(a) PCS to protect CTS (b) VCS and PCS to protect DATA

Figure 4.1: Collision Avoidance Analysis

at the receiver of the CTS packet (A), $r_{i,CTS}$, coincides with or falls inside the area silenced by the RTS ($r_{c,RTS}$), then the CTS frame will be received uncorrupted. We call this the physical carrier sense (PCS) approach and is shown in Figure 4.1(a). Here, although nodes C and D lie in the interference range of the CTS packet(refer to equation 2.6), they cannot initiate any communication while the CTS is being received because they already lie in the silence range of the RTS frame. Both nodes (C and D) are silenced upon hearing the RTS for an Extended Inter-Frame Space (EIFS) [5]. Since EIFS is a sufficient duration for a CTS packet to be received at the transmitter (A), the reception of CTS packet will not be corrupted. A similar approach to that of CTS protection, is adopted for protecting the ACK packet reception by setting $r_{c,DATA} = r_{i,ACK}$.

On the other hand, the EIFS duration is not sufficient to protect larger DATA frames since the transmission duration (which is denoted as the vulnerable period) may be much longer than EIFS period; accordingly, two alternative approaches may be used to protect the transmission of the DATA packet. The first one is a virtual carrier sense (VCS) approach and is achieved by selecting a transmission power and rate for DATA such that the resulting interference range at the receiver (B) is completely covered by the transmission range, $r_{t,CTS}$, of the ensued CTS frame.

The second alternative is a PCS approach; here, the sender (of the DATA frame) will make sure that the area silenced by its transmission covers the interference area around the intended receiver as shown in Figure 4.1(b). Now, in order to prevent collisions while maintaining a high level of spatial reuse, we propose to dynamically switch between the two approaches.

First, we analyze the minimum power requirements for delivering the CTS packet; let P_{RTS} and P_{CTS} be the transmission power of RTS and CTS packets, respectively. The selection of P_{RTS} is presented later in the section. Using equation (2.6), we can obtain the interference range at the receiver of the CTS packet, $r_{i,CTS} = \left(\frac{P_i}{\frac{P_{CTS}}{r^4 \cdot \zeta_{R,CTS}} - P_{cn}}\right)^{\frac{1}{4}}$. Here, $\zeta_{R,CTS}$ is the SINR threshold when receiving a CTS packet at rate R_{CTS} and P_i is the estimated transmission power of an interfering node F. We will explain how to estimate P_i later in the section. Furthermore, from equation (2.3), we can obtain $r_{c,RTS} = (\frac{P_{RTS}}{CS_{th}})^{\frac{1}{4}}$. Since PCS is applied to control the power of the CTS packet as discussed earlier and shown in Figure 4.1(a), we choose $r_{i,CTS} \leq r_{c,RTS}$ in order to prevent collisions from hidden nodes (those in the interference range of the receiver of the CTS but outside the silence range of the RTS frame). Thus, for equality, the lower bound on P_{CTS} can be expressed as:

$$P_{CTS,low} = max[P_{min}, (\frac{CS_{th} \cdot P_i}{P_{RTS}} + P_{cn}) \cdot \zeta_{R,CTS} \cdot r^4] \tag{4.1}$$

where P_{cn} is the current noise measured at the sender node and is encapsulated in the RTS frame.

As we mentioned earlier, there are two approaches for protecting the DATA frame against interference from hidden nodes. In one approach, we set the interference range of DATA ($r_{i,DATA}$) equal to the transmission range of CTS, $r_{t,CTS}$, (note, if the vulnerable period is smaller than EIFS, e.g., case of shorter data frames and higher PHY transmission rates, then the silence range, rather than the transmission range, of CTS may be used). Here, the transmission range of the CTS packet can be expressed

using equation (2.2) as $r_{t,CTS} = (\frac{P_{CTS}}{\kappa_{R,CTS}})^{\frac{1}{4}}$, where $\kappa_{R,CTS}$ is the receiver sensitivity of a transmitted CTS at rate R_{CTS}. Moreover, the interference range of the DATA packet is expressed as $r_{i,DATA} = (\frac{P_i}{\frac{P_{DATA}^{(1)}}{r^4 \cdot \zeta_{R,DATA}} - P_{cn}})^{\frac{1}{4}}$. $P_{DATA}^{(1)}$ is the transmission power of the DATA packet and $\zeta_{R,DATA}$ is the SINR threshold requirement when receiving a DATA packet transmitted at rate R_{DATA}. Accordingly, by making $r_{t,CTS} = r_{i,DATA}$, we obtain:

$$P_{DATA}^{(1)} = max[P_{min}, (\frac{\kappa_{R,CTS} \cdot P_i}{P_{CTS}} + P_{cn}) \cdot \zeta_{R,DATA} \cdot r^4] \leq P_{max} \tag{4.2}$$

where P_{cn} is the current noise measured at the receiver upon receiving the CTS packet and P_{max} is the maximum available transmission power. In addition $P_{DATA}^{(1)}$ is dependent on the SINR threshold, $\zeta_{R,DATA}$, whose value depends on the data transmission rate.

If the PCS approach is used, the silence range of the DATA packet $r_{c,DATA}$ will cover the interference range of the DATA packet receiver. Then, by setting $r_{c,DATA} = r_{i,DATA} + r$ (where r is the sender-receiver distance), we obtain:

$$P_{DATA}^{(2)} = \frac{1}{2} \cdot (\sqrt{2 \cdot u} + \sqrt{2 \cdot u - 2 \cdot g - 4 \cdot u + \frac{2 \cdot q}{\sqrt{2 \cdot u}}} - s) \tag{4.3}$$

where

$u = (\frac{y}{2} + \sqrt{\frac{y^2}{4} + \frac{x^3}{27}})^{\frac{1}{3}} + (\frac{y}{2} - \sqrt{\frac{y^2}{4} + \frac{x^3}{27}})^{\frac{1}{3}} - \frac{1}{3}$

$x = \frac{2 \cdot g^2 - 8 \cdot m}{8} - \frac{8}{3}$

$y = \frac{-2}{27} + \frac{2 \cdot g^2 - 8 \cdot m}{24} - \frac{1}{8}$

$m = (P_i^4) \cdot (r^3 \cdot \zeta_{R,DATA})^4 - (P_i) \cdot (r^3 \cdot \zeta_{R,DATA})^5 \cdot (\frac{P_{cn}}{CS_{th}} + \frac{4 \cdot P_i^3}{r^3 \cdot \zeta_{R,DATA}})$

$g = (4 \cdot P_i^2 \cdot r^3 \cdot \zeta_{R,DATA})^2 - \frac{r^5 \cdot \zeta_{R,DATA}^3}{CS_{th}} - 6 \cdot (4 \cdot P_i \cdot r^3 \cdot \zeta_{R,DATA})^2$

$q = (r^3 \cdot \zeta_{R,DATA})^4 \cdot (\frac{P_{cn}}{CS_{th}} + \frac{4 \cdot P_i^3}{r^3 \cdot \zeta_{R,DATA}}) - \frac{4 \cdot P_i \cdot r^3 \cdot \zeta_{R,DATA}}{2} \cdot (4 \cdot P_i^2 \cdot (r^3 \cdot \zeta_{R,DATA})^2 - \frac{r^5 \cdot \zeta_{R,DATA}^3}{CS_{th}})$
$+ (4 \cdot P_i \cdot r^3 \cdot \zeta_{R,DATA})^3$

$s = P_i \cdot r^3 \cdot \zeta_{R,DATA}$

Since both $P^{(1)}_{DATA}$ and $P^{(2)}_{DATA}$ can protect DATA packet transmission from hidden terminals, we select the smaller between the two; this strategy would indeed decrease the energy consumption and enhance the spatial reuse. Thus, by combining equations (4.2) and (4.3), we obtain the following system:

$$P_{DATA} = min[P^{(1)}_{DATA}, P^{(2)}_{DATA}] \tag{4.4a}$$

$$P_{max} \geq P_{CTS} \geq P_{CTS,low} \tag{4.4b}$$

The solution to the above system is a tuple (P_{CTS}, $\zeta_{R,DATA}$,P_{DATA}), and there may exist more than one feasible solution among which we need to select one that yields the best performance. Recall that the values of P_{CTS}, $\zeta_{R,DATA}$, and P_{DATA} are selected from a set of discrete power and transmission rate levels available for the node with $P_{DATA} \leq P_{max}$ and $P_{CTS} \leq P_{max}$. We consider two alternative approaches ($PRAS1$,$PRAS2$) for determining P_{DATA}, P_{CTS} and $\zeta_{R,DATA}$. For $PRAS1$, we select $P_{CTS} = P_{CTS,low}$. This selection stems from our understanding that a large P_{CTS} may unnecessarily silence more nodes and hence could severely affect the channel spatial reuse. Alternatively, for $PRAS2$, we set $P_{CTS} = P_{max}$ in order to reserve a larger transmission floor for the DATA packet (i.e., eliminate the possibility of collisions).

Algorithm 1 DATA RATE and Power Control Heuristics

1. $P_{CTS} \leftarrow P_{CTS,LOW}$ (for $PRAS_2$ $P_{CTS} \leftarrow P_{max}$)
2. $R \leftarrow$ *the highest rate*
3. $P^1{}_{DATA} \leftarrow \frac{\kappa_{R,CTS} \cdot P_i}{P_{CTS}} + P_{cn}) \cdot \zeta_{R,DATA} \cdot r^4$
4. $P^2_{DATA} \leftarrow$ *equation*4.3
5. $P_{DATA} = min[P^1_{DATA}, P^2_{DATA}]$

if $P_{DATA} > P_{max}$ **then**
  if $p_{c,R} > \theta$ **then**
    6. $R \leftarrow R - 1$
    7. GOTO 3.
  end if
end if

8. $P_{DATA} \leftarrow min[P_{max}, P_{DATA}]$

Given P_{CTS}, we then propose a heuristic (refer to Algorithm 1) that jointly selects transmission power and rate for sending the DATA packet. Initially, a node selects the

highest transmission rate and calculates P_{DATA} according to equation (4.4). Then, the node checks whether P_{DATA} is greater than P_{max} (recall that P_{DATA} is bounded by P_{max}); in this case, the interference area (at the receiver of the DATA frame) resulting for the highest rate may not be completely covered by the transmission range of the CTS or the silence range of DATA, which leaves some hidden nodes uncovered and may corrupt the transmission of the DATA during the vulnerable period. These corrupted packets (whose rate is denoted as the frame error rate) are to be distinguished from packets lost due to collision which are the result of simultaneous transmissions. Note that if the sender reduces the transmission rate, then the frame error or corruption rate may be reduced, as a result of the more robust modulation, and hence a better throughput may be obtained. Therefore, a node needs to decide when it is beneficial to switch to a lower rate; quickly reducing the rate may yield a poor performance since the transmission at lower rates will take longer, although the frame error rate may be reduced. The authors of [76] have noted that a node should switch to a lower transmission rate only if the throughput obtained at the lower rate is at least equal to that obtained at higher rate. Accordingly, a frame error rate threshold (θ) exists, above which it is beneficial to switch the transmission rate. For example, for IEEE 802.11b, one needs to switch from 11Mbps to 5.5Mbps when the frame error rate exceeds 50% [76]. In our PRAS heuristic, the transmission rate is only reduced when the frame error rate exceeds a threshold θ. The DATA frame error rate is easily measured at the receiver by having the sender piggyback to the receiver every unacknowledged DATA frame (1 bit is enough in the next RTS frame); note that since we are using the four way handshake, DATA frames do not experience collision from simultaneous transmission (in the rest we use the term collision probability and frame error rate interchangeably for denoting the DATA frame loss rate due to interference).

Finally, given that the DATA packet is successfully received, the ACK power value

can be derived similar to the way we derived the lower bound for the power of CTS by making $r_{c,DATA} = r_{i,ACK}$. The power of ACK is expressed as:

$$P_{ACK} = max[P_{min}, (\frac{CS_{th} \cdot P_i}{P_{DATA}} + P_{cn}) \cdot \zeta_{R,ACK} \cdot r^4] \tag{4.5}$$

where $\zeta_{R,ACK}$ is the SIR threshold for an ACK frame received at rate R_{ACK}. P_{cn} is the measured noise when receiving the CTS packet and it is encapsulated in the DATA packet.

4.1.3 Analytical Model for PRAS

We extend the model presented in chapter 3 to study the performance of our proposed power and rate adaptive scheme (PRAS). Moreover, we revise and add the following assumptions:

- The receiver sensitivity for all packets is equal and accordingly we denote a_{RTS}, a_{CTS}, a_{DATA}, a_{ACK} to be the transmission ranges of the RTS, CTS, DATA and ACK packets. Moreover, we define a_i to be the transmission range of a neighboring node F (neighbor to a receiver B) whose transmission interferes with the frame reception (at B) and whose transmission power determines the interference range around B (Equation 2.6).

- The current noise P_{cn} equals to zero.

- The system time is slotted with σ seconds. RTS, CTS, DATA and ACK packets are assumed to be with fixed length of L_{RTS}, L_{CTS}, L_{DATA} , L_{ACK} bits. The control channel bit rate is assumed to be R_c (Mbps) and the DATA channel bit rate to be R (Mbps). Thus the transmission of an RTS/CTS/DATA/ACK packets will last for $T_r = \frac{L_{RTS}}{R_c \cdot \sigma}$, $T_c = \frac{L_{CTS}}{R_c \cdot \sigma}$, $T_d = \frac{L_{DATA}}{R \cdot \sigma}$, $T_a = \frac{L_{ACK}}{R_c \cdot \sigma}$ respectively.

- Each node in the network initiates a transmission to one of its neighbors in a

randomly chosen virtual time slot, for a duration of T_{avg}. T_{avg} has been defined and derived in chapter 3 in equation 3.17.

A first parameter of interest is the attempt probability τ that a node transmits in a randomly chosen virtual slot and is given by equation 3.5. Recall that p in equation 3.5 is the probability that a node senses the channel busy and is given by $p = 1-(1-\tau)^{N_c}$, where N_c is the number of active nodes in the carrier sensing zone of the transmitter. When all nodes use the same transmission power, $N_c = \rho \cdot \pi d_{cs}^2$ where d_{cs} is the carrier sense range and ρ is the active density. However, since nodes may use different transmission power when sending out their frames, the carrier sense zone of a node A (CS_A) is no longer circular and takes an arbitrary shape. In order to determine the average number of nodes in CS_A, we assume a circular carrier sense zone whose radius is $\bar{d}_{cs}$(the average carrier sense range) where $(\frac{\kappa}{CS_{th}})^{\frac{1}{4}} = 2$. Hence, $N_c = \rho \cdot \pi \bar{d_{cs}}^2$. Here, $\bar{d}_{cs}$ can be approximated by:

$$\bar{d}_{cs} = (A + B) \cdot C \tag{4.6}$$

where

$A = \tau \cdot a_{RTS} + \tau \cdot (1 - p_{rts}) \cdot a_{CTS} + \tau \cdot (1 - p_{rts}) \cdot (1 - p_{cts}) \cdot a_{DATA}$

and

$B = \tau \cdot (1 - p_{rts}) \cdot (1 - p_{cts}) \cdot (1 - p_{data}) \cdot a_{ACK}$

and

$C = \frac{2}{\tau+\tau\cdot(1-p_{rts})+\tau\cdot(1-p_{rts})\cdot(1-p_{cts})+\tau\cdot(1-p_{rts})\cdot(1-p_{cts})\cdot(1-p_{data})}$

where p_{rts}, p_{cts}, p_{data}, p_{ack} are the collision probabilities of RTS, CTS, DATA, and ACK frames respectively.

Now, according to the methodology of our proposed heuristic (e.g., equations (4.1)-(4.5)), the CTS, DATA and ACK packets are all protected by appropriately selecting their transmission power as well as the data rate (in the case of a DATA frame). However, as we explained in the previous section, DATA frame corruption need not be completely eliminated, especially when the advantages of transmitting at higher rates outweighs the benefits of eliminating the frame error rate (that is by reducing the transmission rate). For example, in a dense network deployment, where the intensity of the interfering signal is strong (i.e., larger a_i), the value of P_{DATA} required to protect the transmission of the DATA frame may be larger than P_{max}; in order to completely protect the frame, the sender must reduce its transmission rate (since P_{DATA} is bounded by P_{max}) to reduce the interference range. Reducing the transmission rate, however, does not necessarily yield better throughput. On the other hand, since control frames are transmitted at the lowest transmission rate, the selection of P_{CTS} and P_{ACK} guarantees that these frames are not corrupted following PRAS methodology. Accordingly, $p_{cts} = p_{ack} = 0$, and equation (3.6) yields $P_c = 1 - (1 - p_{rts}) \cdot (1 - p_{data})$.

Finally the throughput, (S), for each transmitter is calculated from equation 3.19:

$$S = \frac{P_t \cdot L_{DATA}}{T_{avg}}$$

4.1.4 PRAS Analysis

In order to analyze the proposed power and rate control heuristic, we use the model developed in the previous section. Here, we measure the network performance by varying a_i (a_i corresponds to the transmission range of the interfering node F), a_{RTS} and the distance r between the transmitter and the receiver. In our model, the minimum r is initialized to 56 m ($r_{min} = \frac{1}{\sqrt{\rho \cdot \pi}} = 56m$ for $\rho = 100 nodes/km^2$). We first study the throughput as we vary a_i; we set $a_{RTS} = 4 * r_{min}$ and $r = 3 \cdot r_{min}$. We

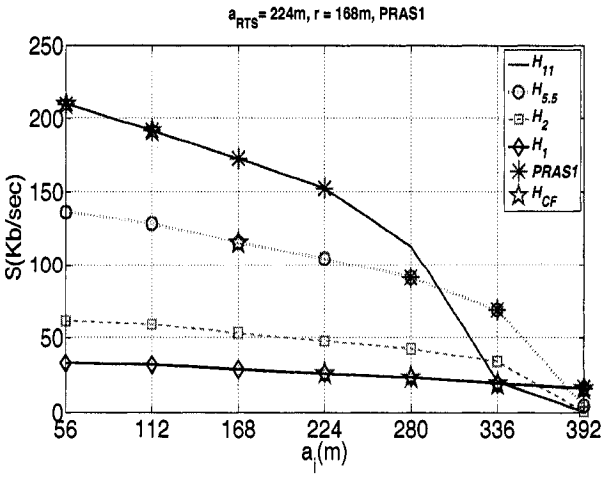

Figure 4.2: $PRAS1$ Throughput versus a_i

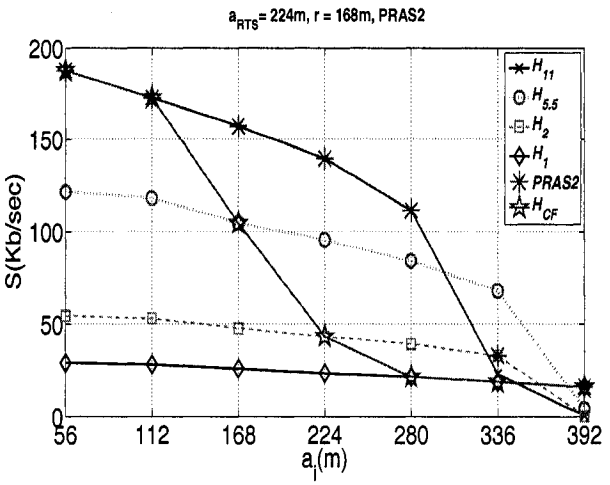

Figure 4.3: $PRAS2$ Throughput versus a_i

consider both PRAS1 ($P_{CTS} = P_{CTS,low}$) and PRAS2 ($P_{CTS} = P_{max}$) and we compare their performances (Figures 4.2 and 4.3) with other heuristics where the transmission rates are fixed (H_{11}, $H_{5.5}$, H_2, H_1), but the power assignment is done according to Equations (4.1)-(4.5). We also include, for comparison purposes, the model for the heuristic wherein hosts attempt to eliminate DATA frame corruption by responding to any packet loss by reducing the transmission rate (H_{CF}). We assume for PRAS a threshold $\theta = 0.6$.

Figures 4.2 and 4.3 show the throughput performance for PRAS1 and PRAS2 schemes respectively, as we vary a_i. Clearly, the figures show that as the strength

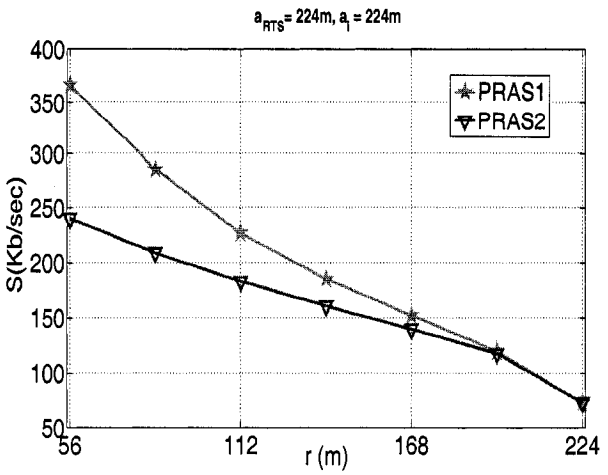

Figure 4.4: Throughput versus distance

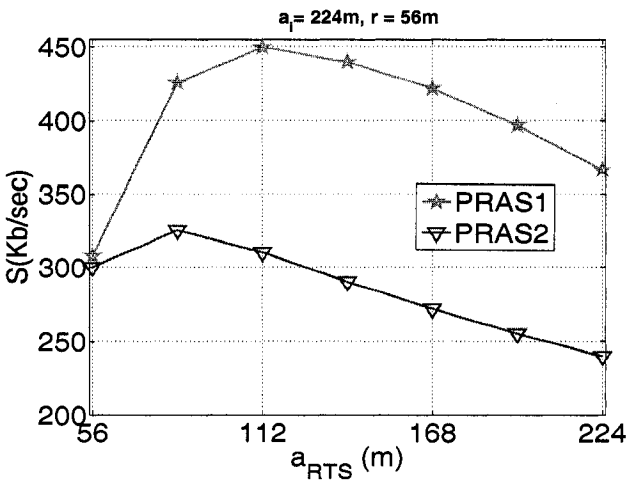

Figure 4.5: Throughput versus a_{RTS}

of the interfering signal(s) increases, the throughput for all schemes decreases. This is intuitive since larger values of a_i implies a larger interference range (Eq. 2.6) and results in a smaller SINR at the receiver, leading either to higher frame corruption rates or forcing the sender to respond by reducing its transmission rate (if the rate is not fixed). In either case, the transmission duration would either be longer (in the latter) resulting in larger value for $T_{transmit}$ or frame retransmission and collision would be excessive (in the former) resulting in larger values of T_{busy} and T_{col} (and hence larger T_{avg}); this explains, the lower throughput obtained when a_i is large. Further, larger a_i requires a larger transmission power for CTS, DATA and ACK frames (Equations (4.1)-(4.5)) to overcome the interference which may unnecessarily silence other senders in the vicinity, limiting the spatial reuse in the network (and as a result, T_{busy} increases).

Figure 4.2 shows that when the interference in the network is strong (i.e., larger a_i), transmitting at smaller rates yields more benefits to the network than larger rates; this is indeed intuitive since smaller transmission rates are more robust to interference. This is shown in the figure as we compare the performances of H_{11} and $H_{5.5}$. It is to be noted also that although H_{11} enjoys a smaller $T_{transmit}$, $H_{5.5}$ has smaller T_{col} and T_{busy} when a_i is large. Now, the performance of PRAS1 is similar to that of H_{11} when a_i is small. Initially, a node deploying PRAS1 always uses the largest transmission rate (11Mbps) for sending out its frames; the transmission power used for sending the frames is the same as that of H_{11} and therefore the same throughput performance is achieved. At larger a_i, the interference range around the receiver becomes larger, and hence the power, P_{DATA}, required to overcome the frame corruption may exceed P_{max}. Since P_{DATA} cannot exceed P_{max}, the DATA frame error corruption (p_{data}) is evaluated and compared with the threshold θ. If the corruption rate exceeds θ, then a node would gain more if it switches to the smaller transmission rate. This is indeed shown in Figure 4.2; as a_i increases, the performance of PRAS1 converges towards

the optimal rate (e.g., that of $H_{5.5}$ or H_2), outperforming H_{11}. It is interesting to note that H_{CF} performs quite good at very low a_i and then rapidly degrades (as a_i increases) due to the premature switching to lower transmission rates as soon as a frame corruption is experienced. Similar performance for PRAS2 can be observed in Figure 4.3.

Next we compare the performance of PRAS1 and PRAS2 as we vary the distance r separating the sender and the receiver (Figure 4.4). We set $a_{RTS} = a_i = 4 \times r_{min}$. When r is small, PRAS1 remarkably outperforms PRAS2; this is due to the fact that in PRAS2, a CTS fame is always transmitted at maximum power (P_{max}) which clearly limits the spatial reuse of the medium. Here, clearly the area silenced by the CTS frame covers more nodes than there are in the interference range of the DATA frame and consequently silencing more nodes, unnecessarily. As a result, T_{busy} is larger for PRAS2 and that explains the lower throughput. The figure also shows that the performance of both PRAS1 and PRAS2 degrades as r increases. First, when r is small, the resulting interference range (Eq.2.6) is small which yields a lower collision rate for the RTS frames. The collision for CTS, DATA and ACK frames is also negligible (here, a sender can always select the suitable transmission power for these frames to protect their reception according to PRAS methodology) and in addition the DATA frame can sustain higher transmission rates. However, as r increases, larger transmission power for the CTS, DATA and ACK frames is required which in turn yields larger $\bar{d}_{cs}$ (Eq. 4.6) and hence larger N_c (the number of nodes which, if they transmit, may silence the current sender) which results in larger T_{busy}, leading to lower throughput. Second, according to our methodology, when r increases, the interference range $r_{i,DATA}$ increases; consequently, either we need to increase P_{DATA} or reduce the transmission rate in order to protect the DATA frame. However, since P_{DATA} cannot exceed P_{max}, a sender will choose to have (i) $r_{i,DATA} \leq r_{t,CTS}$ and $r_{c,DATA} \leq r_{i,DATA}+r$ or (ii) switches to lower transmission rates.

In the former case we allow collision (packet corruption) to exist and hence packet retransmission and larger T_{col} and in the latter case transmission may take longer and hence $T_{transmit}$ would be larger. In either cases, the throughput is affected. Both PRAS1 and PRAS2 shows similar poor performance at larger r since at the CTS will always be transmitted at maximum power (in both schemes).

Finally, we use our model to compare the performance of both PRAS1 and PRAS2 as we vary a_{RTS}; we fix the distance r to 56 m and set $a_i = 4 \times r_{min}$. Figure 4.5 shows the throughput increases as we increase a_{RTS} and then decreases for larger values. Clearly, for larger values of a_{RTS}, the spatial reuse is severely impacted. On the other hand, smaller values of a_{RTS} (i.e., transmission power of RTS) would result in RTS packet corruption since the small transmission power of the RTS cannot overcome the interference at the receiver coming from hidden nodes (note that the strength of the interfering signal is not negligible since a_i is chosen large). This shows that there exists an optimal value for a_{RTS} that yields maximum throughput; in our work we adopt a heuristic for determining the RTS transmission power. Also, since PRAS1 has shown better performance than PRAS2, we will use PRAS1 thereafter in our comparisons and we will refer to it as the PRAS scheme.

4.1.5 P_{RTS} tuning and P_i Estimation

RTS Power Tuning

In PRAS, the tuning of the transmission power of an RTS frame is a key design aspect for enhancing the spatial reuse (as the analysis showed earlier). Note that all the power values of other packets should be correlated with the power of RTS packet. Initially, the RTS frame is sent at a maximum power to a destination node. If N_S consecutive RTS packets were sent successfully to the same destination, then the node decreases its RTS power value to the next lower possible power level which is higher or equal to P_{min} when sending to the same destination. Similarly, after

N_F consecutive packets reception failures, the power of RTS will be increased by one level ($P_{min} \leq P_{RTS} \leq P_{max}$). Here N_S and N_F are simulation parameters.

P_i Estimation

As stated earlier, P_i represents the transmission power of an interfering node F (F is a neighbor, say, to a receiver B); according to Eq. 2.6, determining P_i is critical for determining the interference range around B. Furthermore, according to PRAS (equations (4.1)-(4.5)), P_i is also needed to determine the power assignment of CTS/DATA/ACK frames. Therefore, a heuristic to locally determine the transmission power of a neighboring (interfering) node is needed. We note here that the value of P_i differs from one node to another. For a sender(A)-receiver(B) pair, the receiver maintains an estimate of $P_{i,A}$ ($P_{i,B}$) where $P_{i,A}$ ($P_{i,B}$) represents the transmission power of an interfering node neighbor to A (B). Initially, these values are assigned a value of P_{max} and both values are lower bounded by P_{min}. When B responds to an RTS received from A, it will use the value of $P_{i,A}$ to compute P_{CTS}. Node B will also use the value of $P_{i,B}$ to compute P_{DATA} and the data transmission rate. For every N_{CTS} CTS packets, that a node transmits, and are consecutively received successfully at the sender, $P_{i,A}$ is decreased by a factor of $\alpha \times P_{i,A}$; otherwise, if one frame is lost, $P_{i,A}$ is increased by a factor of $\alpha \times P_{i,A}$ (e.g $\alpha = 0.1$). Note, too, that $P_{i,A}$ is also updated upon the success (loss) of N_{ACK} (one) ACK packets (similar procedure as before). The same methodology applies as well for updating $P_{i,B}$ with N_{DATA} being the consecutive number of successful DATA packets received. Here, N_{CTS}, N_{DATA} and N_{ACK} are all simulation parameters. Note that, whether a CTS or an ACK packet was successfully received at the sender or not is indicated to the receiver through a previously transmitted RTS frame.

Table 4.1: Simulation Parameters

Parameter	Value			
CS_{th} (dBm)	-83.5			
Simulation Time (seconds)	300			
N_s	10			
N_F	1			
N_{DATA}= N_{CTS} = N_{ACK}	10			
θ	60%			
Power Levels (dBm)	1, 3, 5, 7, 10, 14, 18, 22, 24			
Transmission rate(Mbps)	1	2	5.5	11
Receiver sensitivity (κ)(dBm)	-81.5	-79.5	-75.5	-71.5
SINR threshold (ζ)(dB)	7	9	11	15

4.1.6 Network Allocation Vector Adaptation

According to the IEEE 802.11 [5], the NAV contained in RTS is equal to $T_{CTS} + SIFS + T_{DATA} + SIFS + T_{ACK} + SIFS$. Here T_{CTS}, T_{DATA} and T_{ACK} are time durations for transmitting CTS, DATA and ACK packets respectively and SIFS is a short inter-frame space. Recall that in our scheme, the transmission rate of DATA packet is decided at the receiver side, and accordingly the transmitter is unable to calculate T_{DATA} since it does not know the transmission rate for the DATA frame when it transmits the RTS packet. To rectify this issue, in PRAS, the NAV contained in RTS is set to $T_{CTS} + 2SIFS$. This is reasonable due to the collision prevention property in PRAS. We elaborate more on this through the example shown in Figure 3.3. Upon transmitting the RTS frame from node A to node B, nodes in A's RTS transmission range will refrain from transmission for a $T_{CTS} + 2SIFS$ period. When node B replies with a CTS, nodes within B's CTS transmission range will update their NAV value to $T_{DATA} + SIFS + T_{ACK} + SIFS$ period. Nodes in A's RTS transmission range but outside node B's CTS transmission range will update their NAV through the information contained in node A's DATA packet.

4.2 Performance Evaluation

4.2.1 Simulation Setup

We use Qualnet [111] to simulate and the study the performance of our proposed heuristic. The control channel rate is fixed at 2 Mbps and the DATA channel rate varies from 1 Mbps to 11 Mbps. The simulation parameters are shown in Table 4.1. Ad hoc on Demand Vector Routing (AODV) is selected as the routing protocol. Other parameters such as the antenna gains and heights are assumed to be fixed and equal one, and known to all nodes. Five simulation seeds are used and we take the average result. We consider a 10×10 grid network with ten end-to-end CBR (constant bit rate) flows. The distance between each node pair is 50 meters. The other scenario is a network with 100 nodes randomly distributed with 20 random selected CBR flows inside a $1000 \times 1000\ m^2$. We fix the traffic rate to 800 packets/sec for each CBR flow. The mobility factor is 5 m/sec. Thus, by adding the mobility factor into random and grid topology, we have the following four scenarios: 1) Static Grid Topology 2) Dynamic Grid Topology 3) Random Topology 4)Dynamic Random Topology. We compare PRAS with IEEE 802.11, BASIC [29], and *CorePC*(correlative (case ii,B)) [38], Miser [77] and CAPC [39] and Adaptive [40]. Our metrics of comparison are:

- Aggregate Throughput: This counts the total number of the data bytes correctly received by the receivers per time unit.

- Effective Data Delivered per Joule: This counts the total number of received data bytes divided by the entire energy consumption.

4.2.2 Simulation Results and Analysis

Throughput

Figure 4.6 shows that PRAS has a leading performance, followed by Correlative and the rest of the heuristics. Clearly, the reason PRAS outperforms other protocols is due to the fact that a node deploying PRAS will always select a combination of power and transmission rate that will yield the best possible performance. The selection in PRAS is adaptive to the current network conditions (e.g., the values of P_{cn} and P_i). This combination indeed attempts to balance the spatial reuse and the frame corruption in order to achieve higher throughput. This has also been validated through the numerical results we obtained from the model. Correlative (case ii-B is the best case [38]) has also shown remarkable performance, slightly below that of PRAS. In correlative, while doing the power assignments to packets, the impact of the carrier sensing range has not been considered and in addition the control and DATA packets are all sent at maximum data transmission rate. This will be advantageous in low traffic network; however, when the load is high (i.e., the interference in the network is excessive), sending DATA frames at maximum rate is not wise due to high number of potential interfering nodes (as we have shown earlier). The IEEE 802.11 showed throughput limitations for two main reasons: higher rates of RTS collisions and lower spatial reuse since all packets are sent at maximum power. BASIC, on the other hand, severely suffers from hidden nodes since DATA and ACK packets are sent at the minimum required power whereas the RTS/CTS of other communicating nodes are sent at maximum power. Sending frames using the lowest transmission power obviously increases the interference range around the DATA/ACK packet receiver which increases the probability of the DATA/ACK collision. Moreover, transmitting the RTS/CTS at maximum power will unnecessarily suppress neighboring nodes and decreases the throughput. CAPC, Adaptive and Miser show slightly better throughput than IEEE 802.11 and BASIC due to the

fact that DATA and ACK are well protected in these schemes; nevertheless, the RTS frame and in most cases the CTS frame are sent at maximum power which is shown to reduce the spatial reuse. Moreover, the assignment of the DATA power value in Miser, Adaptive, CAPC is done on the assumption that the interfering node always transmits at maximum power, which may not be true in random power-aware topology. Accordingly, the power value assigned to the DATA packet will be more than the sufficient power to protect its reception and thus this, again, impacts the spatial reuse. These are the reasons why these protocols achieve less throughput than PRAS and Correlative. We can see also from Figure 4.6 (Dynamic Grid and Dynamic Random Topology) that mobility has impacted the node throughput. When considered, the source and receiver nodes may not be able to communicate with each other due to the fact that either one of them will be out of range of the other. This may trigger link failures that may occur frequently due to disconnection of adjacent nodes in a route. Routing table entries thus may get stale and may require frequent updates.

Convergence of P_i and P_{RTS}

To study the tuning behavior of P_i, we choose 20 receiver nodes from the random topology and we show in Figure 4.7 the average value of P_i, the estimated power of an interfering node, neighbor to the receiver. The figure also shows the average value of the transmission power of the RTS frames of the 20 sender nodes. As the figure shows, both P_i and P_{RTS} start at a maximum value and quickly converge to *some* steady state values, relatively larger than P_{min} ($P_{min} = 1dBm$ as shown in Table 4.1) but much smaller than P_{max}. Indeed, a smaller value of P_{RTS}, together with the smaller value of P_i, suggests that the network enjoys a good level of spatial reuse with less interference (and hence frame corruption) obtained through the judicious power assignment of PRAS heuristic. In order to support our claim, we go back to

our model for PRAS and look at the throughput vs. a_{RTS} when using the value of P_i obtained in Figure 4.7 (the P_i in Figure 4.7 corresponds to $a_i = 80.5m$). Figure 4.8 shows the throughput (total network throughput) obtained from the model; also shown in the figure is the point that corresponds to the measured P_{RTS} in Figure 4.7 (i.e., $a_{RTS} = 90.5m$). Clearly, a high throughput (of $1030KB/s$) is obtained and is close to the optimal one ($1150KB/s$) that corresponds to an a_{RTS} slightly smaller than $90.5m$. This result indeed supports our claim that our PRAS heuristic balances the tradeoff between better spatial reuse and low frame corruption rate due to hidden nodes in order to achieve a good performance.

Energy Efficiency

Figure 4.9 depicts the energy efficiency (of all schemes) in KBytes/Joule. The IEEE 802.11 has the worst performance since all packets are transmitted at maximum power and that results in unnecessary energy consumption. BASIC scheme severely suffers from packet collision and hence higher energy consumption due to frame retransmissions. Among all schemes, PRAS heuristic achieves the best energy consumption performance in all simulated scenarios. This is indeed due to the fact that frames transmission power in PRAS is carefully decided so that packet collision/corruption is either minimized or avoided while also using just enough power for the frame to reach the destination.

4.3 Conclusions

In this chapter, the tradeoff between spatial reuse and frame error corruption (i.e. signal quality) is investigated and a decentralized heuristic for power and rate control in multihop wireless networks is proposed. The algorithm is also modeled using a realistic analytical model that characterizes the transmission activities governed by the IEEE 802.11 DCF in a single channel, power-aware, multi-rate multihop wireless

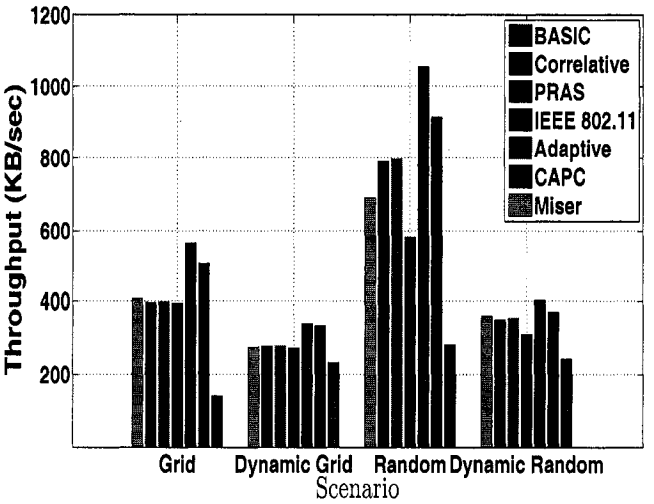

Figure 4.6: Throughput for different Topologies

network. The observations and insights from the model confirm that it is possible to achieve higher throughput performance by tuning the transmit power to allow more concurrent transmissions while appropriately tuning the data transmission rates. The analytical results revealed that adapting the data transmission rate in order to completely avoid packet corruption (loss) due to interference from neighboring transmissions is not always advantageous. This is because when smaller data transmission rates are used, in response to interference, the channel occupation period (or busy time) would be longer, while larger rates yield shorter channel busy period. This shorter period, in addition to the period wasted retransmitting corrupted frames, would offset the benefits of switching to lower rates to avoid frame loss. However, our results also showed that there is a frame loss threshold beyond which it is more advantageous to switch to lower rates. Our simulations revealed a remarkable performance (both throughput and energy consumption) for our proposed heuristic over other existing approaches.

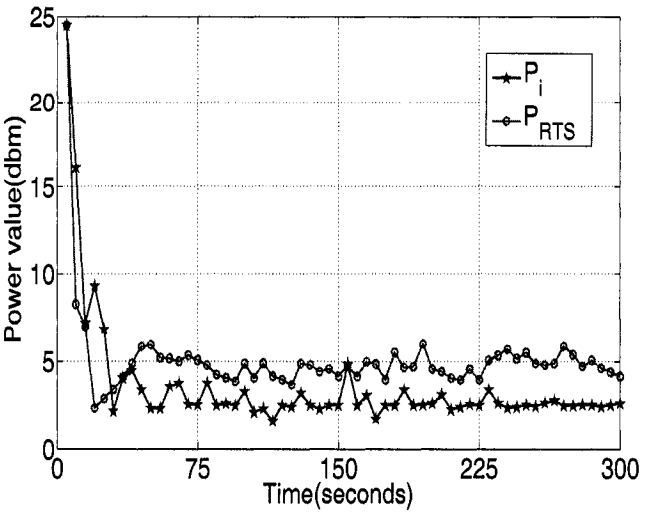

Figure 4.7: Tracing of P_i and P_{RTS}

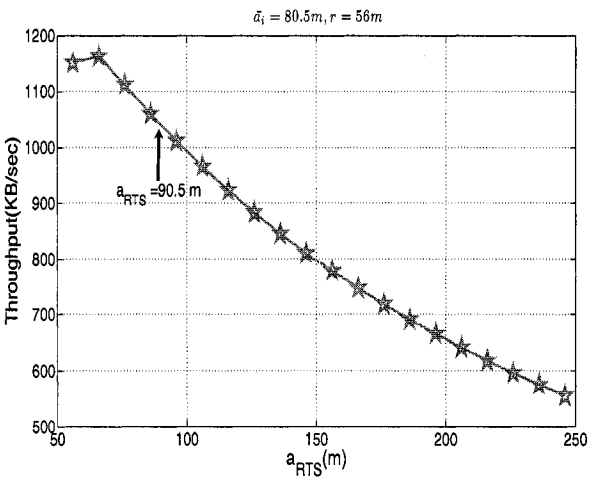

Figure 4.8: Throughput vs. a_{RTS} (model)

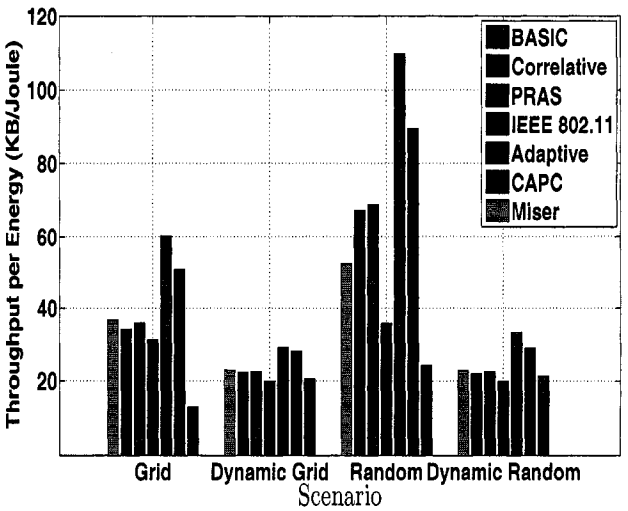

Figure 4.9: Energy Efficiency for different Topologies

Chapter 5

A Spatiotemporal Contention Resolution Algorithm for Enhancing Spatial Reuse in Multihop Wireless Networks

As already mentioned earlier, in wireless ad hoc networks, the physical carrier sensing (PCS) is essentially used to determine whether or not a node may access the medium. Typically, a node senses the medium, before initiating any communication, and defers its transmission if the channel is sensed busy; a channel is considered to be busy if the strength of the received signal exceeds a carrier sense threshold, CS_{th}. The PCS method reduces the likelihood of collision by preventing nodes in the vicinity of each other from transmitting simultaneously, while allowing nodes that are separated by a safe distance (termed as the carrier sensing range, r_c) to engage in concurrent transmissions. The former is referred to as collision avoidance while the latter is known as spatial reuse.

Traditional MAC protocols utilize temporal mechanisms, such as the Binary Exponential Backoff of the DCF access method, to resolve contention among simultaneous transmissions. A node wishing to transmit first senses the channel for a Distributed Inter Frame Space (DIFS) period and then transmits only if the channel is sensed idle. Otherwise, the node waits until the channel is sensed free for another DIFS interval and waits for a random contention time: it chooses a backoff b, an integer distributed uniformly in the window [0, CW] (where CW is the contention window size) and waits for b idle time slots before attempting to transmit. When a node detects a failed transmission, it doubles its CW until it reaches a maximum value (CW_{max}). By separating transmissions in time, successful transmission is achieved and several methods have been proposed to optimize the performance of these temporal mechanisms in single hop networks so that an optimal performance is obtained [6], [76].

Alternatively, to resolve contention among contending hosts and improve the utilization of the channel, recently, the concept of spatial separation has been proposed [74]. Namely, by adjusting the space occupied by each transmission, spatial backoff controls how the channel usage is divided over space such that an appropriate number of concurrent transmissions can exist while a suitable temporal contention level around each transmitter is achieved. In order to control the space occupied by each transmission, a joint control of CS_{th} and transmission rate is proposed by the authors [74]. The authors have shown that substantial gain in channel utilization can be achieved as a result of the improvement in the spatial reuse. Indeed, in addition to tuning the CS_{th}, one can also increase the level of spatial reuse by reducing the transmit power so that multiple transmissions can co-exist without causing enough interference on one another; the authors of [79] analyzed the relation between the transmit power and the CS_{th} in determining the network capacity. Here, a combination of lower transmit power and higher CS_{th} leads to a large number of concurrent

transmissions with each transmission sustaining a lower data rate.

Clearly, the performance of multihop wireless networks is limited both by the interference, caused by neighboring transmissions, in the network as well as the level of contention among contending hosts. In this chapter, the interest is in improving the performance of multihop wireless networks through developing methodologies to deal with the interference caused by hidden nodes as well as combatting frame collisions from simultaneous transmissions. Namely, a MAC-based dynamic adaptation scheme is developed with joint control of carrier sense threshold and contention window size.

By appropriately tuning the CS_{th}, one may detect strong interference and hence avoid unnecessary transmission attempts that could result in a failure (i.e., eliminate collisions from hidden terminals). Further, when selecting an appropriate carrier sense threshold, the exposed terminal problem may be reduced and the channel spatial reuse could be enhanced. When experiencing collisions due to simultaneous transmissions, adapting CW helps in resolving collisions due to simultaneous transmissions. Therefore, it is critical to distinguish the causes of frame loss when deciding which protocol parameter(s) should be tuned such that a good performance is achieved. Various loss differentiation methods have recently been proposed for CSMA-based single hop networks [67], [112], [68], [113] as well as multihop networks [66]. Except the work of [113], none of the other methods can effectively differentiate the frame loss due to interference from hidden nodes or due to collisions. Hence, in this work, an effective method is proposed for differentiating among frame losses. The study reveals that by jointly controlling both parameters (CS_{th} and CW), the network performance can be substantially improved. Also, the study revealed that in a multihop network, there is a tradeoff between spatial reuse and collisions from concurrent transmissions and the optimal performance is obtained with smaller contention windows, which yields a higher collision ratio, but that indeed promotes higher spatial reuse.

The rest of the chapter is as follows. Section 5.1 provides the preliminaries and

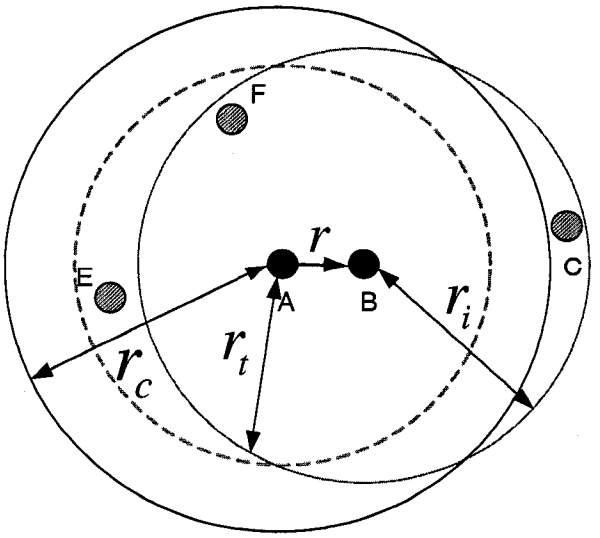

Figure 5.1: Carrier Sensing Range, Silence Range and Interference Range.

motivation of the work. The proposed scheme is presented in Section 5.2 and its performance evaluation, through simulations, is presented in Section 5.3. Finally, the work is concluded in Section 5.4.

5.1 Motivating Issues and Solutions

Although the objective of the algorithms proposed in [48], [49], [50] and [74] is to search for an optimal CS_{th} that can avoid hidden terminals and improve the spatial reuse, these algorithms have some deficiencies due to their purely localized nature. In addition, none of these methods differentiate among collisions from contending nodes and those from hidden terminals, hence their adaptation method may lead to either unnecessary decease of CS_{th} or increase of CW (or both), which would deteriorate the system throughput rather than improving it. We explain in this section the inefficiency of these algorithms in resolving either the hidden terminal problem or contentions through three illustrative examples and provide the motivation for this chapter.

5.1.1 Illustrative Examples

Consider Figure 5.1 where node A is transmitting a frame to node B and where node C is hidden from A and vice versa (nodes A and C cannot sense each other's transmission). Moreover, consider a node (F) that lies in the intersection of the interference area of node B and the carrier sensing range of node A. Below are three different scenarios in which node A may encounter a transmission failure.

- **Scenario 1:** Here, node C starts its transmission to its intended receiver (not shown) first. Since node C is outside the carrier sensing range of A, A senses the channel as idle (i.e., the level of energy detected is below the CS_{th}) and initiates a frame transmission to node B. Since node B suffers from the interference of the on-going transmission (of node C), it is unable to correctly receive the packet transmitted by A. Hence, node A faces a transmission failure. Here in our work, we refer to this kind of collision event as $\mathbf{H_1}$.

- **Scenario 2:** Here, node A starts its transmission to B first. Node C, unaware of this communication (C is assumed to lie outside the silence range of A), initiates a transmission concurrently and thereby corrupts the transmission of node A. We refer to this kind of collision event as $\mathbf{H_2}$.

- **Scenario 3:** Here, nodes A and F initialize their transmission (suppose node C is not involved in any transmission) in the same time slot. Since node F lies in the interference range of B, it will corrupt the transmission of A. Accordingly, let $\mathbf{C}$ represent this kind of collision event.

Next, for each collision event ($\mathbf{H_1}$, $\mathbf{H_2}$ and $\mathbf{C}$) classified above, we propose a solution.

5.1.2 Solution to Scenario 1: Adaptively Adjusting CS_{th} based on Network Performance

In scenario 1, a collision (of $\mathbf{H_1}$-type) can be avoided if a node adjusts its CS_{th} (for instance, based on the network performance, as suggested in [48], [49] and [50]); more specifically, node A can decrease its CS_{th} (i.e., increase its carrier sense range) when it encounters a transmission failure such that if node C transmits in the future, A will be able to sense this transmission and will refrain from initiating any communication. As a result, a collision of this type ($\mathbf{H_1}$) may be avoided. However, a node may need to distinguish this type of failure from others (namely $\mathbf{H_2}$-type and $\mathbf{C}$-type) so that a corresponding reactive scheme can be developed. The method to estimate the packet error rate due to this type of failure will be presented later on.

5.1.3 Solution to Scenario 2: Upper-bounding CS_{th}

Issues with existing solutions

While the algorithms proposed in [48], [49], [50] and [74] can avoid collisions from $\mathbf{H_1}$-type transmission failure, almost none of them address the hidden terminal problem that results in $\mathbf{H_2}$-type transmission failure, as we elaborate in the following example. Suppose node C initializes a transmission (after A's) and corrupts the transmission of A. According to the schemes proposed in [48], [49] and [50], node A should decrease its CS_{th} due to this transmission failure. However, node C does not know that its transmission had corrupted that of A and accordingly C fixes or increases its CS_{th}. As a result, if node A (re)transmits, C will still sense the channel status as idle and initiate a new transmission. Clearly, the transmission of node A will be corrupted again. It is therefore evident that the algorithms of [48], [49] and [50] cannot avoid $\mathbf{H_2}$-type collisions. Furthermore, since the transmission from node C is expected to be successful, the node will consequently increase its CS_{th} for subsequent

transmissions and transmit more aggressively. Therefore, the transmission from C will continue corrupting that of A. As a result, node A will keep decreasing its CS_{th} until ultimately its opportunity of transmission is deprived; these methods have also been shown to deteriorate the fairness among hosts.

The algorithm proposed in [74] can avoid this kind of collision ($\mathbf{H_2}$-type) if node A decreases its transmission rate (i.e., relatively decreases the SINR requirement) until node C falls outside the interference range of node B (the receiver of A's frame). Although the mathematical analysis in [46] has demonstrated that there exists an optimal combination of transmission rate and CS_{th}, the value of such a combination highly relies on the network topology and the channel condition. Hence, it is not always possible for a node to adjust its transmission rate and CS_{th} to achieve this optimal combination by solely depending on its transmission success/failure history. Additionally, and as pointed out in [76], it is only advantageous to transmit at a lower rate when the packet loss rate is high (usually over 50%). That is, transmitting at a lower rate does not necessarily improve the total throughput. Furthermore, neighboring nodes may unnecessarily be suppressed for a much longer time since the transmission duration becomes much longer (and hence the busy time of the channel) with lower transmission rates; consequently, the exposed terminal problem (e.g., node E in Figure 5.1) is exacerbated. Another drawback of the algorithm presented in [74] is that it suffers from the fairness problem, as well, for the same reasons as stated earlier for [48], [49] and [50].

Proposed solution

A solution for avoiding collisions in scenario 2 is introduced; clearly, if node C can, *somehow*, detect the ongoing transmission from node A, then it should defer its transmission to yield to that of A (assuming node C falls in the interference range of A's receiver). However, C would be able to sense a busy channel, when A is

transmitting, only when it falls inside the silence range of A or alternatively when its carrier sense range is large enough to include A. Denote CS_{max} (which will be derived next) as the maximum allowed carrier sensing threshold that node C can use; this maximum threshold (or any value below it) guarantees that node C hears A's transmission and accordingly defers its own. However, evidently it is not feasible for node C to determine whether its transmission may corrupt that of A only based on its own transmission success/failure history. Node C, hence, would need some information regarding the transmission between A and B. The key idea is to allow the receiver (B in this case), through the CTS packet, to distribute necessary information to potential interfering nodes. With this information, all potential interfering nodes (node C in our scenario) can adjust their CS_{max} and limit their CS_{th} not to exceed that value. Potential interferers will, therefore, block their own transmissions in order to allow for the current transmission to complete successfully. The detailed algorithm for determining and dynamically adjusting the CS_{max} is presented later.

Note that, in the proposed solution for $\mathbf{H_2}$-type collision, the RTS/CTS handshake does not silence neighboring nodes; rather these frames only request the neighbors to bound their CS_{th}. That is, nodes receiving an RTS or a CTS frame will not be silenced for the whole 4-way handshake duration, as suggested in the IEEE 802.11 protocol, but rather for only an EIFS[1] (Extended Inter Frame Space) duration. Indeed, this improves the spatial reuse through avoiding unnecessary blocking of neighboring nodes that lie in the transmission range of RTS/CTS frame but outside the interference range of the receiver (for instance node E in Figure 5.1). Namely, in our proposed scheme, the decision on whether to start a new transmission is totally left to the physical carrier sense mechanism, since the PCS mechanism already provides an effective way to protect DATA packets through setting an upper-bound, as discussed earlier, on the CS_{th}. In order to reduce the overhead induced by RTS/CTS

[1]This does not require any changes to the standard; rather a sender would only set the transmission duration in the ensuing frame for EIFS period.

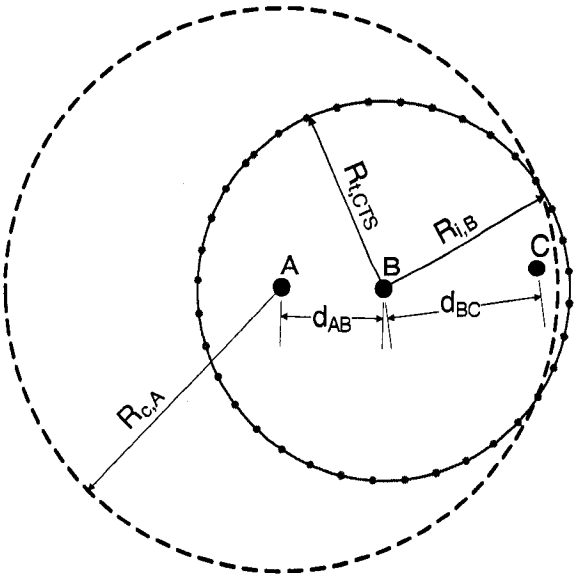

Figure 5.2: Scenario with Hidden Terminals

frames, we deploy a dynamic mechanism that switches between the 2-way and 4-way handshake, as will be shown later.

Deriving CS_{max}

In this section, we present our method for deriving a suitable value for CS_{max}. Initially, node A (Fig. 5.2) transmits an RTS frame to node B. After receiving the RTS packet, node B is able to calculate the distance (d_{AB}) to A as follows:

$$d_{AB} = (\frac{P}{P_{r,B}})^{1/4} \tag{5.1}$$

where, P is the transmission power[2] and $P_{r,B}$ is the received power at node B from A's transmission. Subsequently, using equation (2.6):

$$r_i = \left(\frac{P_i}{\frac{P_t}{r^4 \cdot \zeta} - P_{cn}} \right)^{\frac{1}{4}}$$

[2]In the proposed algorithm, we assume that all the nodes use the same transmission power.

the receiver (node B) calculates its interference range for receiving the DATA packet(s) from node A as:

$$R_{i,B} = \left(\frac{P}{\frac{P}{d_{AB}^4 \cdot \zeta_{DATA}} - CN_B}\right)^{1/4} \tag{5.2}$$

where, ζ_{DATA} is the SINR threshold for DATA packets. In the proposed scheme, we assume a fixed PHY transmission rate for DATA packets, thus the value of ζ_{DATA} is fixed. CN_B represents the current noise measured at node B.

Next, node B encapsulates necessary information about the ongoing transmission from A (such as d_{AB} and $R_{i,B}$) in the CTS packets so that all nodes in its interference range are informed about the ongoing communication; the announced values will be used to derive an upper bound on the CS_{th} to force interfering nodes to defer their transmission. Now, to make sure that all neighboring nodes in B's interference range receive the CTS frame, the frame is transmitted at a rate (the transmit power is fixed) such that the transmission range, $R_{t,CTS}$, is large enough to cover the entire interference range of node B. Note, however, that since the transmission rate is selected from a set of discrete values, we may well have $R_{t,CTS} > R_{i,B}$; this means that some nodes may be outside the interference range of B and still receive the CTS packet. Accordingly, and upon receiving the CTS packet, node C calculates the distance to node B, $d_{BC} = (\frac{P}{P_{r,C}})^{1/4}$ where $P_{r,C}$ is the power of the received CTS frame. C then checks whether it lies in the interference range of node B, or not, by comparing d_{BC} with the value of $R_{i,B}$ carried in the received CTS packet. If $d_{BC} > R_{i,B}$, C concludes that it is outside the interference range of B and accordingly it does not need to limit the CS_{th}. Here, node C discards this CTS packet and waits for EIFS period to contend for the channel again. Otherwise, node C determines that it lies in the interference range of node B and accordingly has to bound its CS_{th}, in order to make sure that A's transmission completes successfully. In other words, C (and other interfering nodes) upon receiving the CTS frame should adjust its CS_{th} such that its carrier sense range includes A and accordingly any transmission from

node A will be sensed by the interfering nodes (that is, the silence range of A now covers the interference range of B). Now, in order for node A to be within the carrier sensing range of C, we should have:

$$R_{c,C} \geq d_{AB} + d_{BC} \tag{5.3}$$

$R_{c,C}$ denotes the carrier sense range of node C (Equation 5.3); the minimum carrier sense range corresponds to $R_{c,C} = d_{AB} + d_{BC}$, and that occurs when node C uses the maximum allowed carrier sense threshold $CS_{max,C}$. For a $CS_{th} < CS_{max,C}$ selected by C, C's carrier sense range is guaranteed to sense the transmission of A and therefore $CS_{max,C}$ is called the upper bound. The minimum carrier sense range should be equal to the silence range of node A ($R_{c,A}$, Equation 3) and is defined as follows:

$$R_{c,C} = R_{c,A} = (\frac{P}{CS_{max,C}})^{1/4} \tag{5.4}$$

Using equations (5.3) and (5.4), $CS_{max,C}$ can be derived as:

$$CS_{max,C} = \frac{P}{(d_{AB} + d_{BC})^4} \tag{5.5}$$

If the current carrier sense threshold of node C is above $CS_{max,C}$, it should limit its threshold (to be lower than $CS_{max,C}$). Otherwise, it maintains the same value and records that of $CS_{max,C}$, which will be used for future adjustment (of CS_{th}) shortly thereafter.

Indeed, the computed value of $CS_{max,C}$ ensures that node C refrains from transmitting when node A transmits. However, in a multi-hop network environment, a node may be surrounded by multiple transmissions (spatially separated) from more than one node pair. Accordingly, every interfering node (e.g., C) maintains a table for its neighboring transmissions; every entry ($< CS^i_{max,C}, T^i_{expire} >$) in the table

corresponds to a node pair i currently communicating. $CS^i_{max,C}$ is the upper bound on the CS_{th} a node determines for a node pair i (determined, using Equation 5.5, upon receiving a CTS frame from the receiver of the node pair i). The maximum carrier sense node C uses is then determined as $CS_{max,C} = min_i\{CS^i_{max,C}\}$. T^i_{expire} is a pre-defined expiration duration for node pair i. If a node does not receive any CTS packet for the same node pair for a T^i_{expire} (we assume $T^i_{expire} = T_{expire}$ for all i) duration, the corresponding entry becomes stale and is deleted from the table. This improves the spatial reuse as can be illustrated in the following example. Suppose node A transmits a packet to node B, and node C accordingly bounds its CS_{th} in order not to corrupt A's transmission. If node A has no more packets to transmit to B, bounding C's carrier sense threshold becomes unnecessary since that forces node C to become too conservative when sensing the medium to transmit its packets, which eventually deteriorates the spatial reuse. Therefore, once node A stops sending frames to B for some time, node C should delete the entry corresponding to this node pair and recompute the upper bound for its CS_{th}.

As discussed, transmitting using the 4-way handshake is an efficient solution to avoid $\mathbf{H_2}$-type collisions. However, it adds extra overhead (through the RTS/CTS exchange), which could ultimately affect the network throughput. To address this problem, we further adopt a policy that dynamically switches between the 2-way and the 4-way handshake to reduce the overhead. Initially, a node transmits using the 4-way handshake. If this transmission is successful, the next frame transmission will use the 2-way handshake; otherwise, a node continues transmitting using the 4-way handshake until the transmission is successful, and thereafter switches to the 2-way access method. Recall that when using the 4-way handshake, all potential interfering neighbors for a receiver limit their CS_{th} for a pre-defined duration T_{expire}. If the sender has another packet to transmit (now using the 2-way access) and it wins the channel directly after it completes its prior transmission, there is a good opportunity

for this initiated packet to succeed. This is due to the fact that the interfering nodes can still sense the transmission of the sender due to the larger carrier sensing range they use (for the period of T_{expire}). Hence, the transmission (using the 2-way handshake) is protected without any additional overhead. Finally, a node operating using the 2-way access switches back to the 4-way handshake only upon a packet loss due to $\mathbf{H_2}$.

5.1.4 Solution to Scenario 3: Increase CW

Recall that scenario 3 corresponds to packet loss from simultaneous transmissions of more than one node in the same time slot. A simple solution to recover from such frame loss is through a temporal contention resolution (e.g., increase of the contention window) that aims to separate transmissions from these contending nodes in time.

Now, for each of the above categories, which may result in a transmission failure, a corresponding solution has been proposed. However, unlike single hop WLANs networks, in a multihop network environment, when a node faces a transmission failure, it is very difficult to distinguish the exact cause ($\mathbf{H_1}$, $\mathbf{H_2}$ or $\mathbf{C}$) of that failure. Next we present our method, with some rules, for distinguishing the causes of frame loss; then, based on the determined causes of transmission failure, we present our algorithm, which adopts different solutions, in order to balance the trade-off between frame collision and spatial reuse to enhance the network capacity.

5.2 Proposed Algorithms

5.2.1 Related Loss Differentiation Methods

Various loss differentiation methods have recently been proposed for CSMA-based single hop networks [67], [112], [68], [113] as well as multihop networks [66]. The authors in [67] introduces a new NAK packet to differentiate packet collision and

channel error. A receiver node transmits an NAK to the sender if it successfully receives the MAC header but fails in receiving the packet payload. Upon receiving the NAK, the sender acknowledges that this transmission failure is due to channel errors but not collisions and accordingly adapts the transmission rate. Another scheme is proposed in [68], which differentiates collisions and errors based on the transmission time information for lost packets. Moreover, the authors in [66] proposed a Collision-Aware Rate Adaptation (CARA). CARA employs RTS probing to differentiate between packet collision or packet error. To reduce RTS/CTS overhead, in CARA, the RTS/CTS exchange is switched off after a certain number of consecutive packet successes and switched on after a certain packet failures. The authors in [112] proposed two algorithms that respectively approximate the packet loss ratio due to collisions and channel errors based on MAC layer measurement. Most recently, the authors in [113] proposed an algorithm in which nodes differentiate interference according to their energy and timing relative to the desired signal, and measure packet error rate (PER) locally at the transmitter for each type of collisions. Except for the work of [113], none of the other methods can effectively differentiate the frame loss due to interference from hidden nodes or due to collisions.

5.2.2 Our Proposed Loss Differentiation Algorithm

In order to differentiate the possible causes of a packet loss upon a transmission, a sender (A) checks whether any of the following conditions (or a combination thereof) are satisfied.

- **Condition** A_1: The ensuing transmission is an RTS transmission.
- **Condition** A_2: The reference transmission is initialized at time t, $t \in [t_{4way}, t_{4way} + T_{expire}]$. Here, t_{4way} denotes the most recent time node A received the CTS packet from its receiver (node B in Figure 1). At that same

time also (i.e., t_{4way}), all potential neighboring nodes receive node B's CTS packet and accordingly are informed to limit their CS_{th}.

- **Condition** A_3: When the transmission is initialized, the sender determines whether its carrier sensing range covers the interference range of the receiver; that is $r_{c,A} \geq r_{i,B} + d$, where $r_{c,A}$ is the carrier sense range of A, $r_{i,B}$ is the interference range of B and d is the distance between A and B. In other words, the carrier sense threshold ($CS_{th,A}$) should be bounded by a "safe threshold", denoted as CS_{safe}, where $CS_{safe} = (\frac{P}{r_{i,B}+d})^{\frac{1}{4}}$, which is easily derived from equation (3) while the value of $r_{i,B}$ can be obtained using equation (5).

Hence, the state of any transmission can be represented by a variable $T = (a_1, a_2, a_3)$ where $a_i = 1$ if condition A_i is satisfied and $a_i = 0$ otherwise. For example, $T = T_1 = (1, 1, 1)$ if all conditions are satisfied for the current transmission. Table 5.1 shows all the possible values of T, each corresponds to a transmission state. Now, recall that a transmission failure may be caused by either of the following events $\mathbf{H_1}$, $\mathbf{H_2}$ or $\mathbf{C}$; upon any transmission failure, the sender determines to which category (as explained above) this transmission belongs and accordingly performs some analysis to determine which event caused the failure.

For example, for those types of transmissions where A_1 (i.e., the ensued frame is RTS) is satisfied (e.g., T_1, T_2, T_3 and T_4), one can determine that a transmission failure is not likely caused by interference of $\mathbf{H_2}$-type (where the interfering signal comes after the reference signal and causes a frame loss) for the following reason; indeed, when A sends out its (RTS) packet, there is a vulnerable period during which if any interfering node (that is outside the silence range of A) attempts to transmit, the transmission from the sender to the receiver (B) will be unsuccessful. This vulnerable period corresponds to the transmission duration of the frame (both header and payload). With an RTS frame that is transmitted at $11Mbps$, the vulnerable period is very small, and hence the RTS collision of type $\mathbf{H_2}$ becomes negligible.

Table 5.1: The Possible Causes for Packet Losses of Each Type

Type of transmission	Possible causes of packet loss
$T_1 = (1, 1, 1)$	**C**
$T_2 = (1, 0, 1)$	**C**
$T_3 = (1, 1, 0)$	**C**, $\mathbf{H_1}$
$T_4 = (1, 0, 0)$	**C**, $\mathbf{H_1}$
$T_5 = (0, 1, 1)$	**C**
$T_6 = (0, 0, 1)$	**C**, $\mathbf{H_2}$
$T_7 = (0, 1, 0)$	**C**, $\mathbf{H_1}$
$T_8 = (0, 0, 0)$	**C**, $\mathbf{H_1}$, $\mathbf{H_2}$

Additionally, for a failed transmission where A_2 is satisfied, all nodes lying within the interference range of the receiver had been informed, through the CTS frame, to bound their CS_{th} in order to sense the transmission of the sender and defer their own transmissions. Accordingly, these interfering (hidden) nodes could not initiate any transmission while the sender is transmitting and hence $\mathbf{H_2}$-type collisions are also unlikely. For those transmissions where A_3 is satisfied (e.g., T_1, T_2, T_5 and T_6), the sender would refrain from sending out its packet if at least one transmission in the vicinity of the receiver is taking place, which may in effect corrupt the sender's frame (here the sender's carrier sense range covers the interference area of the receiver). Hence, $\mathbf{H_1}$-type collision is unlikely for a transmission failure where A_3 is satisfied.

In the above discussion, we have precluded those unlikely causes of packet loss upon every failed transmission; a summary is shown in Table 5.1 where we present the correspondence between a transmission category and the possible cause(s) of failure. Next we present further analysis and the possible reactive schemes for every type of transmission failure.

5.2.3 Solutions

Type T_1, T_2 or T_5 transmissions

When a node encounters a failed transmission of type T_1, T_2 or T_5, both $\mathbf{H_1}$ and $\mathbf{H_2}$ type collisions are not likely (as per our discussion above); the more likely reason for frame loss is that of having multiple senders transmitting in the same time slot (i.e., **C**-type collision, with no hidden nodes). Here, temporal contention resolution (i.e., BEB) is adopted while the CS_{th} is kept fixed in order not to affect the spatial reuse in the network. Additionally, for T_5 transmission category, a node does *not* switch to the 4-way handshake (to reduce the overhead) upon a failure since already hidden nodes have limited their CS_{th} (i.e., $\mathbf{H_2}$-type collisions are unlikely).

Type T_3, T_4 or T_7 transmissions

For these three types of transmissions, a failure results from either **C**-type or $\mathbf{H_1}$-type collision (Table 5.1). Intuitively, one may decide to increase CW or decrease CS_{th}: increasing CW resolves the former type and decreasing CS_{th} resolves the latter type by allowing a node to transmit more conservatively.

However, the authors of [83], using an appropriate analytical model, pointed out that in a wireless multihop network, the attempt probability is jointly determined both by CW and CS_{th}, while the optimal attempt probability (that maximizes the network throughput) can be obtained using a smaller contention window at the expense of a higher collision ratio. This is so because a larger attempt probability promotes the spatial reuse by reducing the channel idle time (there is indeed a trade-off between spatial reuse and collisions from concurrent transmissions). Thus, upon encountering transmission failures that may be caused by either **C** or $\mathbf{H_1}$, increasing CW and decreasing CS_{th} simultaneously may be too conservative and results in a lower channel utilization.

In order to decide which parameter (CS_{th} or CW) should be tuned, we need to

further determine whether the frame loss is due to $\mathbf{C}$ or $\mathbf{H_1}$. Indeed, and unlike single hop WLANs (see for example [112], [67]), it is more challenging to provide an effective loss differentiation in a multihop wireless network. For instance, the authors of [66] proposed to use the RTS/CTS frames to differentiate packet loss due to either collision ($\mathbf{C}$) or interference from hidden nodes (i.e., $\mathbf{H_1}$ and $\mathbf{H_2}$). However, their method strongly depends on the assumption that the RTS/CTS exchange completely silences hidden terminals, which indeed has been shown [11] not to always hold. In addition, this method cannot differentiate $\mathbf{H_1}$-type and $\mathbf{H_2}$-type collisions, and requires the RTS/CTS exchange to be active for all frames.

In our work, we approximate the packet error rate (P_{ER}) for both $\mathbf{C}$ and $\mathbf{H_1}$ through periodic measurement as follows. Among the 8 categories identified earlier, T_1, T_2 and T_5 transmissions can be only corrupted by $\mathbf{C}$, while T_3, T_4 and T_7 can be corrupted by either $\mathbf{C}$ or $\mathbf{H_1}$. Therefore, during a predetermined measurement period, the sender counts the number of frame transmissions (for each category) that have been made as well as the number of failed transmissions. We denote:

- t_1: the number of T_1, T_2 or T_5 transmissions.
- f_1: the number of T_1, T_2 and T_5 failed transmissions.
- t_2: the number of T_3, T_4 and T_7 transmissions.
- f_2: the number of T_3, T_4 and T_7 failed transmissions.

Let $P_{ER,\mathbf{C}}$ denote the collision probability from $\mathbf{C}$, and $P_{ER,\mathbf{H_1}}$ denote the collision probability from $\mathbf{H_1}$. In order to estimate $P_{ER,\mathbf{C}}$ and $P_{ER,\mathbf{H_1}}$, we first assume that the transmission failures caused by $\mathbf{C}$ and $\mathbf{H_1}$ are independent [113]. Therefore, we can write:

$$1 - \frac{f_2}{t_2} = (1 - P_{ER,\mathbf{C}})(1 - P_{ER,H_1}) \tag{5.6}$$

and with the independence assumption, $P_{ER,C}$ can be estimated as:

$$P_{ER,\mathbf{C}} = \frac{f_1}{t1} \tag{5.7}$$

Combining (5.6) and (5.7), we obtain:

$$P_{ER,\mathbf{H_1}} = 1 - \frac{1 - \frac{f2}{t2}}{1 - \frac{f_1}{t1}} \tag{5.8}$$

The values of $P_{ER,\mathbf{C}}$ and $P_{ER,\mathbf{H_1}}$ are updated through periodic measurements of t_1, f_1, t_2 and f_2. Now, according to $P_{ER,\mathbf{C}}$ and $P_{ER,\mathbf{H_1}}$, the sender decides whether it should increase CW or adjust CS_{th}.

More specifically, a node compares the estimated $P_{ER,\mathbf{H_1}}$ value with two predefined thresholds (say P_S and P_F). If $P_{ER,\mathbf{H_1}}$ is above P_F, the node gradually decreases its CS_{th} (to the next lower value) to transmit more conservatively; and if $P_{ER,\mathbf{H_1}}$ is below a certain threshold P_S, a node gradually increases its CS_{th} (to the next higher level) to encourage more concurrent transmissions. Otherwise, a node will fix its CS_{th}. The values of P_S and P_F can be obtained empirically [50]. Further, as mentioned before, in a multihop wireless network, the transmission attempt probability (τ) is jointly determined by the physical carrier sense as well as the contention window ($\tau = p_1 \times p_2$, where p_1 is the attempt probability given that the medium is sensed idle and p_2 is the probability that the medium is idle given that no one transmits in the sender's carrier sensing range). Clearly, a smaller CS_{th} yields a smaller p_2 which results in a smaller τ. However, it has been shown that the optimal attempt probability should remain relatively high to improve the system throughput [83]. Accordingly, one needs to keep p_1 large, which corresponds to a smaller contention window. Furthermore, increasing the contention window upon a frame loss does not necessarily help in controlling the collision when the carrier sensing range does not completely cover the interference range, as has been shown in [83]. Therefore, we

propose to only increase the CW when $P_{ER,\mathbf{C}}$ is larger than $P_{ER,\mathbf{H_1}}$.

Finally, similar to the T_5 transmission, for a failed transmission of type T_7, a node does not switch to RTS/CTS handshake (to reduce the overhead) since the $\mathbf{H_2}$-type collisions are not likely.

Type T_6 transmission

When a node encounters a failed transmission of type T_6, it switches to the 4-way handshake for the next (re)transmission attempt and keeps its CS_{th} and CW unchanged, which is explained as follows. Clearly, the frame loss is not likely to be caused by $\mathbf{H_1}$-type interference (since A_3 is satisfied) and consequently reducing the CS_{th} yields no benefits but rather unnecessarily deteriorates the spatial reuse by forcing nodes to transmit more conservatively. When collisions from **C** and **H2** exit (which is the case of T_6), it has been shown (both from analytical studies [43] as well as simulations [50]) that the frame loss from $\mathbf{H_2}$-type interference dominates that from **C**. Hence, switching to 4-way handshake along with the solution proposed for Scenario 2, presented earlier, can effectively resolve the contention. Moreover, since CS_{th} is smaller than CS_{safe} (recall that A_3 condition is satisfied), CW should not be increased in order to maintain a high transmission attempt probability and accordingly a higher channel utilization. Here, when the next re-transmission fails, the node increases its contention window to resolve the contention temporally.

Type T_8 transmission

When a failed transmission of type T_8 occurs, a node switches to 4-way handshake for the next (re)transmission and decreases its CS_{th} to the next lower level. For these transmissions, hidden terminals greatly corrupt the frame reception and clearly either the transmitter was too conservative estimating the hidden nodes' transmissions (resulting in $\mathbf{H_1}$-type collision) or the hidden nodes were too conservative estimating the

Table 5.2: Transmission Rate Levels Used in Simulation

Rate(Mbits/s)	receiver sensitivity (dBm)	SINR threshold (dB)
11	-83	15
5.5	-79	11
2	-75	9
1	-72	7

sender's transmission (resulting in $\mathbf{H_2}$-type collision). In order to avoid these types of collisions, the CS_{th} for both the sender and the interfering nodes must be tuned, as explained earlier, to ensure a safe spatial separation among concurrent transmissions. Here, we keep the same CW value in order to maintain a higher attempt probability. Note that, since next the sender will retransmit using the 4-way, a retransmission failure would be resolved by appropriately tuning CW.

5.3 Performance Evaluation

In this section, we present a simulation-based study to evaluate the performance of the proposed scheme. Furthermore, we present comparisons with three other schemes: the IEEE 802.11 standard, the *dynamic CCA adaptation* scheme proposed in [48] and the *spatial backoff* scheme recently proposed in [74].

5.3.1 Simulation Setup

The simulation is carried out using Qualnet [111]. The 2-ray model has been adopted as the channel propagation model. The transmission power for all nodes is set to 15dBm. The final result is the average of 5 simulation runs (with different seeds). The available transmission rates and corresponding SINR and receiver sensitivity thresholds for each transmission rate are listed in Table 5.2. In the *dynamic CCA adaptation* scheme, IEEE 802.11 standard and basic (2-way handshake) scheme, all the packets are transmitted at 11Mbps. In the proposed scheme, the transmission

rate for RTS, DATA and ACK packets is fixed to 11Mbps while the transmission rate for CTS packets varies among all available levels. The transmission rate varies in *spatial backoff* scheme. The default CS_{th} for IEEE 802.11 standard is set to -84dBm. On the other hand, for other schemes that adjust the CS_{th}, the adaption step for CS_{th} is set to 1dBm. Moreover, the P_S and P_F for the proposed scheme are set to 0.05 and 0.1 respectively.

In our simulation study, 100 nodes are randomly distributed over a $1000m \times 1000m$ area; we consider constant bit rate (CBR) flows randomly distributed between source-destination pairs and the packet size is assumed fixed to 512 Bytes.

We take the following measurements to evaluate simulated schemes:

- Aggregate Network Throughput, which is the sum of the bytes correctly received by the receivers per time unit (in KB/sec) in the whole network.
- Collision Probability (P_c), which counts the ratio of total number of transmission failures over the total number of transmission attempts that have been made.

5.3.2 Results and Discussions

Impact of CS_{th} and CW

In this section, we try to obtain a deeper insight of the impact of CW and CS_{th} on the system performance through simulation study. In the experiment, the number of CBR flows is fixed to 25 and the traffic load is fixed to 400 packets/second. Figure 5.3 shows the aggregate throughput obtained for the IEEE 802.11 when varying both CS_{th} and CW. Here, the BEB is disabled and the backoff is always selected from the interval $[0, CW]$.

Clearly, a larger contention window (e.g., 512 and 1024) results in a serious throughput degradation regardless of the value of the carrier sense threshold. Indeed,

although a very large CW eliminates the (**C**)-type collisions, it results in longer idle periods, which in turn severely suppresses the spatial reuse of the wireless channel. We recall that the transmission attempt probability (τ) is jointly determined both by CS_{th} and CW ($\tau = p_1 \times p_2$ as mentioned in section 5.2.3) and a large CW leads to a small p_1, which in turn results in a smaller attempt probability. Consequently, the transmitter nodes become too conservative accessing the medium, causing serious throughput deterioration.

Alternatively, larger throughput is obtained when the contention window is small; more specifically, when $CW = 32$, the largest system throughput is obtained when smaller carrier sense thresholds are used (transmitting with $CW = 32$ achieves 10% to 15% of throughput improvement over $CW = 64$ and $CW = 128$). Here, a smaller contention window guarantees a higher access to the channel and a smaller carrier sense threshold guarantees a safe spatial separation among concurrent transmissions. Observe that the optimal network throughput depends on the values of both CW and CS_{th}; for larger CS_{th} (more aggressive senders), the contention windows $CW = 64$ and $CW = 128$ result in a slightly better throughput than $CW = 32$. From the results and discussions above, we can conclude that there exists a balance between the spatial reuse and the collisions due to contentions, and thus the optimal transmission probability, τ, which results in optimal throughput performance is achieved by the appropriate selection of the contention window and the carrier sense threshold.

Impact of network density

We study the impact of network density on the aggregate network throughput by varying the number of CBR flows in the network. As shown in Figure 5.4, in comparison with the IEEE 802.11 standard, the proposed scheme, the *dynamic CCA adaptation* scheme and the *spatial backoff* scheme, all result in higher throughputs, simply because the IEEE 802.11 does not adopt any adaptation mechanism except

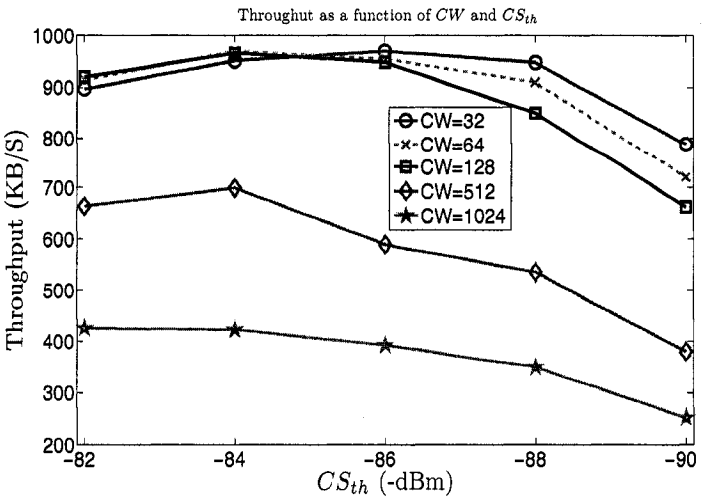

Figure 5.3: Throughput as a function of CS_{th} and CW

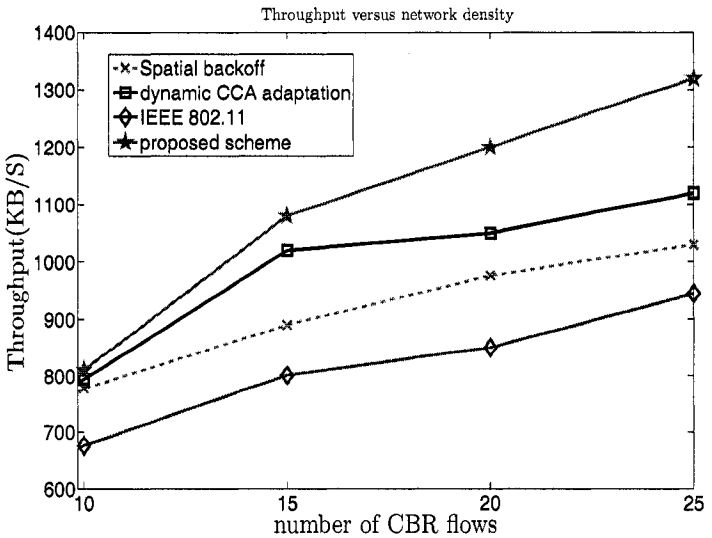

Figure 5.4: Impact of Network Density on Aggregate Throughput

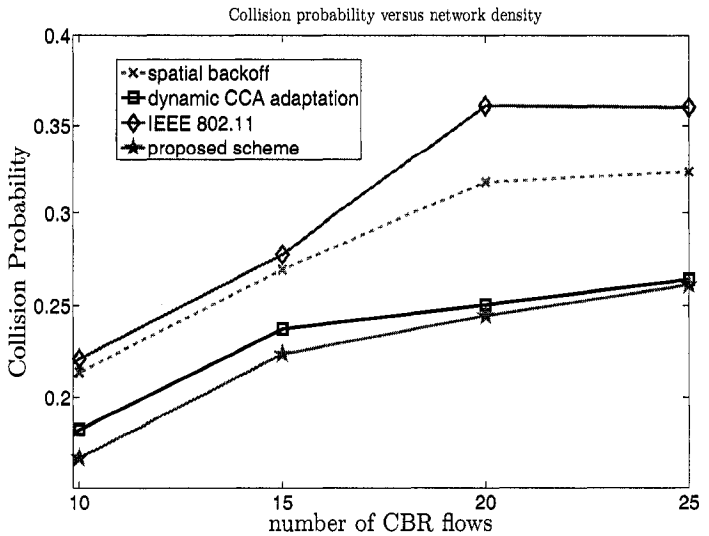

Figure 5.5: Impact of Network Density on Collision probability

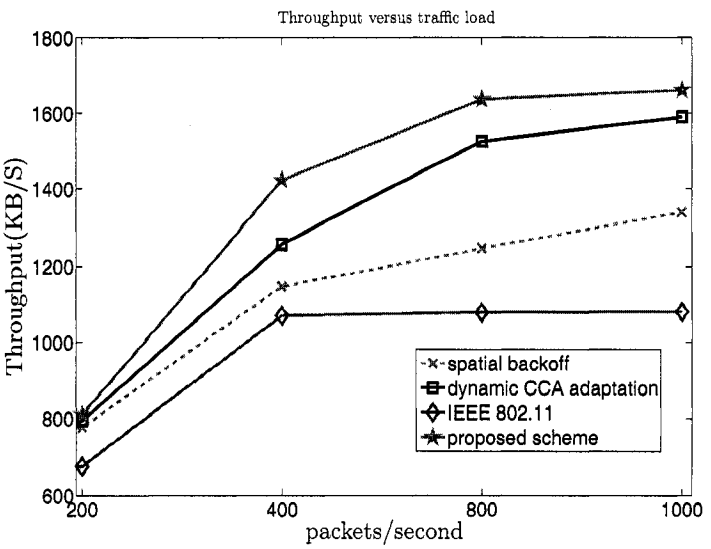

Figure 5.6: Impact of Traffic Load on Aggregate Throughput

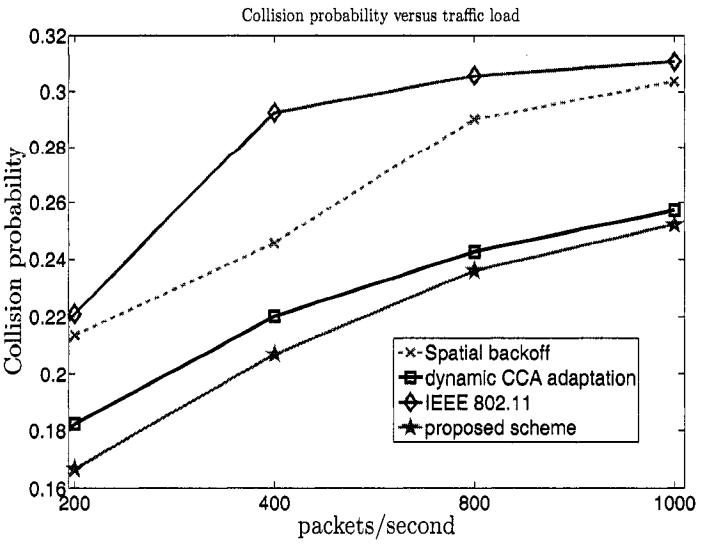

Figure 5.7: Impact of Traffic Load on Collision Probability

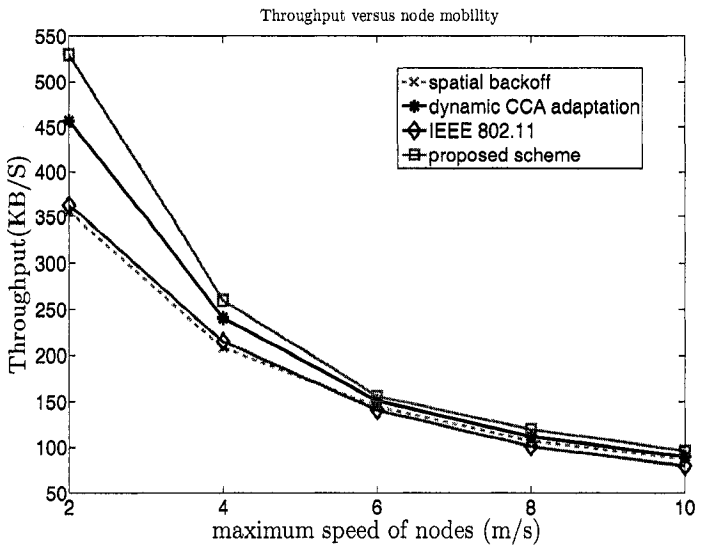

Figure 5.8: Impact of Node Mobility on Aggregate Throughput

that implemented with the binary exponential backoff in response to any packet loss.

The reason why the *dynamic CCA adaptation* scheme performs better than the *spatial backoff* scheme is due to the ineffective adaptation metrics adopted in the latter one. Namely, *spatial backoff* uses consecutive transmission successes/failures in order to estimate the network performance and performs tuning of PHY transmission rate and carrier sense threshold, while the *dynamic CCA adaptation* scheme uses periodic measurements of packet loss ratio. It is to be noted that the use of consecutive transmission successes/failures as a metric may lead to frequent fluctuations and inaccurate estimation due to its dependence on the network topology under investigation [69]. In addition, the *spatial backoff* performs premature decrease of the transmission rate even when the collision probability is low, which indeed affects the throughput since that results in longer busy periods for the wireless channel, as pointed in [76].

When facing a transmission failure, a node operating with the *dynamic CCA adaptation* scheme does not differentiate the causes of transmission failures and correspondingly reacts through decreasing CS_{th} and increasing CW at the same time. Consequently, this may unnecessarily oblige nodes to suppress their transmissions either by waiting for longer backoff period (effect of larger CW) or assuming a high level of interference before initiating a transmission (effect of lower CS_{th}). For example, as the network becomes more saturated, the collisions from $\mathbf{H_2}$ increase and become more dominating [83]. However, when encountering $\mathbf{H_2}$-type collisions, either decreasing CS_{th} or increasing CW can not reduce the collision; rather, this may decrease the transmission attempt probability, and hence deteriorates the spatial reuse. In comparison, the proposed method searches for the best operating point through first effectively differentiating the type of losses and second reacting to frame loss by appropriately adapting either CS_{th} or CW so that a high transmission probability is achieved, encouraging more concurrent transmissions and leading to a better spatial

reuse.

Another key reason for the throughput enhancement obtained by the proposed scheme is that it probes the network for the level of interference and dynamically switches between being conservative and aggressive in accessing the channel, in order to reduce the frame corruption due to $\mathbf{H_1}$-type collisions. Moreover, it efficiently eliminates the collisions from hidden terminals through limiting the CS_{th} of potential interferers (i.e., eliminating $\mathbf{H_2}$-type collisions), while the *dynamic CCA adaptation* and the *spatial backoff* scheme do not completely address $\mathbf{H_2}$-type collisions. This can be observed in Figure 5.5, which shows the collision probability under different network densities. Clearly, the proposed scheme has the lowest collision probability among all the simulated methods. Indeed, it is this property (lower collisions) for our proposed method that leads to over 20% of throughput improvement compared with *dynamic CCA adaptation*, especially as the network becomes denser (e.g., more than 20 flows). We also observe that as the network becomes denser, the measured collision probability of the proposed method approaches that of the *dynamic CCA adaptation* scheme, due to its aggressive nature. However, this impact has been overcome by the high level of spatial reuse and transmission attempt probability, which is achieved by effectively jointly adjusting CS_{th} and CW upon differentiating among failures. Therefore, the proposed scheme continues to be more advantageous in achieving better throughput, when compared with other simulated schemes, as the network gets denser (when there are 25 flows).

Impact of traffic load

Next, we study the impact of the traffic load on the network performance by varying the packet generating rate of the CBR flows from 200 to 1000 packets/second and the results are shown in Figure 5.6; the number of CBR flows is fixed to 10. The network throughput behaves in a similar way to that of Figure 5.4. Initially, when the

traffic load is light (200 packets/sec) for the network to be able to support all flows, the collision probability is small (less than 15%) and the flows are easily separated in time without the need to tune CS_{th} or CW. Hence, all algorithms show almost the same throughput. As the traffic load increases ($\geq$ 400 packets/sec), the collisions from RTS packets increase and the IEEE 802.11 starts showing its limitations in sharing the channel. The *spatial backoff*, *dynamic CCA adaptation* both achieve better throughput than the IEEE 802.11, due to the improvement of spatial reuse achieved by tuning CS_{th}. However, since neither of them completely solves the hidden terminal problem, as the network load increases, the collisions from hidden terminals start to impact the throughput (Figure 5.7). In contrast, the proposed scheme is able to differentiate the transmission failures and accordingly adjust both CS_{th} and CW to avoid collision from hidden terminals while maintaining a high level of transmission attempt probability to yield a high channel usage. Indeed, this enables the proposed scheme to outperform *spatial backoff* and *dynamic CCA adaptation.*

Impact of node mobility

Node mobility has a great impact on the network performance. We select the Random Way-Point mobility model and vary the node's maximum speed from $2m/s$ to $10m/s$. The number of flows is 10 and the packet generating rate is 400 packets/s. Figure 5.8 illustrates the aggregate throughput of all simulated schemes under different mobility levels. It can be seen from the figure that when the speed is low (e.g., $2m/s$), the proposed scheme still posses a leading performance since the network topology does not vary rapidly. However, as the moving speed increases, it can be seen from the figure that all schemes suffer a dramatic throughput drop. This is mainly because the source and destination nodes may become outside the transmission range of each other, which results in more transmission failures. On the other hand, routing table entries may become unstable due to mobility and may require updating, which adds

more congestion on the network.

5.4 Conclusion

In this chapter, a novel dynamic spatiotemporal scheme that balances the tradeoff between collision and spatial reuse in multi-hop wireless networks has been presented. Using this novel approach, a node dynamically adjusts its CS_{th} to eliminate collisions from hidden terminal and enhances spatial reuse by diminishing the effect of the exposed terminals. At the same time, the proposed approach reduces the collisions from among contending hosts while maintaining the level of transmission attempt probability through carefully selecting the contention window. An effective loss differentiation mechanism is proposed to work in concert with the proposed methodology. Moreover, and unlike the DCF access mode, the RTS/CTS handshake does not silence neighboring nodes but rather only informs them to bound their CS_{th} to yield the on-going transmissions. To reduce the overhead from the RTS/CTS handshake, and based on the network performance policy, a policy has been proposed wherein a node can adaptively enable/disable the RTS/CTS exchange. Simulation results and comparisons with other recent methods showed the effectiveness of the proposed method in improving the network performance.

Chapter 6

Distributed Correlative Power Control Schemes for Mobile Ad hoc Networks using Directional Antennas

Signal-to-interference-ratio (SIR) based power control schemes with directional antenna uses the current interference measurement. A source node measures the current interference and encapsulates it in either one of its control or data packets. The receiver node according to a predefined power control scheme will calculate the required transmission power for its ensued control or data packet based on this interference measurement. However, interference may change and thus power assigned to this ensued packet may be insufficient in some cases for successive packet delivery. To the best of our knowledge, no power control schemes with directional antenna use the estimation of the future interference has been proposed in literature.

A distributed correlative power control schemes using interference estimation techniques with directional antenna is proposed. The interference model [85] is extended

to take into account the deafness, hidden terminal and side lobe effects associated with directional transmission. Using this interference model, an analytical study of the power relations that exist between the directional IEEE 802.11 four-way handshaking for successful packet delivery by achieving a target signal to interference ratio (SIR) at both the transmitter and receiver is presented. Based on these correlations, a distributed power control scheme is proposed. Furthermore, and based on the simulation results, the true potentials from the proposed control scheme cannot be shown due to the imperfection of the model derived. From these observation, an enhanced correlative power control scheme deploying prediction filters (Kalman or extended Kalman) is proposed. Prediction filters are shown to achieve more accurate interference estimation in future.

The organization of the rest of the chapter is as follows. In section 6.1, the power control schemes using directional antenna are presented. Section 6.1 presents various simulations carried for different topologies to demonstrate the significant throughput and energy gains that can be obtained under the proposed protocols. Finally, the conclusions is presented in Section 6.3.

6.1 Correlative power control schemes

6.1.1 MAC and Physical Layer Properties

Our proposed protocol schemes will operate based on the following properties:

- IEEE 802.11 directional physical carrier sensing mechanism is adopted [114]. A transmitter cannot initiate any communication in a specific direction if it receives a power level larger than a given carrier-sensing threshold denoted by CS_{th}.

- The D-MAC protocol is adopted with so-called directional virtual carrier sensing (DVCS) [114], a directional version of IEEE 802.11 NAV (network allocation

vector) DNAV. Here, a node is not allowed to send any frame in a specific direction if its DNAV in that specific direction is set.

- Interference power at each time instant can be measured quickly, but probably with errors at each node. The interference power is equal to the difference between the total received power and the power of the desired signal.

- We assume all nodes in ad hoc network are homogeneous and all the radio parameters are the same with two-ray channel model.

- The channel loss gain between a pair of nodes can be determined. The channel loss gain can be measured as follows:

$$Gain = \frac{P_r}{P_t} \tag{6.1}$$

where P_r is the received power from the transmitted power P_t.

- A receiver is able to receive and decode correctly a packet if and only if the defined SINR at the receiver side is larger than or equal to predetermined threshold denoted by ζ; thus we have the condition defined in equation 2.1: Substituting equation 2.1 into equation 6.1, we get

$$P_t \geq \frac{\zeta \times P_n}{Gain} \tag{6.2}$$

Another necessary condition that is defined in chapter 2 for a receiver to be able to receive and correctly decode a packet is that the power of the received packet should be equal to or greater than a threshold power level denoted by κ. Thus, the minimum transmission power is:

$$P_{min} = \frac{\kappa}{Gain}. \tag{6.3}$$

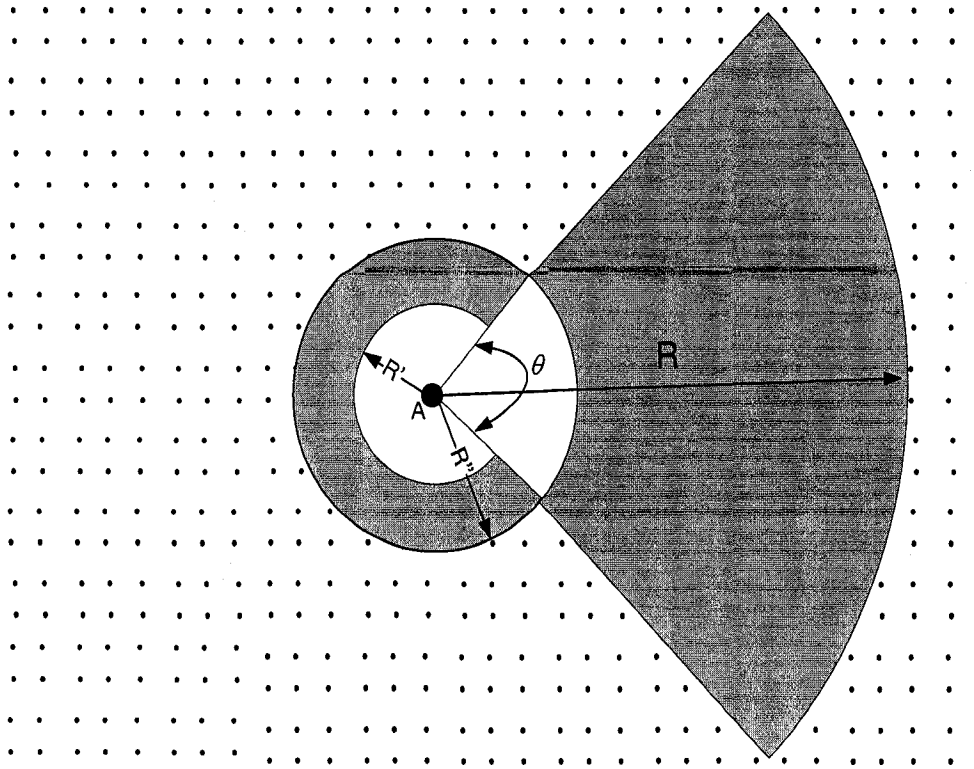

Figure 6.1: Generic Directional Antenna Interference region

6.1.2 Interference Estimation using analytical models

Preliminaries

A generic model of directional antenna for determining the interference is shown in Figure 6.1 [85]. R denotes the maximal permission range of node A. R'' is the maximal range of the side lobe of node A. R' is the constraint range of the side lobe. θ is the beam width of the main lobe. Here, nodes lying in the area of constrained range and in the area formed by the intersection of the node's main beam (the white region in Figure 6.1) with that of side lobe of radius R' are refrained from transmission in any direction since their transmission may highly affect the ongoing communication. We extend and adapt this model to fit the requirements of our proposed power control scheme.

Two types of interferers result from the application of directional antennas, namely the potential interferes and the indirect interferes. All nodes outside the main lobe

and outside the side lobe range (the dotted shaded region in Figure 6.1) are considered potential interfere, and may turn their directional antenna in any direction. All nodes inside the main beam of A within range R and greater than R'' or inside the side lobe of A with a range between R' and R'' are considered indirect interferes (the gray region in Figure 6.1) since they will refrain from transmission in the direction of node A and they will not cause any direct interference to node A. These nodes are free to be engaged in any communication towards other directions.

Directional Interference Model

Let P_t be the transmission power, G_d be the gain of the main lobe, and G_s be the gain of the main side lobe represented by R". The value of G_s is between 0 and 1. h is the antenna height. Using the two-way propagation model, with the exponential attenuation factor equal to 4, and the transmitted power P_t, the values of R, R'' and R' can be found by [85]:

$$R = \left(\frac{P_t \cdot G_d^2 \cdot h^2}{\kappa}\right)^{1/4} \tag{6.4}$$

$$R'' = R \cdot G_s^{1/4} \tag{6.5}$$

$$R' = R \cdot G_s^{1/2} \tag{6.6}$$

Note that, potential interferer nodes may turn their antenna to any direction with equal probabilities. As a result, the antenna gain of these nodes is a random variable given by G_I:

$$G_I = \frac{(2 \cdot \pi - \theta) \cdot G_s + \theta \cdot G_d}{2 \cdot \pi} \tag{6.7}$$

The interference power of any interfere node is a random variable and can be estimated by average value P_{avg}. We now proceed to find the total amount of interference as perceived by node A. Consider the nodes inside the arc-shaped area delimited by the main beam of node A and at distances r and $r + dr$ from node A. Each node in this area is going to contribute an interfering signal $I_1(r)$. Whereas,

each node outside node's A main beam and at distance in $[r, r+dr]$ will contribute an interfering signal $I_2(r)$. Here, $I_1(r)$ and $I_2(r)$ be expressed as follows

$$I_1(r) = \begin{cases} \frac{P_{avg} \cdot G_d \cdot G_I \cdot h^2}{r^4} & r > R \\ \frac{P_{avg} \cdot G_s \cdot G_d \cdot h^2}{r^4} & R'' < r < R \end{cases} \tag{6.8}$$

$$I_2(r) = \begin{cases} \frac{P_{avg} \cdot G_s \cdot G_I \cdot h^2}{r^4} & R'' < r \\ \frac{P_{avg} \cdot G_s \cdot G_s \cdot h^2}{r^4} & R' < r < R'' \end{cases} \tag{6.9}$$

Therefore, the total interference is given by:

$$\begin{aligned} I_{total} = & \rho \cdot (\theta \cdot (\int_{R''}^{R} I_1(r) \cdot r\, dr + \int_{R}^{\infty} I_1(r) \cdot r\, dr) + \\ & ((2 \cdot \pi - \theta) \cdot \int_{R'}^{R''} I_2(r) \cdot r\, dr + \int_{R''}^{\infty} I_2(r) \cdot r\, dr)) \end{aligned} \tag{6.10}$$

where ρ is the uniform active density determined by the number of active nodes on the whole network divided by the area of distribution of all nodes in the network $(nodes/m^2)$,and can be approximated as will be shown next.

Prior to transmitting a packet, a node can approximate the communication activity of its neighbors, i.e those lying mainly in the area $(\pi \cdot R^2)$. This is done via the recorded received control and data packets in the *angle of arrival (AOA)* cache table of every packet not destined to itself from its neighbors. Network nodes that have not transmitted a signal for a while will be removed from the AOA cache table, and thus the node will not consider them in approximating the active density. Through this approximation method, the node predicts the activity of its neighbors; if a node checks the AOA table and finds 4 recorded entries, the node can fortell that there are 4 active nodes that may interfere with its main-lobe or side-lobe transmission and calculates the active density as $\frac{4}{\pi \cdot R^2}$. Note that this estimation is not quite accurate since we are assuming the ratio of total active nodes over the total network area

should be equal to the number of active nodes in a node transmission range over the transmission range area. Another reason for inaccuracy of this estimation is that any neighbor node may become active in the future while the ongoing communication is taking place. To account for this second reason, we propose a safety margin c, that is $c \times \rho$. Note that c is a simulation parameter and may vary depending on the topology under study. Therefore, the estimated network density naturally accounts for dynamically changing traffic flows and mobility in the network.

Simplifying the total interference given by (6.10) by using (6.4), (6.5), (6.6), (6.7) ,(6.8) and (6.9) we obtain:

$$I_{total} = \frac{\rho \cdot P_{avg} \cdot \sqrt{\kappa} \cdot (K_1 + K_2)}{\sqrt{P_t}} \tag{6.11}$$

where

$$K_1 = \frac{\theta \cdot h \cdot (G_I + \sqrt{G_s} - G_s)}{2}$$

and

$$K_2 = \frac{(2 \cdot \pi - \theta) \cdot h \cdot G_s \cdot (\frac{G_I}{\sqrt{G_s}} - \sqrt{G_s} + 1)}{2 \cdot G_d}$$

I_{total} is the total interference estimated; all the variables are known except P_{avg}. Many estimation algorithms [38] have been proposed to find P_{avg}. The worst case scenario is to consider $P_{avg} = P_{max}$. In our model, P_{avg} is determined adaptively from the node performance. The value of P_{avg} at each node starts with an initial value that is equal to P_{max}. Here, P_{avg} is lower bounded by P_{min} and upper bounded by P_{max}. For every N_{frames}, that a node transmits, and are consecutively received successfully at the receiver, P_{avg} is decreased by a factor of $0.1 \times P_{avg}$; otherwise, if one frame is lost, P_{avg} is increased by a factor of $0.1 \times P_{avg}$. Here, N_{frames} is a simulation parameter.

Power Control using Interference Model

Using the derived model, we derive and analyze the relation between RTS and CTS messages, then generalize by induction to four way handshake. As stated before, a necessary condition for receiving an RTS and CTS messages is:

$$\begin{cases} P_{rRTS} \geq \kappa \\ P_{rCTS} \geq \kappa \end{cases} \tag{6.12}$$

where P_{rRTS} and P_{rCTS} are the received power of the RTS and CTS messages. Using equation (6.1) we get:

$$Gain = \frac{P_{rCTS}}{P_{CTS}} \tag{6.13}$$

where P_{CTS} is the power needed to transmit a CTS message. The total noise power estimated at the sender's side assuming $P_{thermal} = 0$ is simply I_{total}. By substituting equations (6.12), (6.13) in equation (6.2) we obtain:

$$P_{CTS} \geq \zeta \cdot \left(\frac{\rho \cdot P_{avg} \cdot \sqrt{\kappa} \cdot (K_1 + K_2)}{Gain \cdot \sqrt{P_{RTS}}} \right) \tag{6.14}$$

where P_{RTS} is the transmitted power of the RTS message. Together (6.12) and (6.14) constitute sufficient condition for both the RTS frame and the ensuing CTS frame transmission to succeed. Similarly, we follow the same procedure to get the transmitted power of DATA frame from CTS frame and the ACK frame from DATA frame. Given that RTS message is sent with the maximum power, the transmission power of the ensuing frames CTS, DATA and ACK are given by:

$$P_{CTS} = max(P_{min}, \psi \cdot \frac{P_{avg}}{\sqrt{P_{RTS}}}) \tag{6.15}$$

$$P_{DATA} = max(P_{min}, \psi \cdot \frac{P_{avg}}{\sqrt{P_{CTS}}}) \tag{6.16}$$

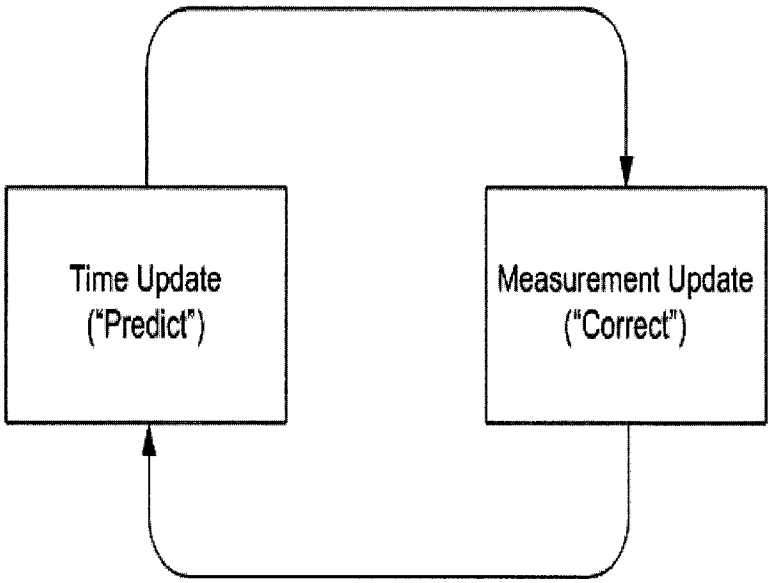

Figure 6.2: The ongoing Kalman filter cycle. The time update projects the current state estimate ahead in time. The measurement update adjusts the projected estimate by an actual measurement at that time

$$P_{ACK} = max(P_{min}, \psi \cdot \frac{P_{avg}}{\sqrt{P_{DATA}}}) \tag{6.17}$$

where $\psi = \zeta \cdot \frac{\rho \cdot \sqrt{\kappa} \cdot (K_1 + K_2)}{Gain}$ and P_{min} is given by equation (6.3).

6.1.3 Interference Power Prediction using Prediction Filters

Preliminaries

Kalman filter has been recently proposed in the literature [115] in different mobile cellular systems applications related to power control such as in interference estimation and channel gain prediction. A Kalman filter method for power control is proposed for broadband, packet-switched TDMA (Time division multiple access) wireless networks in [115]. In this work, a terminal starts sending data packets via an TDMA uplink channel to the base station and upon receiving the first data packet in slot n, the base station measures the channel interference around its area and predicts the future interference using Kalman filter. Based on the predicted interference, the base station calculates the required optimum power for receiving the next data packet in

slot $n+1$. This information is relayed to the terminal via a downlink channel.

The advantages of the Kalman filter are its simplicity due to its recursive structure, robustness over a wide range of parameters and conditions, and the fact that it possibly provides an optimal estimate with minimum mean square error. These features and the successful reported application stories in various research fields (such as target tracking and detection, digital signal processing, digital image processing, etc) for Kalman filter have motivated us to apply it for power control in MANET.

The Kalman filter estimates a process by implementing feedback control form; the filter estimates the process at some time, then obtains feedback in the form of noisy measurement. Thus, Kalman filter prediction equations consist of two types: time update equations and measurement update equations. The time update equations estimate the process a priori value for the next time step by projecting forward in time the current state and error covariance estimates. Moreover, the measurement update equations integrate the new feedback measurement into a priori estimate to obtain an improved posteriori estimate. Indeed the final prediction algorithm shown in Figure 6.2 resembles that of a predictor-corrector algorithm [116] for solving numerical problems where the time update equations are the predictor equations, while the measurement equations are the corrector equations.

Interference Prediction

Let I_n be the actual interference-plus-noise power in dBm received at time event n. I_n is to be considered the process state to be predicted by the Kalman filter. The thermal noise power, which depends on the channel bandwidth, is given and fixed. The total interference is simply the thermal noise plus the measured interference. The system dynamics of the interference plus noise power can be modeled in state-space form as:

$$I_n = I_{n-1} + N_n \tag{6.18}$$

where N_n is the variation of the interference-plus-noise power as new interfering nodes may start to initiate transmissions and/or adjust their transmission power in the time event n. According to the Kalman filter state-space mode, N_n is the process noise. Let X_n be the measured interference plus noise power at time event n. Then,

$$X_n = I_n + E_n \tag{6.19}$$

where E_n is the measurement noise. Equations (6.18) and (6.19) are commonly referred to as the state space generation model. The time equations of the Kalman filter in this case are

$$\tilde{I}_{n+1} = \hat{I}_n \tag{6.20}$$

$$\tilde{P}_{n+1} = \hat{P}_n + Q_n \tag{6.21}$$

where $\tilde{I}_{n+1}$ is the a priori predicted interference at next time event. $\hat{I}_n$ is the a posteriori estimate of I_n. $\tilde{P}_{n+1}$ and $\hat{P}_n$ are a priori and a posteriori estimate of the interference plus noise error covariance at time event $n+1$ and n respectively. Q_n is the covariance of the process noise N_n. The measurement update equations are:

$$K_n = \frac{\tilde{P}_n}{\tilde{P}_n + R_n} \tag{6.22}$$

$$\hat{I}_n = \tilde{I}_n + K_n \times (X_n - \tilde{I}_n) \tag{6.23}$$

$$\hat{P}_n = (1 - K_n) \times \tilde{P}_n \tag{6.24}$$

where $\tilde{I}_n$ and $\hat{I}_n$ are a priori and a posteriori estimate of I_n, $\tilde{P}_n$ is the a priori estimate of the error variance at time event n, K_n is the Kalman gain, and R_n is the covariance for the measurement noise E_n.

In the actual tuning operation of the filter, the measurement noise covariance R_n

and Q_n can be determined as follows :

$$Q_n = \frac{1}{M-1} \times \sum_{n=1}^{M} (X_n - \bar{X}_n)^2 \tag{6.25}$$

$$R_n = C \times Q_n \tag{6.26}$$

where $\bar{X}_n$ is the mean of the last M measured values at time event n. The event n is when a node successfully receives a control or data frame. X_n is the last obtained measured value. C is a constant between 0 and 1. Q_n is an estimate of the variance of the sum of the process and measurement noise because measurements $\bar{X}n$ include the fluctuation of both interference and measurement errors.

A necessary condition for Kalman filter to operate is that the process noise N_n should have a normal distribution [116]. The radio channel model considered in this chapter includes two ray path loss, antenna gain and shadowing. Shadowing is a log-normal distributed random variable caused by terrain features. The received signal power at any node can be formulated as :

$$P_r = P_t \times r^{-4} \times G^2 \times h^2 \times 10^{\Im/10} \tag{6.27}$$

where r is the distance between the two nodes and h is the height of the antenna. G is the antenna gain of the nodes and is considered identical for all nodes. P_r is the received power from the transmitting power P_t. Note that $\Im$ is the shadowing component, which is characterized by a Gaussian random variable with zero mean and standard deviation of σ dB. This makes N_n in dBm normally distributed which verifies the use of Kalman filter in the prediction of interference in MANET environment.

The convergence properties of the Kalman filter is dependent on the values of the variance denoted by (P) [116]. We will show by simulation that P is within limits and has the convergence shape at the end of the performance evaluation section. The

Kalman filter algorithm functions as follows: for event n, the interference measurements are input to (6.25) and (6.26) to estimate Q_n and R_n. Using these values and the current measurement X_n in (6.22) to (6.24), we get Kalman gain K_n, and the posteriori estimates for I_n and P_n, respectively. The a priori estimates for the next time event are given by (6.20) and (6.21). Specifically, I_{n+1} in (6.20) is used as the predicted interference plus noise power for power control as we are going to discuss in the coming section; note that, P_{n+1} is used as an initial value to get the next predicted value.

The extended Kalman filter (EKF) [116] attempts to correct the error induced between the process and measured values, and it is mainly used for non-linear systems. The process in evaluation has been modeled as linear system and thus a small enhancement can be added using the EKF scheme. This enhancement is incorporated with in time equations of the EKF. Thus EKF time update equation is given by:

$$\tilde{I}_{n+1} = \hat{I}_n + (\tilde{I}_n - \tilde{I}_{n-1}) \tag{6.28}$$

Power Control using prediction filters

Before initiating a transmission, node A measures the interference at time instance t, the interference plus noise-power are used as input to the Kalman filter or extended Kalman filter to predict the estimated interference plus noise power I at future time as discussed in previous section. Without loss of generality, I notation will be used as the predicted interference plus noise power ($in\ mw$) in the coming formulas and for all nodes. The RTS message which is sent at maximum power carries the interference information I to node B . Upon receiving the RTS message, node B uses this value I to calculate the required power of CTS as follows. Equations 6.15, 6.16 and 6.17 can be reformulated as follows. The transmission power of the CTS message is given

by:

$$P_{CTS} = max(P_{min}, \zeta \times \frac{I}{Gain}) \tag{6.29}$$

Before sending the CTS message, node B measures interference around its transmission zone and then predicts the interference plus noise power I_+ for the future in order for node A to be able to assign successfully a power value for its data packet. This predicted value is sent to node A in the CTS message. When node A receives the CTS message, it repeats the same procedure taken by node B to assign a suitable power value for DATA frame. The transmission power of the DATA message is given by:

$$P_{DATA} = max(P_{min}, \zeta \times \frac{I_+}{Gain}) \tag{6.30}$$

Node B receiving the DATA frame will assign a power value to the ACK frame as follows:

$$P_{ACK} = max(P_{min}, \zeta \times \frac{I_{++}}{Gain}) \tag{6.31}$$

where I_{++} is the predicted interference plus noise power at node A upon receiving the CTS message and is sent to node B in the DATA message.

6.2 Performance Evaluation

6.2.1 Simulation Setup

We use Qualnet [111] to evaluate by simulation the performance of our proposed power control schemes. We compare the proposed power control schemes with IEEE 802.11b, D-MAC schemes, Directional-BASIC (D-BASIC) [103]. Our comparison with D-BASIC would establish the virtues of the proposed schemes. The power control scheme using interference model for prediction is termed as adaptive. Moreover, we denote the power control scheme using Kalman filter as Adaptive-K and that of extended Kalman filter as Adaptive-EK. The channel rate is 11 Mbps and CBR

Table 6.1: Simulation parameter settings

$\tilde{P}_n$	1	σ	4 dB
σ	4 dB	ζ	10 dB
ζ	10 dB	P_{max}	15 dBm
P_{max}	15 dBm	κ	-78 dBm
κ	-78 dBm	η	-83 dBm
G_d	$15dbi$	G_s	$-6dbi$
h	1	N_{frames}	30
θ	$\frac{\pi}{6}$	Mobility factor	$2\ m\backslash sec$
C	0.8	Simulation Time	300 sec

(Constant Bit Rate) and FTP (File Transfer Protocol) traffic are in our study. Two network topologies are adopted in our simulations; one is 10×10 grid network with ten multi-hop CBR (constant bit rate) or TCP (transport control protocol) flows. The distance between each node pair is 100 meters. The other scenario is a 50 nodes uniform random network with Ten CBR or TCP flows and all nodes are inside a 1000×1000 square of meters. The packet size is 512 bytes and the packet sending rate for CBR is 400 packets/sec.

We are considering the following six scenarios:

1. Grid network with CBR flows;
2. Grid network with TCP flows;
3. Static random network with CBR flows;
4. Static random network with TCP flows;
5. Dynamic random network with CBR flows;
6. Dynamic random network with TCP flows;

Moreover,c for each simulation topology is determined respectively to be: 1.2, 1.2, 1.3,1.3,1.2,1.2; Other simulation parameters are shown in Table 6.1. In each scenario, one node may communicate with another node directly or by using a multihop route, depending on the transmit power. We use three metrics to evaluate 802.11, D-MAC, D-BASIC, Adaptive, Adaptive-K and Adaptive-EK: 1) Aggregate Throughput which is the sum of the data frames correctly received by the receivers per time unit; 2) Effective Data Delivered per Joule which is the received effective data frames divided by the entire energy consumption; 3) Data Frame Corruption Ratio which is the portion of MAC layer frames corrupted by interfering nodes.

6.2.2 Results and Analysis

Average Throughput

Figure 6.3 shows the total network end-to-end throughput for different MAC protocols; namely, IEEE 802.11, D-MAC, D-BASIC, Adaptive, Adaptive-k, Adaptive-EK. Clearly, the throughput of adaptive schemes are higher than that of the others. As can be seen in scenarios 1 and 2, the IEEE 802.11 suffers from channel access problems which make it inefficient in terms of throughput. This is because nodes within the transmission zone of the sender or the receiver are refrained from initiating any transmission for the duration of the ongoing communication between the sender and the receiver nodes. Thus, as traffic load increases, the duration to win the channel decreases. As a result, packets will be dropped because their transmission retry limit threshold is reached. The traffic load of 400 packets/sec is considered high and thus the IEEE 802.11 starts to show its limitations in sharing the channel in the time domain.

D-MAC and D-BASIC outperform the IEEE 802.11 due to their directivity gains and due to the lack of deafness events in the grid topology. D-MAC reduces the number of blocked nodes, so spatial reuse increases and hence throughput increases.

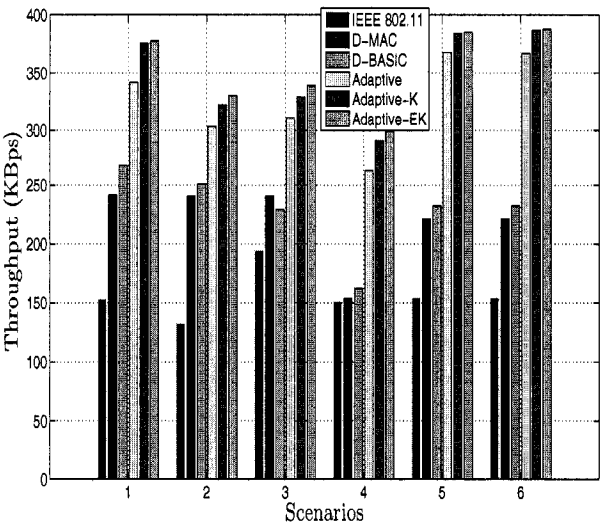

Figure 6.3: Network End-to-End Throughput

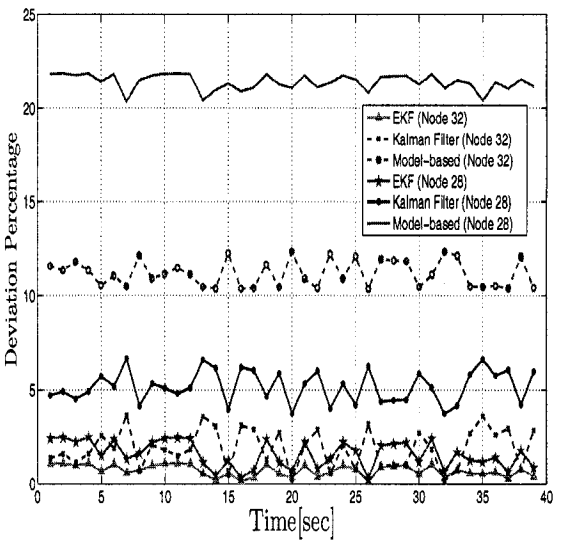

Figure 6.4: Interference Error percentage

D-BASIC effectively avoids interference, reduces the contention between nodes, and as well reduces the number of blocked nodes. This is the reason why D-BASIC outperforms D-MAC in terms of throughput in most of the scenarios. Nevertheless, D-BASIC suffers from hidden nodes problem, which clearly shows its effect in scenario 5 (Figure 6.3).

The proposed adaptive scheme can detect the active density and based on this estimation, can assign consecutive power to frames which differentiate it from others in terms of achieving better throughput gains. In case of no detected activity within the sender's region, packets are transmitted with a sufficient minimal power P_{min} for correct reception. This in turn decreases the interference and accordingly enhances the spatial reuse which results in better throughput gain. The Adaptive method uses an interference model to estimate the interference whereas tuned prediction filters predict this interference. Figure 6.4 shows an intuitive deviation comparison for the first 40 *sec* between these two techniques for random node 28 in scenario 3 and node 42 in scenario 6. As shown, prediction filters are able to follow the measured value with less deviation. It is to be noted here that deviation is defined as the measured value minus the estimated or predicted value. Figure 6.5 shows the average error considering all the scenarios for the interference estimation using Kalman, and extended Kalman filters and the model-based. An interference estimation value that is higher than the measured actual interference with an error that is more than 10% may highly affect the overall performance of the network. This is because nodes with higher interference estimation value may increase their transmission power to overcome this high interference; thus, the higher the transmission power, the more the interference effect on other nodes. As a result this may highly affect the overall network performance which is shown in Figure 6.5. Moreover, nodes with lower interference estimate value with an error greater than or equal to 10% will decrease their packet transmission power. In such a case, there is a likelihood that these packets may be corrupted

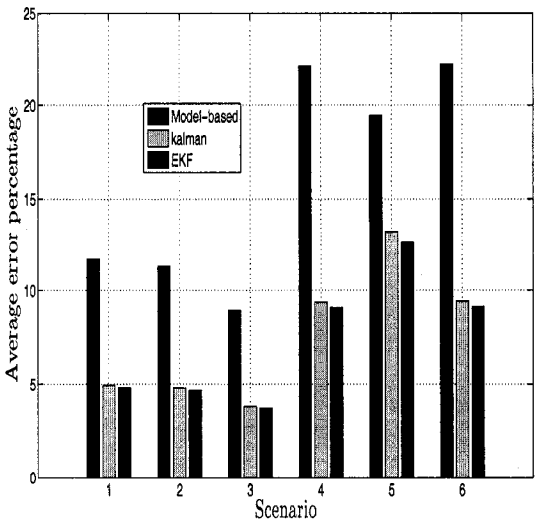

Figure 6.5: Average Interference error percentage

along the path due to actual interference that nodes were not aware of when they assigned power values to their consecutive packets. In conclusion, tuned prediction filters outperform the model based by an average error enhancement of 12.4% and this was the reason behind the prediction filters achieving higher throughput gain.

A slight improvement in terms of CBR end-to-end throughput for IEEE 802.11 is reported in scenario 3. The randomness of nodes enhances the IEEE 802.11 performance due to the fact that there exists cases where fewer nodes may lie in the vicinity of the transmission range of the sender. On the other hand, D-BASIC transmits data packets at low transmission power; there is high probability for data reception failure and accordingly this aspect decreases network throughput as can be seen in scenarios 3 to 6. When the load is high, the interference is large. Thus, D-MAC and D-BASIC protocols are not be able to use all their antenna beams due to the mutual interference problem. The adaptive schemes are shown to perform better in scenarios 3 to 6 since they resolve mutual interference problem.

Prediction Filters

To test the effectiveness of prediction filters, we consider scenario 5 and try to vary the interference fluctuation by adding additional flows between two simulation instances. Initially 10 CBR flows were running. We injected an additional 10 CBR flows between 5 sec and 200 sec to increase the interference. A snapshot for the same random node 28 is reported in Figure 6.6. The predicted value in Figure 6.6 is simply estimated at previous event for the next event. Thus, this figure shows the estimated value predicted at event t for the next event Vs the value measured at time instance $t+1$. As can be seen, the measured interference increases between these two time instances. The prediction filters were able to accurately follow the actual measured interference.

Throughput/Energy

Figure 6.7 depicts the ratio of throughput to average energy consumption per node in KBps/Joules. Energy consumption includes the energy of a successful transmission of packets, the lost energy in retransmitting a packet in case of collisions and the energy of the node while receiving a packet and when it is in idle state. The power savings are attributed to the gain of the directional antennas and to the correct assignment of power values for the adaptive schemes. Reduction in the mutual interference makes it feasible for nodes to deliver packets efficiently with less energy consumption.

Mobility

We study the impact of mobility on the average throughput for scenario 5. By increasing the mobility, the source and receiver nodes may not be able to communicate with each other due to the reason that either one of them will be out of range of the other. This may trigger link failures that may occur frequently due to disconnection of adjacent nodes in a route. Route table entries thus may get stale due to node mobility

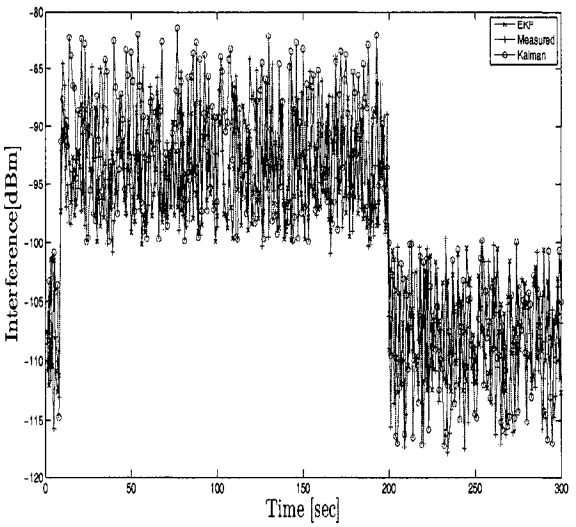

(a)

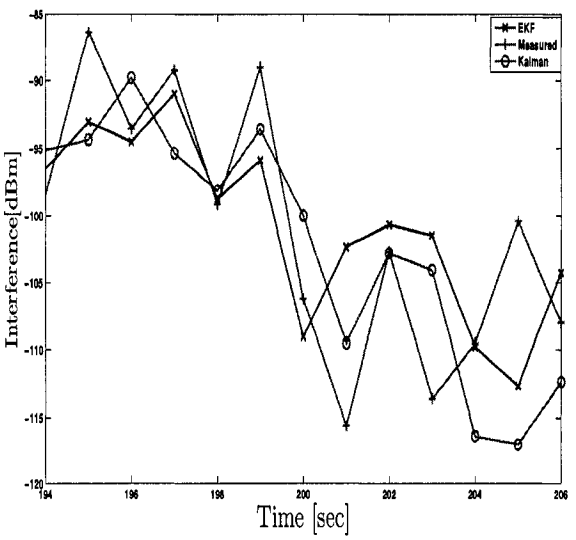

(b)

Figure 6.6: Interference prediction under variable traffic load

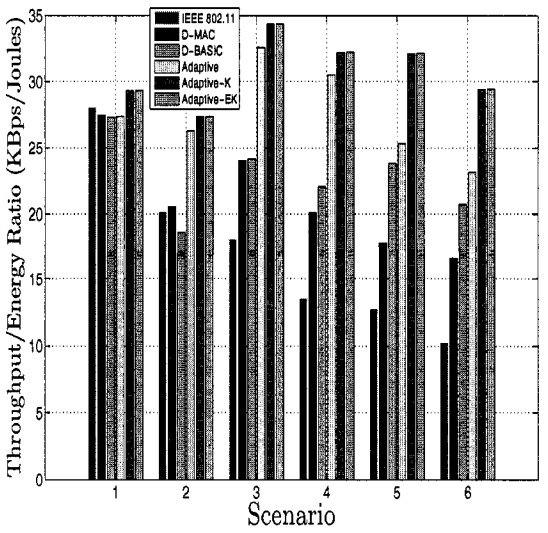

Figure 6.7: Ratio of Throughput by average energy consumption per node

and may require updating. This will add more congestion on the network. This is the reason why for all case studies (IEEE 802.11, D-MAC,D-BASIC, Adaptive, Adaptive-K, Adaptive-EK), the throughput starts to decrease as the mobility increases. As can be shown from Figure 6.8, the percentage decrease in throughput as mobility increases in the case where nodes are equipped with directional antennas is much less than the omnidirectional transmission. This is due to the directional transmission properties (directivity gains - higher range of communication) which may keep a link between two nodes stronger if one of the nodes is moving in the same direction as the directional antenna. This is, however, not the case with omnidirectional transmission where the range is limited and usually much shorter. However, directional transmission may suffer more frequent link breakages resulting from nodes that are moving outside the main lobe beamwidth area. This explains the fact that with directional transmission, the throughput decrease starts at lower mobility than the case of omnidirectional, as shown in Figure 6.8.

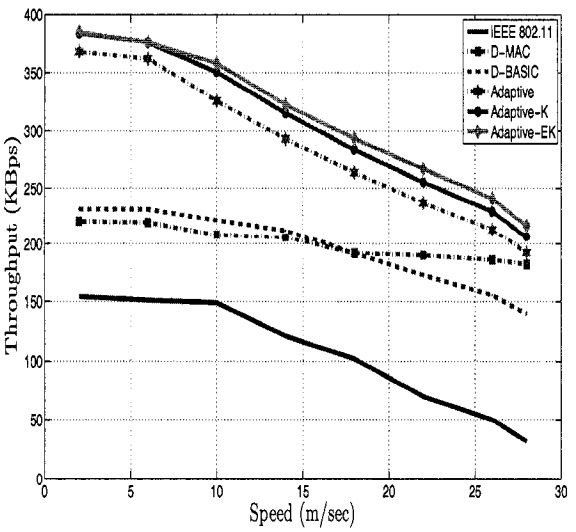

Figure 6.8: Scenario 5 CBR End-to-end throughput (KB/sec)

Data Frame corruption Factor

Figure 6.9 shows the data frame corruption ratio in all scenarios. Power control using adaptive schemes causes less corruption than the others. The reason behind this aspect is that all packets with IEEE 802.11 are transmitted with maximum power, thus the interference increases, and this results in more packet corruption. D-MAC suffers from deafness and mutual interference. This causes higher data corruption. D-BASIC and Adaptive schemes also suffer from deafness since both are based on D-MAC. Nevertheless, power control integrated with their operation decreases the mutual interference, thus achieving higher packet delivery rate. The effectiveness of the power assignment in the power control scheme adopting prediction filters is intuitively shown to decrease the number of packets dropped.

Deafness

In all the schemes considered, deafness played a major role in decreasing the throughput anticipated. D-MAC and D-BASIC suffer from this problem and this could be viewed mainly in the random topology (i.e. cases 3 to 6). Deafness has not been

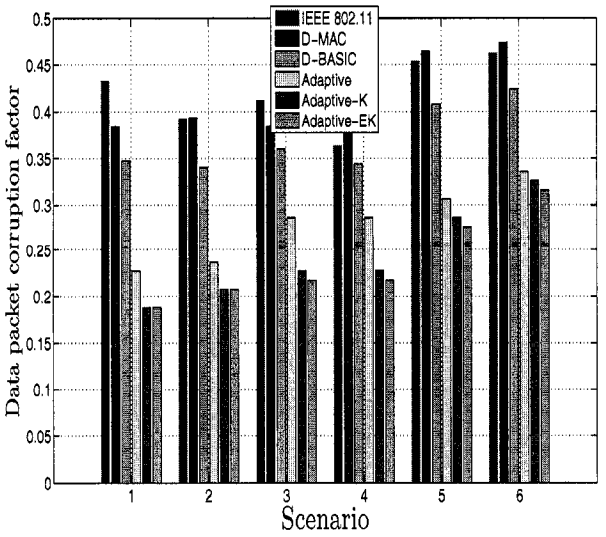

Figure 6.9: Data Frame Corruption Ratio

completely rectified with the proposed power control scheme since, as mentioned before, the scheme was built on D-MAC. Nevertheless, we verify that the efficient assignment of the directional CTS has decreased to high extent the deafness consequences. To verify our proposition, let us take a look at Figure . Figure 6.10 shows the probability of RTS retransmission due to timeout in scenario 5. The probability of RTS retransmission is simply the ratio of RTS packet retransmitted due to timeout to the total number of RTS packets sent throughout the simulation time. Deafness has a major effect on the RTS transmission parameter. IEEE 802.11 has the least value since it does not suffer from this problem. D-MAC and D-BASIC have nearly the same value since both of them send the CTS packet at fixed power value. The adaptive scheme sends the RTS packet at fixed power then adapts the value of the transmission power of the CTS packet to fit the node's activity around sender. If the node activity density is high, the power assigned to the CTS packet transmission will give it the potential to reach most of the active nodes. Consequently, this results in a decrease of the deafness phenomena but not complete elimination. Suggested solution for deafness is to add a busy tone channel, which is out of scope of this work.

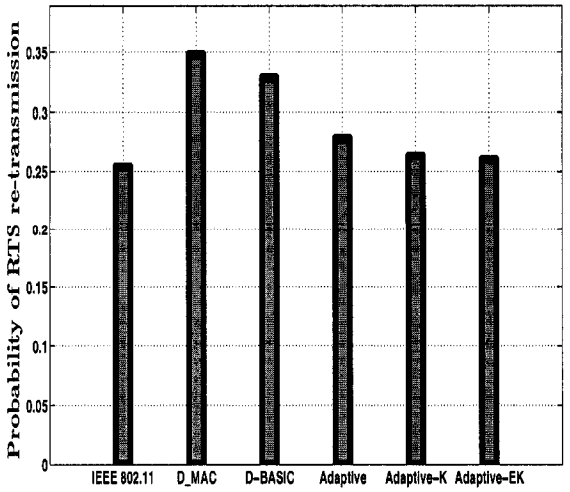

Figure 6.10: Probability of RTS re-transmission due to timeout

Kalman Filter convergence

Figure 6.11 shows the convergence of the error of interference plus noise power covariance $\tilde{P}$ estimates for a random node 28 in scenario 5 under normal traffic conditions for simulation time 500 *sec.* $\tilde{P}$ is within a value between 0 and 1 and has a convergence shape at the end of the simulation time. This result shows that Kalman filter has operated successfully and has maintained the convergence shape. We verify the Kalman convergence conditions [117], [116] with other nodes from other topologies and almost the same convergence shape has been depicted.

6.3 Conclusion

A power control scheme for directional MAC protocol which requires the use of a single channel for the transmission and for the reception of both control and data packets has been proposed. the temporal transmission power correlations that exist between the directional MAC protocol 4-way handshake packets (RTS/CTS/DATA/ACK)

for successful communication have been derived taking into accounts directional operational access problems such as hidden terminal problems, deafness and side lobe interference. Based on the node activity density, an interference model was estimated and together with the correlations derived, we were able to induce efficient constraints that ensure the correct delivery of each individual frame in this 4-way handshake. Moreover, the kalman and extended kalman filter has been introduced as another solution to estimate the interference in future. It is shown that the prediction filters outperform the model-based techniques by average error 14.3%.

It has been shown by simulation that the proposed power control schemes are efficient in terms of throughput and energy consumption. The performance of our proposed schemes have been compared with the performance of mobile ad-hoc networks using different MAC protocols such as the standard IEEE 802.11b MAC protocol, the D-MAC protocol with no power control and the D-MAC protocol with D-BASIC power control scheme. Our simulation results showed that the correlated power control schemes are improving the throughput compared to D-MAC by 48.6% on average. The proposed schemes outperform the IEEE 802.11 by 78.1% factor. At the same time, 74.2% reduction in energy consumed over the IEEE 802.11 are achieved by the correlated schemes.

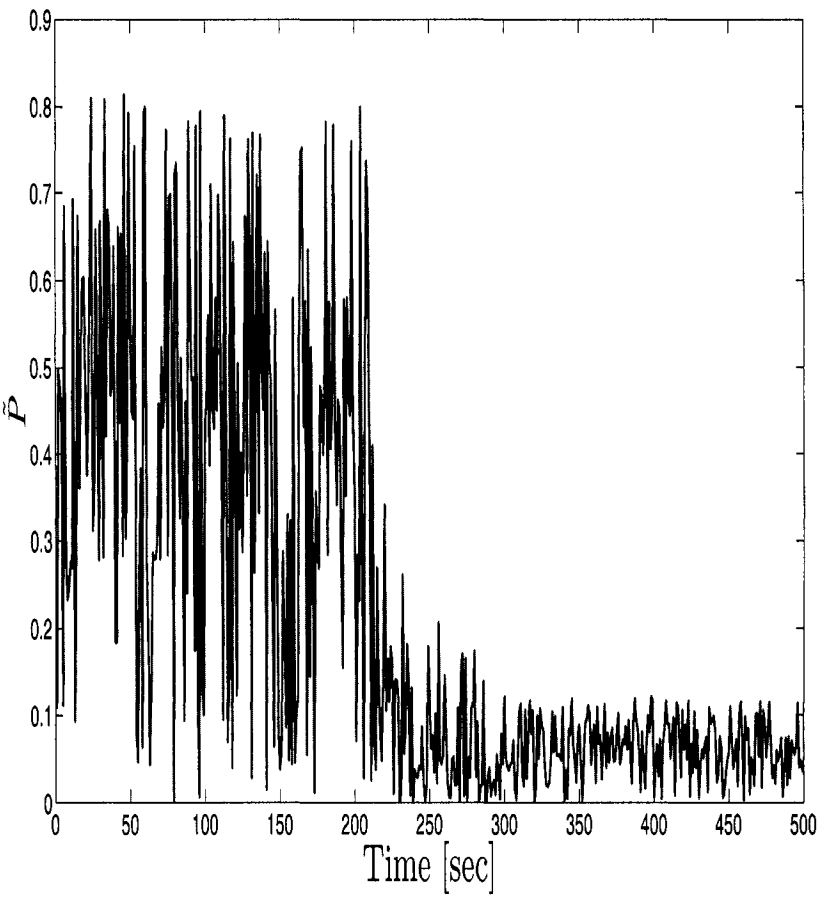

Figure 6.11: Convergence of Kalman filter

Chapter 7

Power-Aware Ad Hoc Networks with Directional Antennas: Models and Analysis

In this chapter, a theoretical study on the performance limits of power-aware multi-hop ad hoc network is presented where nodes are equipped with directional antennas. Specifically, the interactions of both the interference and collision in a power aware multi-hop wireless network are studied analytically and their impacts on the overall network capacity and energy consumption are analyzed. Furthermore, the transmission power adjustment gains in minimizing the overall energy consumption is investigated. To achieve the objective, an integrated interference/collision-aware analytical model is developed. A directional honey grid interference model [118] is constructed based on the directional antenna generic model proposed in [85]. Additionally, a collision model is constructed. Using the integrated interference/collision models with SIR constraints requirements, the expressions for the maximum throughput and energy consumption are calculated. The maximum throughput is the throughput that

could be achieved under the worst-case scenario, and that is the maximum interference. The energy consumption model shows both the energy consumed in collision resolution and the energy disbursed to meet the SIR constraints.

The rest of the chapter is organized as follows. Sections 7.1, 7.2 and 7.3 presents the model background. In Sections 7.4, 7.5 and 7.6 the interference, collision and energy models are developed respectively. Section 7.7 presents a comprehensive study of the directional IEEE 802.11 DCF mentioned attributes using the derived model after which the reliability of the model, is verified using discrete event simulations in Section 7.8. Finally, the conclusion is presented in Section 7.9.

7.1 Antenna Model

We adopt the generic model of the directional antenna presented in section 5.1.2 and shown in Figure 6.1 [85]. Accordingly, let P_t be the transmission power, G_t be the transmitter gain of the main lobe, G_r be the receiving gain. G_s be the gain of the main side lobe represented by R'', and h is the antenna height. The receiver is able to receive and decode the packet correctly if the received power P_r of a frame from a transmitter node in its transmission zone is higher than or equal to κ (the reception sensitivity). Furthermore, using the two-ray propagation model, with the exponential attenuation factor equal to 4, the transmitted power P_t of a frame can be written as:

$$P_t = \frac{\kappa R^4}{G_t G_r h^2} \tag{7.1}$$

The values of R, R' and R'' are given by equations 6.4, 6.5, 6.6 [85].

7.2 Medium Access Control

We consider that a directional version of IEEE 802.11 MAC (DMAC) is being adopted by all ad-hoc nodes, in order to access the shared channel using their directional antennas. We briefly summarize the protocol features that are needed in our analysis

- All nodes have two modes of operation, directional and omni-directional.
- When nodes are idle, they are listening to the media omni-directionally. All control and data packets (i.e. RTS, CTS, DATA and ACK) are transmitted directionally.
- On reception of an RTS packet, a node switches to directional mode and points its antenna back to the transmitting node, based on the direction-of-arrival of the RTS packet or knowledge of the location of that sender.
- Directional virtual carrier sensing [114] is implemented as follows. Each node keeps a directional NAV table with a similar use to the NAV value in 802.11. When it overhears an RTS or CTS packet, not destined to itself, it marks the direction-of-arrival in its NAV table as "busy" for the time duration contained inside the packet.
- When a node has a packet to transmit, it checks the direction of the intended recipient in its NAV table to see whether there is any ongoing transmission in that direction. If there is, it backs off and tries again later.

7.3 Network Topology

We assume that all nodes have a uniform setting (identical beamwidth and antenna gains) and the nodes are uniformly distributed over a large two-dimensional area with node density ρ. The sender and the receiver can be either in directional or

omni-directional mode when receiving or transmitting packets. Thus, four possible connectivity scenarios exist: 1) directional transmission and omni-directional reception (D-O) 2) omni-directional transmission and omni-directional reception (O-O) 3) omni-directional transmission and directional reception (O-D) 4) directional transmission and directional reception (D-D). Accordingly, we let R_{oo}, R_{od}, R_{do}, R_{dd} to be the ranges of the four connectivity scenarios **and G_d and G_o are the directional gain and the omni-directional gain respectively.** Thus, we have:

$$R_{oo} = \left(\frac{P_t G_o^2 h^2}{\kappa}\right)^{1/4} \tag{7.2}$$

$$R_{do} = R_{od} = \left(\frac{P_t G_d G_o h^2}{\kappa}\right)^{1/4} \tag{7.3}$$

$$R_{dd} = \left(\frac{P_t G_d G_d h^2}{\kappa}\right)^{1/4} \tag{7.4}$$

Moreover, let the average number of nodes in a transmission area of (O-O) neighbors with a radius R_{oo} be N, then we have: $N = \rho\pi R_{oo}^2$, $\rho\pi R_{do}^2 = \lambda N$, $\rho\pi R_{dd}^2 = \lambda^2 N$ **where $\lambda = \frac{G_d}{G_o}$.**

In our work, we assume that RTS/CTS messages are sent with fixed power to cover a range r_t ($r_t = a_{RTS} = a_{CTS}$), while DATA/ACK are sent with power value that is less than the fixed power to cover the distance between the sender and the receiver range ($r_t = r = a_{data} = a_{ack} \leq a_{RTS}$). Thus, the power of RTS and DATA packets assuming fixed bit error rate are related as:

$$P_{RTS} = P_{data}\left(\frac{a_{RTS}}{a_{data}}\right)^4 \lambda \tag{7.5}$$

7.4 Interference Model

7.4.1 Preliminaries

We assume that the system time is slotted with σ seconds. RTS, CTS, DATA and ACK packets are assumed to be with fixed length of L_{RTS}, L_{CTS}, L_{DATA} , L_{ACK} bits (including the physical header). The channel bit rate is assumed to be R (Mbps). Thus the transmission of RTS/CTS/DATA/ACK packets will last for $T_r = \frac{L_{RTS}}{R}$, $T_c = \frac{L_{CTS}}{R}$, $T_d = \frac{L_{DATA}}{R}$, $T_a = \frac{L_{ACK}}{R}$ respectively.

We assume that each node generates traffic with arrival rate of μ messages per second; we refer to this traffic as "own" traffic. Additionally, on average there are (H - 1) relay nodes between any source and destination pair. Consequently $\mu(H-1)$ will be the average volume of relay traffic reaching any node. Thus, the total traffic per node is calculated as node's own traffic + relay traffic which is equal to $\mu+\mu(H-1) = \mu H$.

Now, assuming that packets arrive at a node using a Poisson process with exponential arrival rate of $\mu \times H$, one can derive the probability that the station's buffer has no packets awaiting transmission, ζ. Assuming $M/M/1/Q/\infty$ queuing model [119], and denote l as the packet processing rate and Q as the queue length at the node, then, ζ can be obtained as follows:

$$\zeta = \frac{1 - \frac{\mu H}{l}}{1 - (\frac{\mu H}{l})^{Q+1}} \tag{7.6}$$

Next, we derive the probability that a station transmits in a time slot, τ. Similar to Bianchi's model [15], a modified Markov chain can be used to model the operation of the station' access to the channel with one additional state representing a station with no packet in its queue to transmit. Therefore, the probability that a node transmits in a time slot is given by [119]:

$$\tau = \frac{2(1-P_c^{m+f+1})}{\frac{2\zeta(1-P_c)}{(1-\zeta)} + (1-P_c^{m+f+1}) + W[\frac{(1-(2P_c)^{m+1})(1-P_c)}{1-2P_c} + P_c(2P_c)^m(1-P_c^f)(1-2P_c)]} \tag{7.7}$$

where $m = log_2(W_m/W_0)$, W_0 and W_m are the minimum contention window and maximum contention window respectively. P_c is the conditional collision probability (to be derived next). Furthermore, when the node reaches the m'th backoff stage, the contention window is increased up to the maximum value and then the station tries at most f retransmissions. When the node reaches stage $m+f$ and the backoff timer decreases to zero, the frame will be either transmitted successfully or discarded.

Finally, the average number of hops, H, required for forwarding a message from the source to the destination and assuming a random traffic pattern is given by [120], [121]:

$$H = \frac{L}{a_{data}} \tag{7.8}$$

where L is the average path length of a message.

7.4.2 Interference Derivation

According to the antenna model presented in Section 7.1, we derive the maximum interference that a node receiving a data packet encounters. We assume an ongoing communication between two nodes A and B. We then extend the analysis of the honey grid model presented in [30] to take into account the directional antennas application. Our honey grid model will be constructed based on the constraint range of the side lobe R'.

Based on equations (6.5) and (6.6), we assume that the value of G_s is chosen such that the ratio $n = \frac{R}{R''}$ ($R = a_{RTS,do}$) is an integer value not equal to 1 so that a deterministic grid model can be easily built. In this chapter, we consider the case when $n = 2$; for other values of n, the same methodology of analysis can be applied

to derive the final interference model. Accordingly, when $n = 2$, $R = 4R'$, $R'' = 2R'$ ((6.5) and (6.6)). Thus, the honey grid model is constructed and is shown in Figure 7.1. Based on Figure 7.1, we analyze and determine the number of nodes that might cause interference to the ongoing communication between A and B.

Nodes that lie in the region of $2\pi - \theta$ cause interference on node's A side lobe. As illustrated in section 7.1, these interfering nodes are classified as direct and indirect interfering nodes. Moreover, the number of interfering nodes relies also on the selection of θ. Here, we derive the interference for the case of $\theta = \frac{\pi}{4}$. For other values of θ, the same methodology of analysis can be used. Thus, the number of indirect interfering nodes at distance $R'' + \epsilon$ will be 5, 10, 15 at distances R', $2R'$, $3R'$ respectively. These indirect interfering nodes add interference that is multiple of $G_s G_d$ since they cause interference on node's A side lobe.

Nodes lying outside the circular region of $R+\epsilon$ are considered potential interfering nodes and these nodes will point their beams toward node A when sending the DATA packet and they interfere with the main lobe of node A. The number of interfering nodes for this case are 24, 48, 72, 96, and so on. These nodes are located respectively at distances $4R'$, $8R'$, $12R'$, $16R'$ and so on. These direct interfering nodes add interference that is multiple of $G_d G_d$.

Moreover, nodes lying in the main lobe area of the sender and at a distance less than $R + \epsilon$ and greater than $R'' + \epsilon$ can cause interference on node's A side lobe as illustrated in section 7.1. However, given the case where all the direct interfering nodes are transmitting, such nodes will be silenced.

Now, when node A sends its RTS frame successfully, node B replies back with a CTS packet. Here, nodes lying in the main lobe of the CTS packet have already been silenced by direct interfering nodes, and as shown in Figure 7.1, at most two nodes will be silenced by B's side lobe of radius R'. Thus, we have 22 direct interfering nodes at distance $4R'$ (instead of 24). However, to keep the analysis simple, we decided to

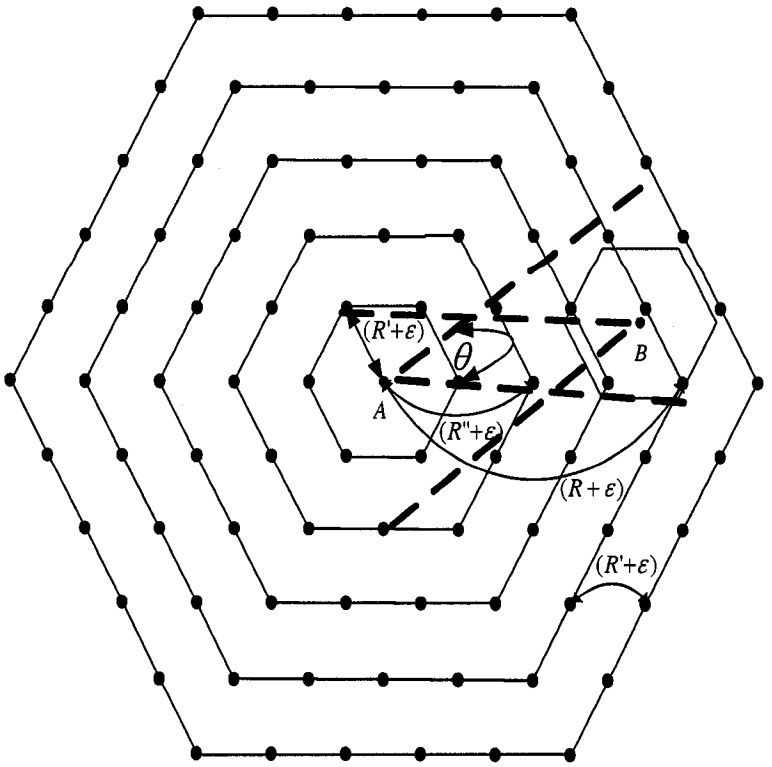

Figure 7.1: Interference

neglect this minimum effect of the CTS frame. By using equations (7.5) and (6.6), the interference level I_r is composed of interference level I_d from direct interfering nodes and I_i from indirect interfering nodes that are located at a distance r from the receiver. I_r is:

$$I_r = \tau(I_d + I_r) \tag{7.9}$$

where

$$I_d = \frac{\theta}{2\pi}(P_{data} r^{-4} G_d^2 (\frac{T_d + T_a}{T_r + T_c + T_d + T_a} + (\frac{a_{RTS}}{a_{data}})^4 \frac{G_d}{G_o} \frac{T_r + T_c}{T_r + T_c + T_d + T_a}))$$

and

$$I_i = \frac{2\pi - \theta}{2\pi}(P_{data} r^{-4} G_d G_s (\frac{T_d + T_a}{T_r + T_c + T_d + T_a} + (\frac{a_{RTS}}{a_{data}})^4 \frac{G_d}{G_o} \frac{T_r + T_c}{T_r + T_c + T_d + T_a}))$$

Here, τ is the probability that this interfering node transmits and has been derived

earlier. Moreover, $\frac{T_d+T_a}{T_r+T_c+T_d+T_a}$ resembles the portion of time needed to send the DATA and ACK packets over the whole 4-way handshake duration.

The total interference I by all interfering nodes derived in the honey grid model and after mathematical manipulation takes the form:

$$I = (\tau \frac{P_{data} G_d}{a_{RTS}^4} (\sum_{i=1}^{\infty} \frac{1}{i^3} \frac{24\theta G_d}{2\pi} + \sum_{i=1}^{\frac{R}{R'}-1} 5i \frac{G_s(2\pi-\theta)}{2\pi}) \\ (\frac{T_d+T_a}{T_r+T_c+T_d+T_a} + (\frac{a_{RTS}}{a_{data}})^4 \frac{G_d}{G_o} \frac{T_r+T_c}{T_r+T_c+T_d+T_a}) \tag{7.10}$$

Note that a receiver is able to receive and decode correctly a packet if and only if the signal to interference plus noise ratio (SIR) at the receiver side is larger than or equal to a predetermined threshold denoted by SIR_{min}.

$$SIR = G \frac{P_{data} {a_{data}}^{-4}}{I} \geq SIR_{min} \tag{7.11}$$

where G is the processing Gain used in the network physical layer.

Assuming a worst case interference, $SIR = SIR_{min}$, and rearranging (7.10), we obtain:

$$\tau = \frac{G \times a_{RTS}^4}{G_d \times SIR_{min} \times a_{data}^4 (\sum_{i=1}^{\infty} \frac{1}{i^3} \frac{24\theta G_d}{2\pi} + \sum_{i=1}^{\frac{R}{R'}-1} 5i \frac{(2\pi-\theta)}{G_s 2\pi})} \\ (\frac{1}{\frac{T_d+T_a}{T_r+T_c+T_d+T_a} + (\frac{a_{RTS}}{a_{data}})^4 \times \frac{G_d}{G_o} \times \frac{T_r+T_c}{T_r+T_c+T_d+T_a}}) \tag{7.12}$$

The τ obtained in (7.12) represents the transmission attempt probability under worst case interference, which together with (7.6) and (7.7) would give the maximum allowable traffic into the network , μ. Clearly, an closed formula for μ cannot be derived and hence we numerically solve this non-linear system to obtain its value.

7.5 Collision Model

We present in this section a model for deriving the effect of collisions on the throughput under the maximum interference. For this reason, we modify the model presented in [30] for a uniformly distributed multihop ad hoc network using directional antennas. Both the channel and node state models are used to derive the various parameters needed to determine the system throughput.

7.5.1 Channel State Model

Figure 7.2(a) depicts the wireless channel state transition at a given time slot σ. There exists 4 transition states within this Markov chain model.

- *IDLE* is the state that indicates that the channel around node A is sensed idle. The duration of this transition state is $T_{idle} = \sigma$.

- *TRANSMIT* is the state that a successful four-way handshake transmission has been completed and its duration is $T_{transmit} = T_r + T_c + T_d + T_a + 3SIFS + 4\omega + DIFS$.

- *RTS-col* is the transition state when two or more nodes accessing the same channel transmit at the same slot their RTS packets and thus their transmissions collide. The duration of this state is $T_{rr} = T_r + \omega + DIFS + SIFS$.

- *CTS-col* is the state that indicates that a hidden node from either node A or node B sends a packet and this packet will collide with the CTS packet. The duration of this state is $T_{cc} = T_r + T_c + 2\omega + 2SIFS + DIFS$.

where ω is the propagation delay.

Now we define the transition states. The states (*TRANSMIT-to-IDLE*, *RTS-col-to-IDLE* and *CTS-to-IDLE*) have respective transition probabilities equal to 1 since no node is allowed to transmit immediately after the channel becomes idle. The

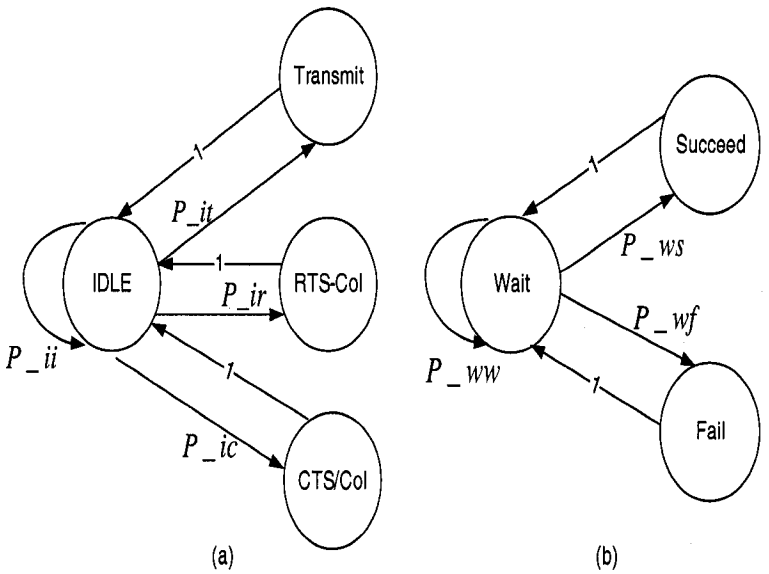

Figure 7.2: Channel and Node Wireless State

probability of the transition state *IDLE-to-RTS-col* is P_{ii}. Here, P_{ii} is the probability that there is not any directional neighboring nodes initiating any transmission:

$$P_{ii} = (1 - \frac{\theta\tau}{2\pi})^{\lambda N} \tag{7.13}$$

The transition *IDLE-to-TRANSMIT* has a probability P_{it} that exactly one node transmits at this time slot and starts a successful four way handshake while the other nodes in areas S_1 (as shown in Figure 7.3) refrain from transmitting in the direction of node A, and nodes in the area S_2 refrain from transmitting. P_{it} is given by:

$$\begin{aligned} P_{it} = P_s[\rho S_1(1 - \frac{\tau\theta}{2\pi})^{\rho S_1 - 1} + (\rho S_2 \\ (1-\tau)^{\rho S_2 - 1}] \end{aligned} \tag{7.14}$$

where P_s is the probability that a node begins a successful four-way handshake at this time slot and S_1 and S_2 are determined as follows:

$$S_1 = \frac{\theta a_{RTS,do}^2}{2} + \frac{(2\pi - \theta)a_{RTS,do}^2(G_s - G_s^{\frac{1}{2}})}{2} \tag{7.15}$$

$$S_2 = \frac{(2\pi - \theta)a_{RTS,do}^2 G_s^{\frac{1}{2}}}{2} + \frac{\theta a_{RTS,do}^2 G_s}{2} \tag{7.16}$$

Moreover, the transition state *IDLE-to-RTS-Col* has a probability P_{ir}. Here, P_{ir} is the probability that more than one node initiates a transmission of an RTS packet at the same time slot (i.e., P_{ir} = 1 - probability that none of the nodes in the area S_1 and S_2 transmits - probability that exactly one node in the area S_1 transmits towards node A - probability that exactly one node in the area S_2 transmits):

$$\begin{aligned} P_{ir} = 1 - (1-\tau)^{\rho(S_1+S_2)} - (\rho S_1(1 - \frac{\tau\theta}{2\pi})^{\rho S_1 - 1} \\ + \rho S_2(1-\tau)^{\rho S_2 - 1}) \end{aligned} \tag{7.17}$$

Finally, the probability of the *IDLE-to-CTS-Col* transition state, P_{ic}, is obtained:

$$P_{ic} = 1 - P_{ii} - P_{it} - P_{rts} \tag{7.18}$$

Now, we can solve for the Transmit state limiting probability β_t of the wireless channel state, by writing the equilibrium equations of the channel state diagram. β_t is simply the portion of time a node is successfully transmitting; in other words, it is the ratio between the successful transmission time to the total network time. The total time is defined as the sum of total transmission time and contention time. Hence, β_t can be derived as:

$$\beta_t = \frac{P_{it} L_{DATA}}{\sigma + P_{it} T_{transmit} + P_{ir} T_{rr} + P_{ic} T_{cc}} \tag{7.19}$$

Now in order to calculate β_t, we need to determine P_s.

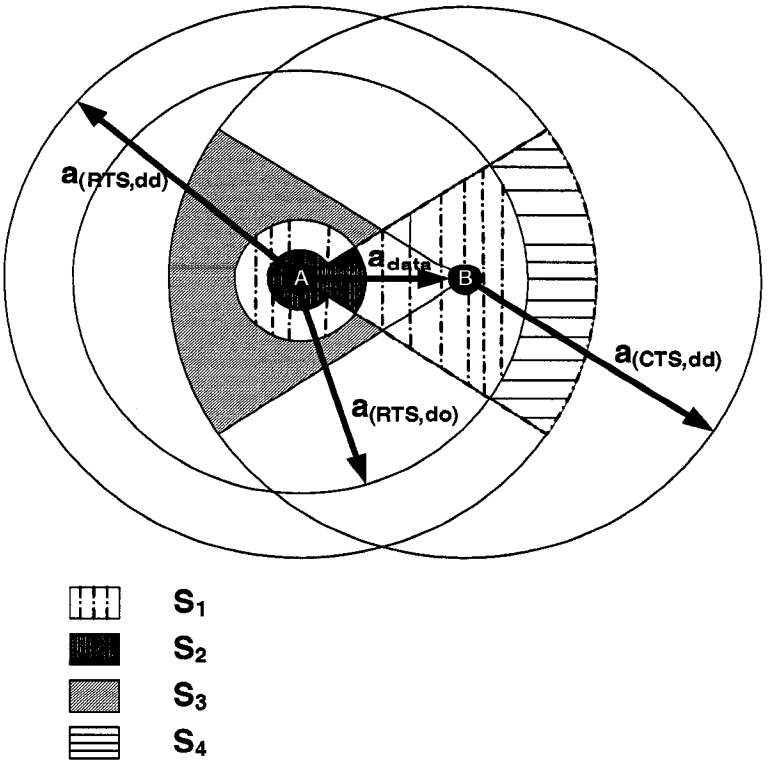

Figure 7.3: Hidden Areas

7.5.2 Node State Model

The states of the transmitting node can be modeled by a three state Markov chain, which is shown in Figure 7.2(b). Three states are defined in this model: *wait*, *succeed*, and *fail*. The *wait* state is when nodes defer for other nodes or backs off, *succeed* state is when a node completes a four way successful handshake and *fail* state is when the node's four way handshake is unsuccessful. Accordingly, we define the transition probabilities. Because of the assumption of collision avoidance, no node is allowed to transmit packets continuously, therefore the transition probabilities from *succeed* to *wait* and from *fail* to *wait* are both one, and the transition probabilities from *fail* to *wait* are both one and the transition probabilities from *succeed* to *succeed* and from *fail* to *fail* are both zero. Given that the node listens omni-directionally, the transition probability P_{ww} that a node having a packet to transmit continues to stay in *wait* state in a time slot is equal to the probability that it does not start any

transmission. In addition, there should be no node initiating a transmission in the direction towards the sending node. P_{ww} is given by:

$$P_{ww} = (1-p)(1-(\frac{\theta\tau}{2\pi}))^{\lambda N-1} \tag{7.20}$$

We define S_3 and S_4 to be the hidden areas from node B (Figure 7.3) when replying with the CTS packet to node A; thus the nodes existing in S_3 may collide with the CTS transmission. Note that the existence of the hidden nodes in S_4 results when both transmitter and receiver are (D-D) neighbors i.e., the range extended with a $\frac{G_d}{G_o}$. Therefore S_3 and S_4 are calculated as follows:

$$S_3 = \frac{\theta a_{RTS,dd}^2}{2} - \frac{a_{data}^2 tan(\frac{\theta}{2})}{2} - \frac{(2\pi-\theta)(a_{RTS,dd}^2 G_s^{2/\alpha})}{2} \tag{7.21}$$

$$S_4 = \frac{\theta(a_{RTS,dd}^2 - a_{RTS,do}^2)}{2} \tag{7.22}$$

The transition probability, P_{ws}, from the *wait* state to the *succeed* state is the probability that node A transmits at this time slot, node B does not transmit, none of the nodes existing in area S_1 transmit in the same direction towards node A, none of the nodes existing in area S_2 transmits, and none of the hidden terminals in areas S_3 and S_4 transmits for $T_r + SIFS + T_c + 2\omega$. This probability is then calculated as follows:

$$\begin{aligned} P_{ws} = \tau(1-\tau)(\rho S_1(1-\frac{\tau\theta}{2\pi})^{\rho S_1} + \rho S_2(1-\tau)^{\rho S_2}) \\ (1-(\frac{\theta\tau}{2\pi}))^{\rho(\frac{T_r+T_c+SIFS+2\omega}{\sigma})S_3} \\ ((1-(\frac{\theta\tau}{2\pi}))^{\rho(\frac{T_r+T_c+SIFS+2\omega}{\sigma})S_4} \end{aligned} \tag{7.23}$$

Now to consider the spatial reuse of the wireless medium, define the spatial reuse

factor $\nu(a_{data})$ which is the number of possible concurrent transmissions in the combined region covered by nodes A and B. Indeed, $\nu(a_{data})$ is the ratio between the total region covered by nodes A and B and the actual area that excludes the region covered by the handshake between nodes A and B (Figure 7.3). If there is one handshake in areas 1 and 4, then in theory there may be $\frac{S_{total}}{S_1+S_2+S_3+S_4}$ concurrent handshakes in the region excluding 1 and 4. Here, S_{total} is simply:

$$S_{total} = 2(\pi a_{RTS,dd}^2) - a_{RTS,dd}^2 \times (arccos(\frac{a_{data}}{2a_{RTS,dd}}) - \frac{a_{data}}{2a_{RTS,dd}} \times \sqrt{1 - \frac{a_{data}^2}{4a_{RTS,dd}^2}}) \tag{7.24}$$

Upon integrating the spatial reuse factor, P_{ws} can be re-written as $\nu(a_{data}) \times P_{ws}$. Finally, the transition probability P_{wf} from the wait state to fail state can be derived as:

$$P_{wf} = 1 - P_{ww} - P_{ws} \tag{7.25}$$

The limiting probability of the state succeed P_s is obtained by solving the equilibrium equations of the wireless node state transition diagram:

$$P_s = \frac{P_{ws}}{2 - P_{ww}} \tag{7.26}$$

The value of P_s is then inserted in equation (7.13) and the value of P_{it} is used in equation (7.19) to obtain β_t. Moreover P_c in equation (7.7) is calculated as $1 - P_s$. Assuming that the network is divided into several flows, each flow is assumed to reach its destination without causing collision, then the total throughput can be defined as the sum of the throughput of each flow. We define η as the ratio of the number of nodes that can simultaneously transmit at the same time slot without causing any

collision to the total number of nodes.

$$\eta = \nu(a_{data}) \times \frac{\chi}{\pi a^2_{RTS,dd}} \tag{7.27}$$

where χ is the network size.

Finally, the total network throughput (Thr) can be simply written as:

$$Thr = \eta \times \mu \times \beta_t \tag{7.28}$$

7.6 Energy Model

The total energy consumption [122], [123] is calculated as the energy needed to transmit control and data packets and their retransmissions due to collisions. The total power P_{RTS} consumed by the transmission and retransmission due to collision of the RTS control frames. P_{RTS} is simply the summation of power needed to send RTS frames multiplied by the probability that i nodes existing either in areas S_1 or S_2 transmit an RTS frame at the same time slot. Taking into account the power dissipated in the side lobes P_{RTS} can be derived as:

$$\begin{aligned} P_{RTS} = \frac{1}{2\pi}\theta(\sum_{i=1}^{\rho S_1}\binom{\rho S_1}{i} iCa^4_{RTS,do}(1+G_s\frac{2\pi-\theta}{\theta})(\frac{\theta\tau}{2\pi})^i \\ (1-(\frac{\theta\tau}{2\pi}))^{\rho S_1 - i} + \sum_{i=1}^{\rho S_2}\binom{\rho S_2}{i} iCa^4_{RTS,do} \\ \tau^i(1-\tau)^{\rho S_2 - i}) \end{aligned} \tag{7.29}$$

where $C = \frac{\kappa}{G_d G_o h^2}$.

The retransmission of CTS packets will be due to the hidden nodes existing in the S_3 and S_4 area. P_{CTS} is:

$$P_{CTS} = \frac{\theta}{2\pi}((\sum_{i=1}^{\rho S_3} \binom{\rho S_3}{i} iCa^4_{RTS,dd}(1 + G_s\frac{2\pi - \theta}{\theta})(\frac{\theta\tau}{2\pi})^i$$
$$(1 - (\frac{\theta\tau}{2\pi}))^{\rho S_3 - i}) + (\sum_{i=1}^{\rho S_4} \binom{\rho S_4}{i} iCa^4_{RTS,dd}(\frac{\theta\tau}{2\pi})^i \quad (7.30)$$
$$(1 - (\frac{\theta\tau}{2\pi}))^{\rho S_4 - i}))$$

The total consumed time T_{total} is calculated as:

$$T_{total} = \frac{T_{transmit}}{\beta_t} \quad (7.31)$$

Going back to the equilibrium equation of the wireless state transition diagram, we find β_r and β_c, the ratio of *IDLE-to-RTS*-col and *IDLE-to-CTS*-col relative times to the total time β_t respectively. β_r and β_c are given simply by:

$$\beta_r = P_{ir} \times \frac{\beta_t}{P_{it}} \quad (7.32)$$

$$\beta_c = P_{ic} \times \frac{\beta_t}{P_{it}} \quad (7.33)$$

P_{it} ,P_{ir}, P_{ic} are given by equations (7.14),(7.16) and (7.17) respectively. The total contention time during frame collisions has an RTS component and CTS/DATA/ACK component equal to

$$T_{RTS} = \beta_r \times T_{total} \quad (7.34)$$

$$T_{CTS} = \beta_c \times T_{total} \quad (7.35)$$

Having derived all the above parameters, we can derive the total energy (E) wasted in the network by multiplying the expected number of hops (H) by the energy per hop:

Table 7.1: Analytical parameter settings

Parameter	Value	Parameter	Value
SIFS	10 μs	DIFS	50 μ s
σ	20 μs	SIR_{min}	10dB
Packet size	1000 bytes	$[W_o, W_m]$	[31, 1023]
RTS packet	20 bytes	CTS/ACK packets	14 bytes
$MACheader$	34 bytes	R	2 Mb/sec
G	10.4 dB	L	$16d$
G_d	7 dB	G_s	-6 dB

$$E = H \times (P_{data} \times T_{transmit} + P_{RTS} \times T_{RTS} + P_{CTS} \times T_{CTS}) \tag{7.36}$$

where $P_{data} = Ca_{data}^4$.

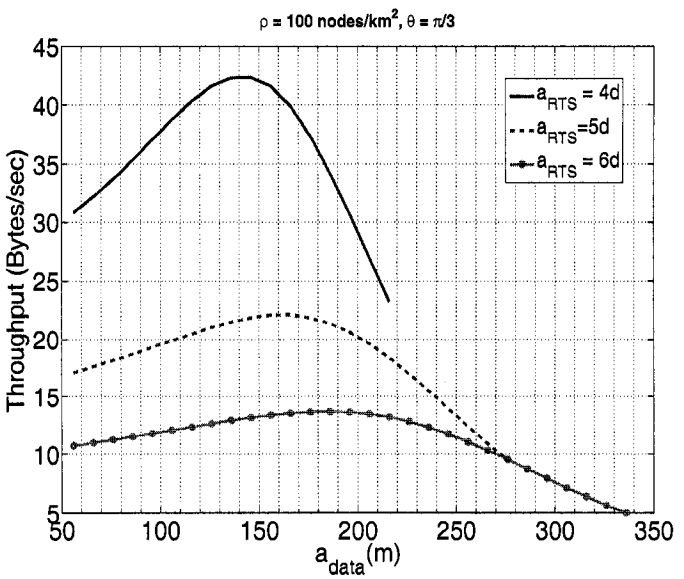

Figure 7.4: Network Throughput for different a_{RTS}

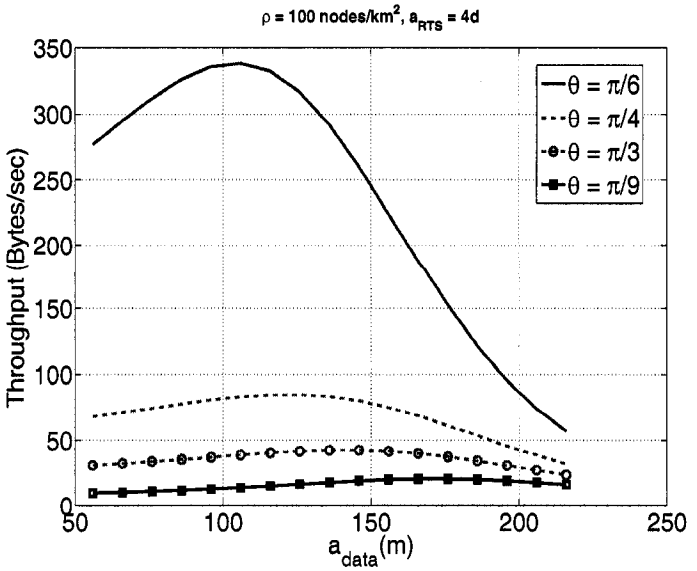

Figure 7.5: Total Network Throughput vs beam angle

7.7 Results and Analysis

Table 7.1 presents the various MAC and PHY parameters we used for obtaining our numerical results as well as in our simulation experiments. In our model verification, a_{data} is initialized to $d = \frac{1}{\sqrt{\rho\pi}} = 56m$ for $(\rho = 100 nodes/km^2)$, which is the average distance for a receiver to exist within the transmission range of the sender. a_{RTS}, the transmission range of RTS/CTS control packets is also a function of d and $a_{data} \leq a_{RTS}$.

7.7.1 Varying the Transmission Ranges: a_{RTS}/a_{data}

We start by first analyzing the throughput performance as we vary the transmission power for DATA packets (i.e., a_{data}) and for different transmission ranges for RTS/CTS packets (i.e, a_{RTS}). Figure 6 shows the performance result of the RTS/CTS handshake when $\theta = \frac{\pi}{6}$. Figure 7.4 shows that the highest throughput is obtained for shorter ranges of RTS (i.e., lower transmission power for the RTS packets), while the throughput decreases for higher transmission power. This is due to the fact that by increasing the RTS transmission range (a_{RTS}), the control messages will silence larger

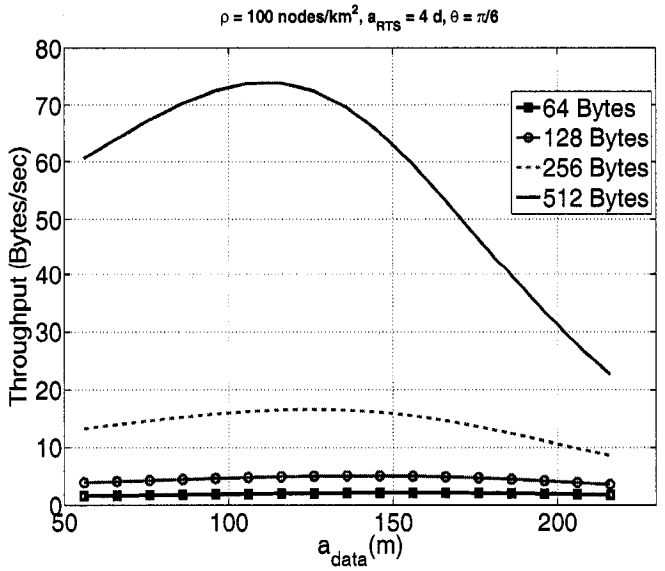

Figure 7.6: Network Throughput for different packet size

number of nodes, i.e., larger transmission range as well silence range, which indeed has the effect of suppressing other senders which would have successfully initiated concurrent transmissions. Ultimately, transmission RTS packets at higher higher power affects the spatial reuse and results in lower system throughput, as shown in the figure. Moreover, at a larger a_{RTS}, the RTS collision rate increases and the interference (I, Eq. 7.10) increases as well, which reduces the throughput as well.

Next, we analyze the effect of varying the transmission power of the DATA packet. When a_{data} is small (e.g., $a_{data} << a_{RTS}$), the transmission range of DATA is also small while the interference is large, and thus a lower throughput is obtained. On the other hand, as a_{data} increases, the DATA frame would have better chances to be successfully received at the receiver (the higher transmission power yields received signal with higher power and hence better signal to interference plus noise ratio), and accordingly the system throughput is improved. As the DATA frame transmission power continues to increase, the transmission range, a_{data}, becomes very large, and the sender starts to unnecessarily silence other neighboring senders preventing simultaneous transmissions and limiting the spatial reuse. This is verified by Figure

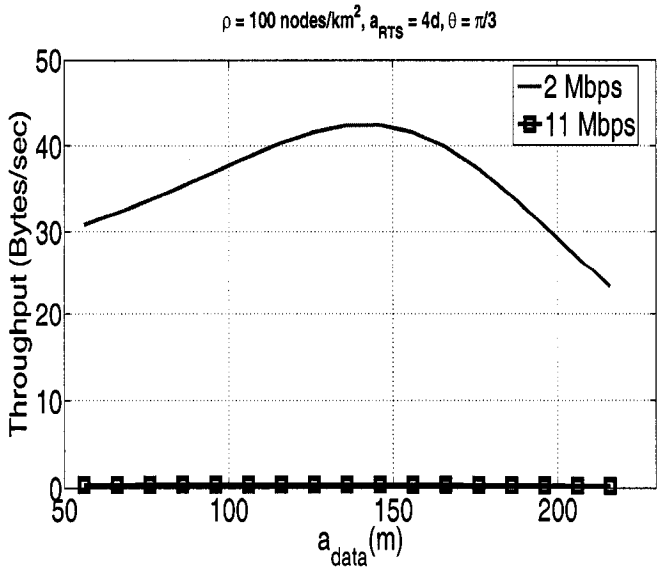

Figure 7.7: Network Throughput for different transmission rate

7.4.

7.7.2 Varying the beam width θ

The effect of controlling the transmission power and the beam width θ is shown in Figure 7.5. Clearly, narrower beams result in higher throughput gains. Decreasing the beam width will increase the number of interfering nodes. Nevertheless, by reducing the beam width, the number of hidden terminals and contending terminals decreases since the areas S_1, S_2 , S_3, and S_4 in Figure 7.3 decrease. Therefore, the spatial reuse factor $\nu(a_{data})$ is enhanced.

Additionally, the transmission power decreases since it is directly proportional to the directional beam width. Hence, the resulting interference will be diminished by the factor of beam width reduction. It can be verified from Figure 7.5 that by reducing the beam width, the enhancement in spatial reuse is more dominant than the effect due to the increase in the number of interfering nodes and hence in determining the throughput.

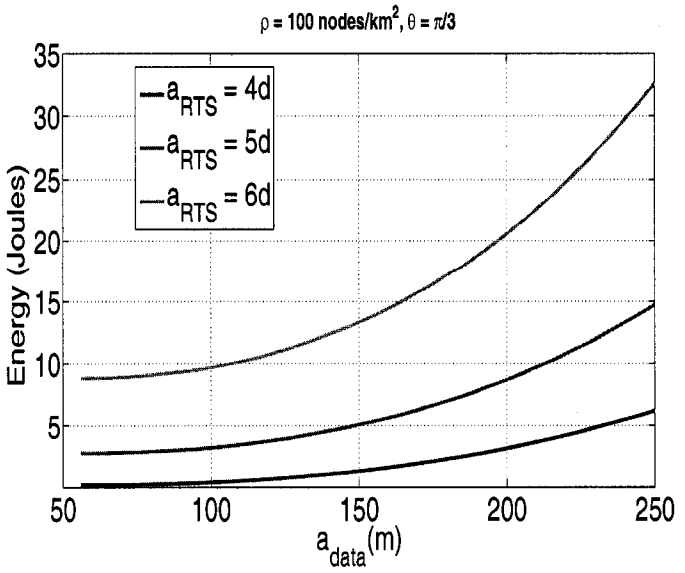

Figure 7.8: Total Energy Consumption for different transmission ranges

7.7.3 The impact of packet size and transmission rate

We measure the network performance by varying the packet size and we study the impact of controlling the transmission power. We set $a_{RTS} = 4d$. Unlike our earlier observation, the smaller the size of the data frame (e.g., 64 bytes and 128 bytes), the greater the impact of interference becomes. This is due to the fact that, the term $\frac{T_r+T_c}{T_r+T_c+T_d+T_a}$ in equation (7.10) increases and as a result a lower throughput is obtained. As a_{data} increases, the reduction of the term in equation (7.9) $((\frac{a_{RTS}}{a_{data}})^4)$ is more pronounced and yields better throughput as shown in Figure 7.6. Moreover, for smaller packet sizes, it is verified from the analytical model that β_t is also reduced.

Figure 7.7 shows the throughput when using higher transmission rates (e.g., 11Mbps) for DATA frames whereas control messages are always transmitted at 2Mbps [5]. Clearly, as the PHY data rate increases, the SIR threshold increases (for example, for a data rate of 11 Mbps , SIR_{min} becomes 15dB [5]); at this new SIR threshold, a lower attempt probability is allowed which indeed limits the amount of traffic (μ) a node can transmit which results in a lower throughput.

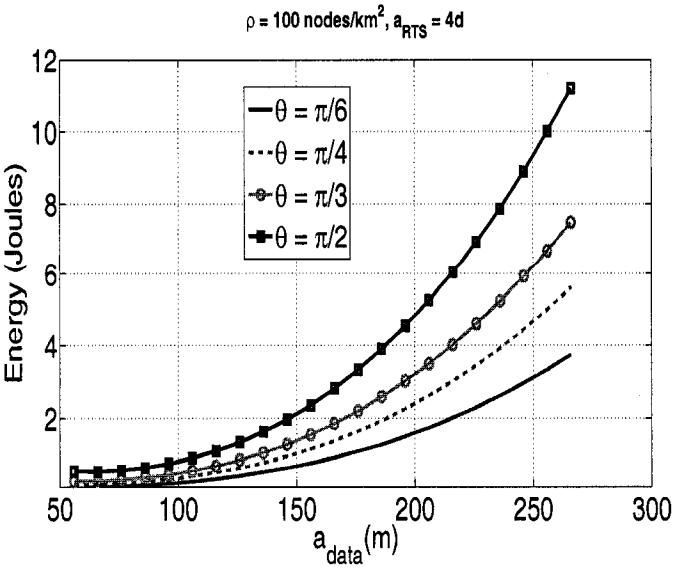

Figure 7.9: Total Energy Consumption for different beam width

7.7.4 Energy Consumption

The effect of controlling the transmission power on energy is investigated in Figure 7.8. Here, Figure 7.8 shows the results for the total energy consumption for $\frac{\pi}{3}$ beam width and for different a_{RTS}. Increasing a_{RTS} will decrease the interference level since more nodes will defer their transmissions. Nevertheless the collision rate due to nodes contending for channel access will increase and thus more energy is wasted in collisions. The consumed energy increases with the increase of a_{data}. As a_{data} increases, the transmission power increases and more energy will be consumed. Furthermore, the increase of a_{data} increases the probability of CTS collision (although the hidden nodes in S_3 decreases but the increase of hidden nodes S_4 is more pronounced) and thus the energy due to packet collision and packet retransmission increases which sums up in an increasing manner with the energy for transmission. At lower a_{data}, the energy consumption are almost the same due to the balance that occurs between the energy disbursed to overcome the interference and the energy consumed in collision resolution. Figure 7.9 presents the effect of increasing the beam width. When the beam width increases, energy consumption needed to transmit and retransmit

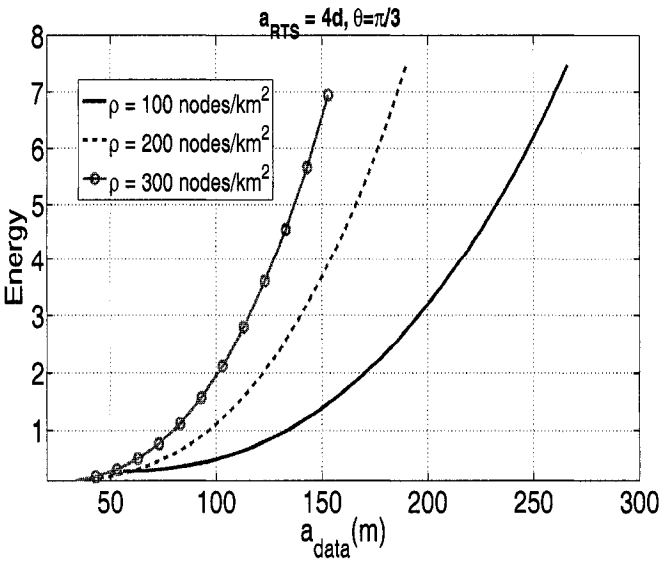

Figure 7.10: Total Energy for different network densities

the packet increases, since the power as mentioned before is directly proportional to the beam width. Furthermore, with the increase of the beam width, the collision rate increases since the number of nodes contending for channel access increases, and thus the energy will definitely sums up in an increasing manner with the energy for transmission.

Figures 7.10 and 7.11 show the effect of changing the node density on the network. Clearly, as the number of nodes increases, the collision rate increases and thus the interference increases which decreases the throughput and increases the energy consumption.

7.7.5 Results summary

To summarize, increasing the RTS transmission range, the control messages will silence larger number of nodes which has the effect of reducing the spatial reuse and moreover it increases the interference level on other communicating nodes which leads to lower throughput. Given the fact that in using smaller beamwidth, more hidden nodes exist, nevertheless the spatial reuse factor gain is more pronounced

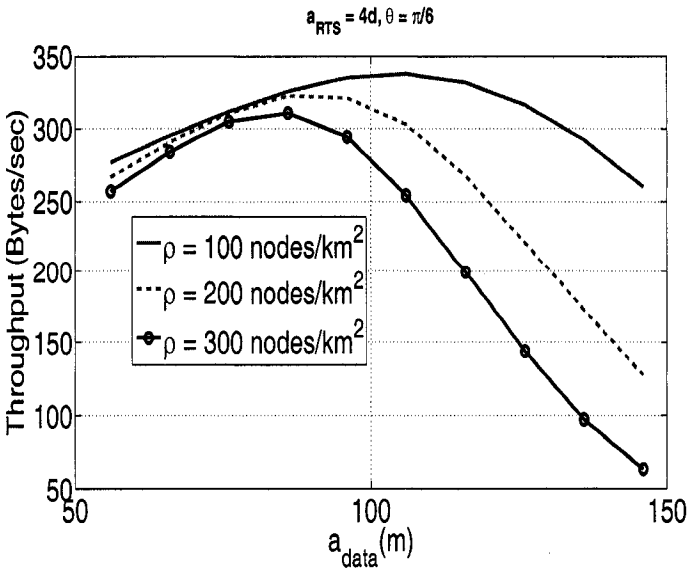

Figure 7.11: Network Throughput for network densities

and thus higher throughput is achieved. In addition, our model has also been used to expose the performance of the RTS/CTS access scheme; although these control messages may slightly reduce the collisions among contending hosts, their impacts on spatial reuse and the added overhead outweighs their benefits and specifically when using higher rates under the worst case scenario. Furthermore, using smaller size packets is not beneficial, due to the higher control overhead. Finally, we noticed that the energy consumption is more effected by the transmission range rather than the collision factor.

7.8 Model Verification

Here, we validate the accuracy of the proposed analytical model by comparing the numerical results with results we obtained from simulations. We use Qualnet [111] to perform the various simulation experiments. The Switched beam antenna has been adopted in this simulation with beamwidth equals $\frac{\pi}{4}$. In the network, 36 nodes are regularly placed in a 4x4 grid topology within an area of $300m \times 300m$. The distance between a node and its closest neighbor is 50m. We consider CBR (constant bit rate)

Table 7.2: Simulation vs Analytical

$a_{data}(m)$	Simulation (Throughput(Bytes/sec))	Analytical(Throughput(Bytes/sec))
50	12.73	10.484
100	13.77	11.5668
150	8.933	7.05707
200	5.373	4.94316

traffic flows of packet size 1000 bytes. The RTS transmission range is set to 200m. We recall that in our model, we derived an expression for the throughput under the worst case network interference; however in our experiment, in order to best simulate this scenario, we select a random transmitter-receiver pair and accordingly fix the rest of nodes to have their traffic in the direction of the receiver. The random source node transmits packets to its receiver at a distance $a_{data} = r$ and r is varied for different experiment runs. We use 5 simulation seeds to calculate the average single node throughput. The corresponding transmission power values used to reach 50, 100, 150, 200 meters are respectively 0.5dBm, 12.5dBm, 20dBm, 24dBm. The results of both model and simulations are presented in Table 7.2. The simulation results differ from those of the analytical by 10% at higher a_{data} to around 17% at smaller values for a_{data}. Indeed, the results of the analytical model provide only a lower bound for the throughput since the throughput expression is derived under the worst case interference. However, simulating this worst case interference scenario is not quite feasible and indeed this is a major reason for the gap between results obtained from the model and the simulation.

7.9 Conclusion

An analytical model for power-aware multi-hop wireless networks with nodes equipped with directional antennas is presented to study transmission power control. The expressions to evaluate a lower bound on throughput under maximum interference are derived. Furthermore, an energy consumption model that utilizes both kinds of energy consumption has been presented: The energy consumed in collision resolution and the energy consumed to overcome interference. The parameter effects (θ,a_{data}, a_{RTS}) on the overall network performance have been analyzed. Finally, simulation results verified the accuracy of the model.

Chapter 8

Conclusion and Future Directions

8.1 Conclusions

In wireless multihop ad hoc networks where decentralized MAC such as IEEE 802.11 DCF is deployed, spatial reuse has an enormous influence on the channel reservation. This in turn determines the number of communicating nodes which are allowed to transmit simultaneously and thus has tremendous effect on the throughput. In this thesis, the effectiveness of spatial reuse on enhancing the throughput has been investigated.

First, the effects that transmission power control, data rate adaptation and tuning carrier sensing threshold have on network throughput have been explored and the interplay between them has been investigated. To accomplish this, a realistic analytical model that characterizes the transmission activities governed by the IEEE 802.11 DCF in a single channel, power-aware, multihop wireless network has been developed. The results showed that both carrier sensing threshold and transmit power have major impact on network performance. While decreasing the CS threshold impacts the spatial reuse, a larger CS threshold will yield severe interference among concurrent transmissions rendering power control ineffective. Moreover, an optimal CS threshold that strikes a balance between spatial reuse and collisions

resulting from interfering nodes has been observed. Controlling transmission power while selecting an appropriate CS threshold showed to be quite effective. Further, the smaller the size of the data frame is, the more advantageous to tune the CS rather than controlling the transmission power. The model has also been used to expose the performance of the RTS/CTS access scheme; although these control messages may slightly reduce the collision among contending hosts, their impacts on spatial reuse and the added overhead outweighs their benefits and specifically when using higher rates. The comparative study showed that the basic access always outperforms the RTS/CTS access method. Thus, adapting the DATA rate in order to prevent collision is not advantageous in most of the times. Based on the observations and insights from the results generated from the proposed model, appropriate heuristics for tuning the carrier sensing threshold and performing power and rate control have been developed. Specifically, a localized, distributed power and rate control scheme has been proposed through which nodes, in a multihop wireless network, dynamically adjust their transmission power and data rates to balance the tradeoff between collisions and spatial reuse. Simulation results under different topologies were then used to demonstrate the significant throughput and energy gains that can be obtained by proposed scheme.

Then, a novel dynamic spatiotemporal scheme that balances the tradeoff between collision and spatial reuse in multi-hop wireless networks has been presented. Using this novel approach, a node dynamically adjusts its CS_{th} to eliminate collisions from hidden terminals and enhances spatial reuse by diminishing the effect of the exposed terminals. At the same time, the proposed approach reduces the collisions from among contending hosts while maintaining the level of transmission attempt probability through carefully selecting the contention window. An effective loss differentiation mechanism is proposed to work in concert with the proposed methodology.

Moreover, and unlike the DCF access mode, the RTS/CTS handshake does not silence neighboring nodes but rather only inform them to bound their CS_{th} to yield for the on-going transmissions. To reduce the overhead from the RTS/CTS handshake, and based on the network performance policy, a policy has been proposed wherein a node can adaptively enable/disable the RTS/CTS exchange. Simulation results and comparisons with other recent methods have shown the effectiveness of the proposed method in improving the network performance.

Finally, the effect of coupling power control with the use directional antenna on multihop ad hoc networks environment has been studied. Mainly, a power control scheme has been proposed for directional MAC protocol. The temporal transmission power correlations that exist between the directional MAC protocol 4-way handshake packets (RTS/CTS/DATA/ACK) have been derived for successful communication taking into accounts directional operational access problems such as hidden terminal problems, deafness and side lobe interference. Based on the node activity density, an interference model was estimated and together with the correlations derived, efficient constraints have been induced that ensure the correct delivery of each individual frame in this 4-way handshake. Moreover, the kalman and extended kalman filter have been introduced as another solution to estimate the interference in future. It has been shown that the prediction filters outperform the model-based techniques by an average error of 14.3%. We later verified through simulations the performances of the proposed scheme with the performances of mobile ad-hoc networks using different MAC protocols such as the standard IEEE 802.11b MAC protocol, the D-MAC protocol with no power control and the D-MAC protocol with D-BASIC power control scheme. Later, analytical model that shows the benefits of coupling directional antenna with transmission power control in a uniformly distributed multihop ad hoc networks where nodes are equipped with directional antennas. An interference model

has been constructed for directional antenna based on a honey grid model to calculate the maximum interference. Further, a directional collision avoidance model has been derived and based on the integrated inteference/collision model and Signal to Interference Ratio (SIR), the maximum end-to-end throughput under the maximum interference has been calculated. Further, the effect of collision on the energy consumption has been investigated. Conclusions drawn from the proposed model that in using smaller beamwidth, more hidden nodes exist, nevertheless the spatial reuse factor gain is more pronounced and thus higher throughput is achieved. In addition, the model has also been used to expose the performance of the directional RTS/CTS access scheme; although these control messages may slightly reduce the collision among contending hosts, their impacts on spatial reuse and the added overhead outweighs their benefits and specifically when using higher rates under the worst case scenario. Furthermore, using smaller size packets is not beneficial, due to the higher control overhead. Finally, the energy consumption is more effected by the transmission range rather than the collision factor.

8.2 Future Work

The work presented in this thesis provided considerable benefits in performance enhancement for wireless ad hoc networks. However, there are still several future directions that can provide additional benefits.

In the loss-differentiation algorithm presented in Chapter 5, we made the assumption that the transmission failures caused by collisions from contenting nodes ($\mathbf{C}$) and collisions from hidden terminals ($\mathbf{H_1}$) are independent. However, this may not be strictly true, since when collisions from $\mathbf{H_1}$ exist, the contribution of type-$\mathbf{H_2}$ or type-$\mathbf{C}$ collisions to packet loss depends on the number of $\mathbf{H_1}$ collisions. Thus, applying mathematical analysis to further exactly characterize more accurately the different types of packet loss is one possible extension.

One future direction is to apply game theory to study the behavior of tuning protocol parameters in wireless ad hoc networks. Because nodes in a wireless ad hoc network decide their channel accesses independently in a selfish behavior, and the channel access of a node has an influence on those of its neighboring nodes, game theory naturally offers certain benefits as a tool to analyze distributed algorithms and protocols for ad hoc networks. Specifically, game theory is an effective tool to investigate the existence, uniqueness, and convergence to a steady state operating point when nodes perform independent adjusting of network parameters (e.g. power, rate and CS_{th}). Moreover, game theory can also provide deeper insight into cross layer optimization designs [124]. Therefore, applying game theory to distributed power control and tuning of CS_{th} would be one of our future research directions.

Another future direction is to apply artificial intelligent schemes such as fuzzy logic, neural networks, or genetic algorithms to select which attribute (power control, rate adaptation or tuning the CS_th or CW) to use and tune based on collision probability and distance.

Bibliography

[1] S. Kumar and V. S. Raghavan and J. Deng, "Medium Access Control Protocols for Ad-hoc Wireless Networks: A Survey," *Elsevier Ad-Hoc Networks Journal*, vol. 4, no. 3, pp. 326–358, May 2006.

[2] Bay Area Wireless User Group, "www.bawug.org."

[3] H Dai, K.W. Ng and M.Y Wu, "An Overview of MAC Protocols with Directional Antennas in Wireless Ad hoc Networks," in *Proceedings of the IEEE International Multi-Conference on Computing in the Global Information Technology - ICCGI*, Washington, DC, USA, July 2006, pp. 84–90.

[4] H. Zhai, J. Wang, X. Chen, and Y. Fang, "Medium access control in mobile ad hoc networks: challenges and solutions," *Wireless Communications and Mobile Computing*, vol. 6, no. 2, pp. 151 – 170, February. 2006.

[5] "IEEE 802.11b working group part 11: Wireless LAN media access control (MAC) and physical layer (PHY) Specifications," 1999.

[6] K. Medepalli and F. Tobagi, "On Optimization of CSMA/CA based Wireless LANs: Part I - Impact of Exponential Backoff," in *Proceedings of the IEEE International Conference on Communications - ICC*, Istanbul, Turkey, June 2006, pp. 2089–2094.

[7] K. Medepalli and F. Tobagi and D. Famolari and T. Kodama , "On Optimization of CSMA/CA based Wireless LANs: Part I - Mitigating Efficiency Loss," in

Proceedings of the IEEE International Conference on Communications - ICC, Istanbul, Turkey, June 2006, pp. 4799–4804.

[8] C. Lau and C. Leung, "Capture Models for Mobile Packet Radio Networks," *IEEE Transactions on Communications*, vol. 40, no. 5, pp. 917–925, 1992.

[9] C. Ware, J. Chicharo, and T. Wysocki, "Modelling of Capture Behaviour in IEEE 802.11 radio modems," in *Proceedings of the IEEE International Conference on Telecommunications- ICT*, Bucharest, Romania, June 2001, pp. 213–217.

[10] Y. Yang, J. C. Hou, and L.-C. Kung, "Modeling the Effect of Transmit Power and Physical Carrier Sense in Multi-hop Wireless Networks ," in *Proceedings of the IEEE International Conference on Computer Communications - INFOCOM*, Alaska, USA, May 2007, pp. 2331–2335.

[11] K. Xu, M. Gerla, and S. Bae, "Effectiveness of RTS/CTS handshake in IEEE 802.11 based ad hoc networks," *Elsevier Ad Hoc Network Journal*, vol. 1, no. 1, pp. 107–123, May 2003.

[12] L. Kleinrock and F. A. Tobagi, "Packet switching in radio channels: Part I -carrier sense multiple-access modes and their throughput-delay characteristics," *IEEE Transactions on Communications*, vol. 23, no. 12, pp. 1400–1416, December 1975.

[13] F. Tobagi and L. Kleinrock, "Packet Switching in Radio Channels: Part II–The Hidden Terminal Problem in Carrier Sense Multiple-Access and the Busy-Tone Solution," *IEEE Transactions on Communications*, vol. 23, no. 12, pp. 1417–1433, December 1975.

[14] H. Chaya and S. Gupta, "Performance Modeling of Asynchronous Data Transfer Methods of IEEE 802.11 MAC protocol," *Wireless Networks*, vol. 3, pp. 217–234, August 1997.

[15] G. Bianchi, "Performance Analysis of the IEEE 802.11 distributed coordination function," *IEEE Journal of Selected Areas in Communications - JSAC*, vol. 18, no. 3, pp. 535–547, March 2000.

[16] F. Cali, M. Conti, and E. Gregori, "Dynamic Tuning of the IEEE 802.11 Protocol to Achieve a Theoretical Throughput Limit," in *IEEE/ACM Transactions on Networking*, vol. 8, no. 6, December 2000, pp. 785–799.

[17] Y. Wang and J. J. Garcia-Luna-Aceves, "Collision avoidance in single-channel ad hoc networks using directional antennas," in *Proceedings of IEEE International Conference on Distributed Computing Systems - ICDCS*, Washington, DC, USA, May 2003, pp. 640–646.

[18] J. He, D. Kaleshi, A. Munro, Y. Wang, A. Doufexi, J. McGeehan, and Z. Fan, "Performance investigation of IEEE 802.11 MAC in multihop wireless networks," in *Proceedings of the IEEE/ACM International Symposium on Modeling, Analysis and Simulation of Wireless and Mobile Systems - MSWiM*, Hawaii, USA, October 2005, pp. 242 – 249.

[19] S. Narayanaswamy, V. Kawadia, R. Sreenivas, and P. Kumar, "Power control in ad-hoc networks: Theory, architecture, algorithm and implementation of the COMPOW protocol," in *Proceedings of the European Wireless Conference*, Florence, Italy, Feburuary 2002, pp. 23–28.

[20] V. Rodoplu and T. H. Meng, "Minimum energy mobile wireless networks," *IEEE Jounal on Selected Areas in Communications*, vol. 17, no. 8, pp. 1333–1344, 1999.

[21] R. Wattenhofer, L. Li, P. Bahl, and Y. Wang, "Distributed topology control for wireless multihop ad-hoc networks," in *Proceedings of the IEEE International Conference on Computer Communications - INFOCOM*, Anchorage Alaska, April 2001, pp. 1388–1397.

[22] A. Muqattash and M. Krunz, "Power Controlled Dual Channel (PCDC) Medium Access Protocol for Wireless Ad Hoc Networks," in *Proceedings of the IEEE International Conference on Computer Communications - INFOCOM*, San Francisco, USA, April 2003, pp. 470–480.

[23] N. Li, J. C. Hou, and L. Sha, "Design and analysis of a mst-based distributed topology control algorithm for wireless ad-hoc networks," *IEEE Trans. on Wireless Communications*, vol. 4, no. 3, pp. 1195–1207, 2005.

[24] N. Li and J. C. Hou, "Localized fault-tolerant topology control in wireless ad hoc networks," *IEEE Transaction on Parallel and Distributed Systems*, vol. 17, no. 4, pp. 307–320, 2006.

[25] L. Li , J. Halpern, P. Bahl, Y. Wang and R. Wattenhofer, "A cone-based distributed topology-control algorithm for wireless multi-hop networks," *IEEE/ACM Transactions on Networking*, vol. 13, no. 1, pp. 147–159, 2005.

[26] A. Behzad and I. Rubin, "Impact of power control on the performance of ad hoc wireless networks," in *Proceedings of the IEEE International Conference on Computer Communications - INFOCOM*, Miami, USA, April 2005, pp. 102–113.

[27] R. Zheng, J. C. Hou, and N. Li, "Power management and control in wireless networks," in *Ad Hoc and Sensor Networks*, Y. Pan, Y. Xiao, and J. Li, Eds. Nova Science Publishers, 2006.

[28] N. Li and J. C. Hou, "Topology control in wireless sensor networks," in *Combinatorial Optimization in Communication Networks*, M. Cheng, Y. Li, and D.-Z. Du, Eds. Springer Publishers, 2006.

[29] E. Jung and N. H. Vaidya, "A Power Control MAC Protocol for Ad Hoc Networks," in *Proceedings of the ACM International Conference on Mobile Computing and Networking - Mobicom*, Atlanta, USA, September 2002, pp. 36–47.

[30] S. Gobriel, R. Melhem, and D. Moss, "A Unified Interference/Collision Analysis for Power-Aware Ad Hoc Networks," in *Proceedings of the IEEE International Conference on Computer Communications - INFOCOM*, Hong Kong, China, March 2004, pp. 608–620.

[31] A. Sheth and R. Han, "SHUSH: Reactive Transmit Power Control for Wireless MAC Protocols," in *International Wireless Internet Conference - WICON*, Budapest, Hungary, July 2005, pp. 18–25.

[32] S. Agarwal, R. Katz, S. Krishnamurthy, and S. Dao, "Distributed power control in ad-hoc wireless networks," in *Proceedings of the IEEE International Symposium on Personal, Indoor and Mobile Radio Communications - PIMRC*, San Diego, USA, October 2001, pp. 59–66.

[33] J. Rao , S. Biswas, "Transmission power control for 802.11: a carrier-sense based NAV extension approach," in *Proceedings of the IEEE International Global Telecommunications Conference - GLOBECOM*, vol. 6, St. Louis, USA, November 2005, pp. 6–11.

[34] A.A. Pires, J.F. de Rezende and C. Cordeiro, "ALCA: a new scheme for power control on 802.11 Ad Hoc networks," in *Proceedings of the IEEE International Symposium on a World of Wireless, Mobile and Multimedia Networks - WoWMoM*, Taormina - Giardini Naxos, June 2005, pp. 475–477.

[35] J. P. Monks, V. Bharghavan, and W. W. Hwu, "A Power Controlled Multiple Access Procotol for Wireless Packet Networks," in *Proceedings of the IEEE International Conference on Computer Communications - INFOCOM*, Anchorage, USA, April 2001, pp. 219–228.

[36] S. Wu, Y. Tseng, and J. Sheu, "Intelligent medium access for mobile ad hoc networks with busy tones and power control," *IEEE Journal on Selected Areas in Communications*, vol. 18, no. 9, pp. 1647–57, 2000.

[37] A. Muqattash and M. Krunz, "A Single-Channel Solution for Transmit Power Control in Wireless Ad Hoc Networks," in *Proceedings of the ACM International Symposium on Mobile Ad Hoc Networking and Computing - MobiHoc*, Tokyo, Japan, May 2004, pp. 276 – 283.

[38] J. Zhang and B. Bensaou, "Core-Pc: A Class of Correlative Power Control Algorithms for Single Channel Mobile ad hoc Networks," *IEEE Transactions on Wireless Communications*, vol. 6, no. 9, pp. 3410–3417, September 2007.

[39] K.P. Shih and Y.D. Chen, "CAPC: a collision avoidance power control MAC protocol for wireless ad hoc networks," *IEEE Communications Letters, Vol (9), Issue (9)*, pp. 859– 861, Sep 2005.

[40] K.P. Shih, Y.D. Chen, and C. Chang, "Adaptive Range-Based Power Control for Collision Avoidance in Ad Hoc Networks," in *Proceedings of the IEEE International Conference on Communications - ICC*, Glasgow, Scotland, June 2007, pp. 3672–3677.

[41] J. Zhu, X. Guo, L. L. Yang, and W. S.Conner, "Leveraging spatial reuse in 802.11 mesh networks with enhanced physical carrier sensing," in *Proceedings of the IEEE International Conference on Communications - ICC*, Paris, France, June 2004, pp. 4004– 4011.

[42] A.Vasan, R. Ramjee and T. Woo, "ECHOS - enhanced capacity 802.11 hotspots," in *Proceedings of the IEEE International Conference on Computer Communications - INFOCOM*, Miami,USA, March 2005, pp. 1562 – 1572.

[43] H. Ma, H.M.K Alazemi and S. Roy, "A stochastic model for optimizing physical carrier sensing and spatial reuse in ad hoc networks," in *Proceedings of the IEEE International Conference on Mobile Ad-hoc and Sensor Systems - MASS*, Washington, USA, November 2005, pp. 615–622.

[44] E. Wong and R. Cruz, "A spatio-temporal model for physical carrier sensing wireless ad-hoc networks," in *Proceedings of the IEEE International Society Conference on Sensor, Mesh and Ad Hoc Communications and Networks - SECON*, Reston, VA, USA, September 2006, pp. 276–285.

[45] J. Deng, B. Liang, and P. K. Varshney, "Tuning the Carrier Sensing Range of IEEE 802.11 MAC," in *Proceedings of the IEEE International Global Telecommunications Conference - GLOBECOM*, Texas, USA, December 2004, pp. 2987– 2991.

[46] X. Yang and N. H. Vaidya, "On the Physical Carrier Sense in Wireless Ad-Hoc Networks," in *Proceedings of the IEEE International Conference on Computer Communications - INFOCOM*, Miami,USA, March 2005, pp. 2525–2535.

[47] K. Jamieson, B. Hull, A. Miu, and H. Balakrishnan, "Understanding the Real-World performance of carrier sense," in *Proceedings of ACM Workshop on experimental approaches to wireless network design and analysis - EWIND*, Philadelphia, USA, August 2005, pp. 52–57.

[48] J. Zhu, B. Metzlerand, X. Guo and Y. Liu, "Adaptive csma for scalable network capacity in high-density wlan: a hardware prototyping approach," in *Proceedings of the IEEE International Conference on Computer Communications -*

INFOCOM, Barcelona, Spain, April 2006, pp. 1–10.

[49] J. Zhu, X. Guo, L. L. Yang, W. S. Conner, S. Roy, and M. Hazra, "Adapting physical carrier sensing to maximize spatial reuse in IEEE 802.11 mesh networks," *Wireless Communications and Mobile Computing*, vol. 4, no. 8, pp. 933–946, 2004.

[50] H. Ma, S. Shin, and S. Roy, "Optimizing Throughput with Carrier Sensing Adaptation for IEEE 802.11 Mesh Networks Based on Loss Differentiation," in *Proceedings of the IEEE International Conference on Communications - ICC*, Glasgow, Scotland, June 2007, pp. 4967–4972.

[51] S. Desilva and R. Boppana, "On the Impact of Noise Sensitivity on Performance in 802.11 Based Ad Hoc Networks." in *Proceedings of the IEEE International Conference on Communications - ICC*, Paris, France, July 2004, pp. 4372–4376.

[52] C. C. Chen, E. Seo, H. Kim, and H. Luo, "Self-Learning Collision Avoidance for Wireless Networks," in *Proceedings of the IEEE International Conference on Computer Communications - INFOCOM*, Barcelona, Spain, April 2006, pp. 2987– 2991.

[53] Y. Zhu, Q. Zhang, Z. Niu, and J. Zhu, "On Optimal Physical Carrier Sensing: Theoretical Analysis and Protocol Design," in *Proceedings of the IEEE International Conference on Computer Communications - INFOCOM*, Alaska , USA, May 2007, pp. 2351–2355.

[54] D. Qiao and S. Choi, "Goodput enhancement of IEEE 802.11a wireless LAN via link adaptation," in *Proceedings of the IEEE International Conference on Communications - ICC*, Helsinki, Finland, June 2001, pp. 1995–2000.

[55] D. Qiao, S. Choi and K. G. Shin,, "Goodput analysis and link adaptation for IEEE 802.11a wireless LANs," *IEEE Trans. on Mobile Computing,*, vol. 1, no. 4, pp. 278–292, December 2002.

[56] M. Borgo, A. Zanella, P. Bisaglia, and S. Merlin, "Analysis of the hidden terminal effect in multi-rate IEEE 802.11 b networks," in *Proceedings the International Symposium on Wireless Personal Multimedia Communications - WPMC*, Abano Terme, Italy, September 2004, pp. 240– 248.

[57] I. Tinnirello, S. Choi and Y. Kim, "Revisit of RTS/CTS Exchange in High-Speed IEEE 802.11 Networks," in *Proceedings of the IEEE International Symposium on a World of Wireless, Mobile and Multimedia Networks - WoWMoM*, Taormina, Italy, June 2005, pp. 232– 235.

[58] P. Chatzimisios, A. Boucouvalas, and V. Vitsas, "Effectiveness of RTS/CTS handshake in IEEE 802.11a wireless LANs," *Electronic Letters*, vol. 40, no. 14, pp. 915–916, July 2004.

[59] G. Holland, N. Vaidya and P. Bahl, "A rate-adaptive MAC protocol for multi-hop wireless networks," in *Proceedings of the ACM International Conference on Mobile Computing and Networking - Mobicom*, Rome, Italy, July 2001, pp. 236–251.

[60] A. Kamerman and L. Monteban, "WaveLAN II: A high-performance wireless LAN for the unlicensed band," *Bell Labs Technical Journal*, pp. 118–133, summer 1997.

[61] J. Bicket, "Bit-rate selection in wireless networks," Master's thesis, MIT, 2005.

[62] MadWiFi project, "www.MadWiFi.org."

[63] I. Haratcherev, K. Langendoen, R. Lagendijk, and H. Sips, "Hybrid rate control for ieee 802.11," in *Proceedings of the second international workshop on Mobility*

management & wireless access protocols - MobiWac, Philadelphia, PA, USA, 2004, pp. 10–18.

[64] M. Lacage, M. Manshaei, and T. Turletti, "IEEE 802.11 rate adaptation: a practical approach," in *Proceedings of the ACM international symposium on Modeling, analysis and simulation of wireless and mobile systems - MSWiM*, Venice, Italy, 2004, pp. 126–134.

[65] B. Sadeghi, V. Kanodia, A. Sabharwal and E. Knightly, "Opportunistic media access for multirate ad hoc networks," in *Proceedings of the ACM International Conference on Mobile Computing and Networking - Mobicom*, Atlanta, Georgia, September 2002, pp. 24–35.

[66] J. Kim, S. Kim, S. Choi, and D. Qiao, "CARA: Collision-Aware Rate Adaptation for IEEE 802.11 WLANs," in *Proceedings of the IEEE International Conference on Computer Communications - INFOCOM*, Barcelona, Spain, 2006, pp. 1–11.

[67] Q. Pang, V. C. M. Leung, and S. C. Liew, "A rate adaptation algorithm for IEEE 802.11 WLANs based on MAC-layer loss differentiation," in *Proceedings of the IEEE International Conference on Broadband Networks - BROADNETS*, Boston, USA, October 2005, pp. 709–717.

[68] J.H.Yun, S.W.Seo, "Collision Detection based on Transmission Time Information in IEEE 802.11 Wireless LAN," in *Proceedings of the IEEE International Conference on Pervasive Computing and Communications - PerCom*, Pisa , Italy, 2006, pp. 410–414.

[69] S. Wong, S. Lu, H. Yang, and V. Bharghavan, "Robust rate adaptation for 802.11 wireless networks," in *Proceedings of the IEEE 12th annual international*

conference on Mobile computing and networking, Los Angeles, CA, USA, 2006, pp. 146–157.

[70] J. Choi, J. Na, K. Park, and C. Kim, "Adaptive Optimization of Rate Adaptation Algorithms in Multi-Rate WLANs," in *Proceedings of the IEEE International Conference on Network Protocols - ICNP*, Beijing, China, October 2007, pp. 144–153.

[71] K. Wang, F. Yang, Q. Zhang, D. O. Wu, and Y. Xu, "Distributed cooperative rate adaptation for energy efficiency in ieee 802.11-based multi-hop networks," in *Proceedings of the 3rd International Conference on Quality of service in heterogeneous wired/wireless networks - QShine*, Waterloo, Canada, September 2006.

[72] Y. Eunho, C. J. Kim, Chong-Kwon, and L. Jaewha, "An enhanced link adaptation strategy for ieee 802.11 wireless ad hoc networks," in *Proceedings of the IEEE International Conference On Wireless Communications, Networking and Mobile Computing - WiCom*, Dalian, China, September 2007, pp. 1672–1676.

[73] T. Kim, J. Hou, and H. Lim, "Improving spatial reuse through tuning transmit power, carrier sense threshold, and data rate in multihop wireless networks," in *Proceedings of the ACM International Conference on Mobile Computing and Networking - Mobicom*, California, USA, October 2006, pp. 366–377.

[74] X. Yang and N. Vaidya, "A Spatial Backoff Algorithm Using the Joint Control of Carrier Sense Threshold and Transmission Rate," in *Proceedings of the IEEE International Society Conference on Sensor, Mesh and Ad Hoc Communications and Networks - SECON*, San Diego,USA, June 2007, pp. 501–511.

[75] C. Chen, E. Seo, H. Luo, and N. Vaidya, "Rate-adaptive Framing for Interfered Wireless Networks," in *Proceedings of the IEEE International Conference on*

Computer Communications - INFOCOM, Anchorage, Alaska, USA, May 2007, pp. 219–230.

[76] M. Heusse, F. Rousseau, R. Guillier, and A. Duda, "Idle sense: an optimal access method for high throughput and fairness in rate diverse wireless lans," in *Proceedings of the ACM Special Interest Group on Data Communications - SIGCOMM*, Philadelphia, USA, October 2005, pp. 121–132.

[77] D. Qiao, S. Choi, A. Jain, and K. G. Shin, "MiSer: an optimal low-energy transmission strategy for IEEE 802.11a/h," in *Proceedings of the ACM International Conference on Mobile Computing and Networking - Mobicom*, San Diego, USA, September 2003, pp. 161–175.

[78] H. Ma and S. Roy, "Simple and Effective Carrier Sensing Adaptation for Multi Rate Ad-Hoc MESH Networks," in *Proceedings of the IEEE International Conference on Mobile Ad-hoc and Sensor Systems - MASS*, Vancouver, Canada, 2006, pp. 795–800.

[79] J. A. Fuemmeler, N. H. Vaidya, and V. V. Veeravalli, "Selecting transmit powers and carrier sense thresholds in CSMA protocols for wireless ad hoc networks," in *Proceedings of the ACM International Wireless Internet Conference - WICON*, August 2006, pp. 15–21.

[80] A. Kumar, E. Altman, D. Miorandi, and M. Goyal, "New insights from a fixed point analysis of single cell IEEE 802.11 WLANs," in *Proceedings of the IEEE International Conference on Computer Communications - INFOCOM*, Miami, USA, April 2005, pp. 1550–1561.

[81] T. Lin and J. Hou, "Interplay of Spatial Reuse and SINR-Determined Data Rates in CSMA/CA-Based, Multi-Hop, Multi-Rate Wireless Networks," in *Proceedings of the IEEE International Conference on Computer Communications*

- *INFOCOM*, Anchorage, Alaska, USA, May 2007, pp. 803–811.

[82] H. Zhai and Y. Fang, "Physical carrier sensing and spatial reuse in multirate and multihop wireless ad hoc networks," in *Proceedings of the IEEE International Conference on Computer Communications - INFOCOM*, Barcelona, Spain, April 2006, pp. 1–12.

[83] Z. Zeng, Y. Yang, and J. Hou, "How Physical Carrier Sense Affects System Throughput in IEEE 802.11 Wireless Networks," in *Proceedings of the IEEE International Conference on Computer Communications - INFOCOM*, Alaska, USA, April 2008.

[84] R. Ramanathan, *Antenna Beamforming and Power Control for Ad Hoc Networks.*

[85] A. Spyropoulos and C. Raghavendra, "Capacity bounds for ad-hoc networks using directional antennas," in *Proceedings of the IEEE International Conference on Communications - ICC*, Los Angeles, CA, USA, May 2003, pp. 348–352.

[86] M. M. Carvalho and C. B. Margi and K. Obraczka and J.J. Garcia-Luna-Aceves, "Modeling energy consumption in single-hop ieee 802.11 ad hoc networks," in *Proceedings of the IEEE International Conference on Computer Communications and Networks - ICCCN*, Chicago, IL USA, October 2004, pp. 367–372.

[87] S. Yi, Y. Pei, and S. Kalyanaraman, "On the capacity improvement of ad hoc wireless networks using directional antennas," in *Proceedings of the ACM International Symposium on Mobile Ad Hoc Networking and Computing - MobiHoc*, Annapolis, Maryland, USA, May 2003, pp. 108 – 116.

[88] A. Spyropoulos and C.S. Raghavendra., "Asympotic capacity bounds for ad-hoc networks revisited: the directional and smart antenna cases," in *Proceedings of*

the IEEE International Global Telecommunications Conference - GLOBECOM, vol. 3, San Francisco, USA, December 2003, pp. 1216–1220.

[89] R. Choudhury and N. H. Vaidya, "Performance of Ad Hoc Routing using Directional Antennas," *Elseiver Journal of Ad Hoc Networks*, vol. Volume 3, Issue 2, pp. 157–173, March 2005.

[90] A. Arora, M. Krunz, and A. Muqattash, "Directional Medium Access Protocol DMAP with Power Control for Wireless Ad Hoc Networks," in *Proceedings of the IEEE International Global Telecommunications Conference - GLOBECOM*, Dallas, USA, November 2004, pp. 2797– 2801.

[91] J. Wang, Y. Fang, and D. Wu, "SYN-DMAC: A Directional Mac protocol for Ad Hoc Networks with Synchronization," in *Proceedings of the IEEE Military Communications Conference*, New Jersy, USA, October 2005, pp. 2254–2263.

[92] K. Kiran and P. Sai, "A survey on mobility support by mac protocols using directional antennas for wireless ad hoc networks," in *proceedings of the IEEE International Symposium on on Ad Hoc and Ubiquitous Computing - ISAUHC*, Mangalore, India, December 2006, pp. 148–153.

[93] R. Vilzmann and C. Bettstetter, "A survey on MAC protocols for ad hoc networks with directional antennas," in *Proceedings of EUNICE Open European Summer School*, Colmenarejo, Spain, July 2005, pp. 187–200.

[94] G. Li, L. L. Yang, W. S. Conner, and B. Sadeghi, "Opportunities and challenges for mesh networks using directional antennas," in *Proceedings of the First IEEE Workshop on Wireless Mesh Networks*, Florida, USA, April 2005, pp. 32–41.

[95] R. R. Choudhury and N. H. Vaidya, "Deafness: a mac problem in ad hoc networks when using directional antennas." in *Proceedings of the IEEE International Conference on Network Protocols - ICNP*, Annapolis, Maryland, USA, September 2004, pp. 283 – 292.

[96] C. M. Cordeiro, H. Gossain, and D. P. Agrawal, "A directional antenna medium access control protocol for wireless ad hoc networks," *Brazilian Telecommunications Society*, vol. 2, no. 1, pp. 842–854.

[97] H. Gossain, C. Cordeiro, and D. P. Agrawal, "Minimizing the effect of deafness and hidden terminal problem in wireless ad hoc networks using directional antennas: Research articles," *Wirel. Commun. Mob. Comput.*, vol. 6, no. 7, pp. 917–931, 2006.

[98] M. Takata, M. Bandai, and T. Watanabe, "A Directional MAC Protocol with Deafness Avoidance in Ad Hoc Networks," *IEICE Transactions on Communications*, vol. 90, no. 4, p. 866, 2007.

[99] S. S. Kulkarni and C. Rosenberg, "DBSMA: A Mac Protocol for Multi-hop Ad-hoc Networks with Directional Antennas," in *Proceedings of the IEEE International Symposium on Personal, Indoor and Mobile Radio Communications - PIMRC*, Berlin, Germany, September 2005, pp. 57– 61.

[100] J. Zander, "Slotted Aloha Multihop Packet Radio Networks with Directional Antennas," *IEE Electronics Letters volume 26, number 25*, pp. 2098–2100, September 1990.

[101] R. Ramanathan, "On the Performance of Ad Hoc Networks with Beamforming Antennas," in *Proceedings of the IEEE International Symposium on Mobile Ad Hoc Networking and Computing - MobiHoc*, Long Beach, USA, October 2001, pp. 95 – 105.

[102] N. Fahmy, T.D. Todd and V. Kezys, "Ad hoc Networks with Smart Antennas Using IEEE 802.11-based Protocols," in *Proceedings of the IEEE International Conference on Communications - ICC*, New York, USA, April 2002, pp. 3144–3148.

[103] A. Nasipuri, K. Li, and U. Sappidi, "Power Consumption and Throughput in Mobile Ad Hoc Networks using Directional Antennas," in *Proceedings of the IEEE International Conference on Computer Communications and Networks - INFOCOM*, Miami, USA, October 2002, pp. 620– 626.

[104] N. Fahmy and V. Kezys, "Distributed Power Control for Ad hoc Networks with Smart Antennas," in *Proceedings of the IEEE Vehicular Technology conference - VTC*, September 2002, pp. 2141– 2144.

[105] A. Arora and M. Krunz, "Interference-limited MAC protocol for MANETs with directional antennas," in *Proceedings of the IEEE International Symposium on a World of Wireless, Mobile and Multimedia Networks - WoWMoM*, Taormina, Italy, June 2005, pp. 2–10.

[106] Z. Xiaodong, L. Jiandong, and Z. Dongfang, "A Novel Power Control Multiple Access Protocol for Ad Hoc Networks with Directional Antennas," in *Proceedings of the IEEE International Conference on Advanced Information Networking and Applications - AINA*, Vienna, Austria, April 18-20 2006, pp. 822–826.

[107] L. Song and C. Yu, "Improving Spatial Reuse with Collision-Aware DCF in Mobile Ad Hoc Networks," in *Proceedings of the IEEE International Conference on Parallel Processing - ICPP*, Columbus, USA, August 2006, pp. 219–228.

[108] T. Nadeem, L. Ji, A. Agrawala, and J. Agre, "Location Enhancement to IEEE 802.11 DCF," in *Proceedings of the IEEE International Conference on Computer Communications - INFOCOM*, Miami, USA, March 2005, pp. 651– 663.

[109] Z. Li, S. Nandi, and A. Gupta, "Improving MAC Performance in Wireless Ad Hoc Networks using Enhanced Carrier Sensing (ECS)," in *Proceedings of IFIP Networking Conference*, Athens, Greece, April 2004, pp. 600–612.

[110] F. Ye, S. Yi, and B. Sikdar, "Improving Spatial Reuse of IEEE 802.11 Based Ad Hoc Networks," in *Proceedings of the IEEE International Global Telecommunications Conference - GLOBECOM*, San Francisco,USA, December 2003, pp. 1013– 1017.

[111] Qualnet Simulator, "www.scalablenetworks.com."

[112] D. Malone, P. Clifford, D. J. Leith, "Mac layer channel quality measurement in 802.11," *IEEE Communications Letters*, vol. 11, Issue: 2, pp. 143–145, Feb 2007.

[113] J. Zhu, X. Zhu, S. Zhu, and K. Papagiannaki, "Csma self-adaptation based on interference differentiation," in *Proceedings of the IEEE Global Telecommunications Conference - GLOBECOM*, Washington DC, USA, November 2007, pp. 4946–4951.

[114] M. Takai, J. Martin, R. Bagrodia, and A. Ren , "Directional virtual carrier sensing for directional antennas in mobile Ad Hoc networks," in *Proceedings of the ACM International Symposium on Mobile Ad Hoc Networking and Computing - MobiHoc*, Lausanne, Switzerland ,December 2002, pp. 183 – 193.

[115] K. K. Leung, ""Power Control by Interference Prediction for Broadband Wireless Packet Networks"," *IEEE Transactions on Wireless Communications*, vol. 1, no. 2, pp. 256–265, April 2002.

[116] G. Welch and G. Bishop, "An Introduction to the Kalman Filter," Department of Computer Science University of North Carolina at Chapel Hill, Tech. Rep., August 2006.

[117] R. Brown and P. Hwang., *Introduction to Random Signals and Applied Kalman Filtering.*, 1997.

[118] R. Hekmat and P. Mieghem, "Interference in wireless multihop ad hoc networks," in *Proceedings of Mediterranean Ad Hoc Networking Workshop - Med-hoc-net*, Sardegna, Italy, September 2002, pp. 36–41.

[119] L. Lin, H. Fu, and W. Jia, "An efficient admission control for IEEE 802.11 networks based on throughput analyses of (Un)saturated channel," in *IEEE Global Telecommunications Conference. GLOBECOM*, St. Louis, USA, December 2005, pp. 3017– 3021.

[120] P. Mieghem and G. Hooghiemstra and R. Hofstad, "A scaling law for hop count," Delft University, Tech. Rep., October 2000.

[121] R Lou, D. Bellis, and R.M. Edwards, "Estimation of the average hop count using grid pattern in multihop wireless ad hoc networks," in *Proceedings of London Communication Symposium*, London,UK, September 2002, pp. 19–23.

[122] L. Feeney and M. Nilsson, "Investigating the energy consumption of a wireless network interface in ad hoc networking environment," in *Proceedings of the IEEE International Conference on Computer Communications - INFOCOM*, Alaska, USA, April 2001, pp. 1548–1577.

[123] M. Kubisch and H. Karl, "Analyzing energy consumption in wireless networks by relaying," University of Berlin, Tech. Rep., June 2001.

[124] V. Srivastava, J. Neel, A. Mackenzie, R. Menon, L. Dasilva, J. Hicks, J. Reed, and R. Gilles, "Using game theory to analyze wireless ad hoc networks," *IEEE Communications Surveys and Tutorials*, vol. 7, no. 4, pp. 46–56, 2005.